A Study of Coupled-Cluster Methods for infinite matter

by

Fredrik Wilhelm Holmen

Thesis

for the degree of

Master of Science

Faculty of Mathematics and Natural Sciences
University of Oslo

Autumn 2016

Abstract

In this thesis, we present the formalism of many-body methods, with an emphasis on the Coupled Cluster method with double excitations. The methods are tested on three physical systems, the finite size pairing model and two infinite homogenoeus systems, the electron gas in three dimensions and infinite nuclear matter. We have developed a software suite which can easily be extended to other physical systems, as well as to include more complicated correlations. The results have been benchmarked against existing literature, with excellent agreement.

Acknowledgements

The work I have done in this thesis could never been done without the help of Morten Hjorth-Jensen, my advisor. You have taught me everyting I have used in this thesis, through your many great courses and personal interactions. I want to thank you for the amazing work you have done for the group Computational Physics and for the way you inspire everyone you meet. The material I present in this thesis are built heavily upon the work of others. A special thank you to Audun Skau Hansen. My work is influenced by your great thesis.

I would like to thank Henrik Sveinsson for being a great inspiration and a good friend. You taught me the value of hard work and high ambitions. It was you who sparked my interest in physics at Oslo katedralskole when I followed your path in natural sciences. I would also like to thank Bjørnar Pettersen and Marit Ingebrigtsen, two of my teachers at Oslo katedralskole.

The last five years have been an amazing experience. I have learned way more than I thought was possible, I have met great people and been given opportunities by the institute to develop my skills as a tutor. Much of the positive experience is owed to the community at Lillefy, the home of Fysikkforeningen and Fysisk Fagutvalg, where I have emptied countless cups of coffee. Vetle Wegner Ingeberg, Henrik Limseth, Torgeir Mo, Sigve Smedsrud Harang, Anders Lauvland have been my best friends for the last five years. You have selflessly shared your knowledge, good humour and beers.

I am thankful for my time at Computational Physics, a splendid master group, filled with brilliant and caring people. You have created a relaxed atmosphere, where interesting discussions and competitive card games light up the day. A special thank you to Marte Julie Stra, Jonas van den Brink, Sean Bruce Miller and Emilie Fjørner for sharing my office and giving me loads of help.

Thank you My Tien Diep for always keeping my motivation high and reducing my nerdy obsessions to a tolerable level.

Contents

1 Introduction **1**

1.0.1 Motivation 1

1.0.2 Goals for the Work 2

1.0.3 Structure 3

2 Quantum Mechanics **5**

2.1 Postulates 5

2.2 The Many-Body Wave Function 6

2.3 Pauli's Exclusion Principle 7

2.4 Slater Determinant 8

2.5 An ansatz for the Wave Function 9

2.6 The Hamiltonian 10

2.7 Matrix Elements 11

2.7.1 Calculation of matrix elements 12

2.8 The Variational Principle 14

3 Second Quantization **15**

3.1 Annihilation and Creation operators 15

3.2 Strings of Operators 16
3.3 Anticommutator Relations 17
3.4 Inner products 18
3.5 Representation of Operators 19
3.5.1 One-Body Operator 20
3.5.2 Two-body Operator 21
3.5.3 The Hamiltonian 22
3.6 Normal Ordering and Wick's Theorem 23
3.6.1 Normal Ordering 23
3.6.2 Contractions 24
3.6.3 Time-independent Wick's theorem 24
3.7 Particle-Hole Formulation 25
3.8 Normal ordering of Operators 26
3.8.1 One-Body Operator 26
3.8.2 Two-Body operators 27
3.9 Partitioning the Hamiltonian Operator 28
3.10 Normal Ordering of Hamiltonian 30
3.11 Correlation Energy 32

4 Diagramatic Representation **33**

4.1 The Slater determinant 33
4.2 Operators 35
4.3 Contractions and Inner products 39
4.4 Interpreting Diagrams 41

5 Many-Body Methods **43**

5.1 Full Configuration Interaction Theory 44

5.1.1 The Hamiltonian Matrix 45

5.1.2 Computational cost 46

5.2 Many-body Perturbation Theory 47

5.2.1 General derivation of Many-Body Particle Theory equations 48

5.2.2 Equations for Rayleigh-Schrödinger Perturbation Theory . 49

5.3 Linked Diagram theorem 50

5.4 Hartree-Fock calculations 51

6 Coupled-Cluster Theory **53**

6.1 The Exponential Ansatz 53

6.2 Comparison with Configuration Interaction 54

6.3 Truncating the Exponential Ansatz 55

6.4 The Variational Principle 57

6.5 Size-Extensivity 57

6.6 The Coupled-Cluster Doubles Equations 58

6.7 Intermediates 60

7 The Pairing Model **63**

7.1 The Hamiltonian 63

7.2 Configuration Interaction theory 66

7.3 Hartree-Fock calculations 67

7.4 Many-Body Perturbation Theory 69

7.4.1 Interpreting diagrams 70

7.4.2 Label all lines 71
7.4.3 Identify the operators 71
7.4.4 Identify the denominator 71
7.4.5 Including phase factor 72
7.4.6 Identify equivalent lines 72
7.4.7 Second Order Perturbation Theory 72
7.4.8 Third Order Perturbation Theory 73
7.4.9 Fourth Order Perturbation Theory 73
7.5 Spin Summations 78

8 Infinite Matter **81**

8.1 The Infinite Electron Gas 81
8.1.1 The Hamiltonian 81
8.1.2 The Reference Energy 83
8.1.3 The Fock Matrix Elements 83
8.1.4 Anti-Symmetric Matrix Elements 84
8.1.5 The Plane Wave Basis 84
8.2 Infinite Nuclear Matter 87
8.3 Nuclear Interaction 87
8.3.1 The Minnesota Potential 88

9 Implementation of CCD **91**

9.1 Implementing the CCD equations 91
9.2 Matrix Representation of Contractions 92
9.2.1 Aligning elements 93

9.3 Block Implementation 95
9.3.1 Two-state configurations 96
9.3.2 Unaligned channels 97
9.3.3 Permutations 100
9.4 Setting Up Basis 100
9.5 Parallelization 101

10 Results **103**

10.1 The Pairing Model 103
10.1.1 Comparison of CCD solvers 105
10.1.2 Comparison of various solvers 107
10.2 The Homogeneous Electron Gas 109
10.2.1 The Reference Energy 109
10.2.2 Comparison of solvers 109
10.2.3 The Thermodynamic limit 111
10.3 Neutron Matter 117

11 Conclusion and future prospects **121**

Chapter 1

Introduction

The aim of this thesis is to utilize many-body methods for computing the ground state energy for three different systems. The pairing model, the homogeneous electron gas and infinite nuclear matter. Well-performing many-body methods are very computationally costly, and a brute force implementation of configuration interaction theory, many-body perturbation theory and coupled-cluster theory is only a viable option for small systems. The thesis investigates how one can implement a more efficient solver for the coupled-cluster equations in order to gain a better understanding of large systems.

1.0.1 Motivation

The pairing model is an interesting model to solve, not because of its direct representation of real matter, but because it lives in a small and finite Hilbert space. This allows us compute the exact ground state energy with full configuration interaction theory. The result is an important tool for comparing the performance of different solvers. Because it is a small and confined system, it is easy to calculate matrix elements, leading to an exact solution that lends itself for comparisons with methods like many-body perturbation theory and coupled-cluster theory. The system is therefore exceptionally good at benchmarking the implementation of many-body methods.

Moving on to the homogeneous electron gas, we present an infinite system of electrons interacting with each other and a background charge. By only taking care of the electron-electron interaction, we generate a system that can be dealt with using common tools of many-body quantum mechanics. This is one of the first systems to be evaluated by many-body methods, and the literature on this

topic contains many different benchmarks.

The main goal of nuclear physics, is to understand the fundamental physics of the nucleus, its constituents and their interaction. We can generate experimental data on ground state energies, and by applying known many-body quantum mechanics, we hope to reproduce these results and gain larger insights into the forces and laws of motion which govern nuclear physics. Studies of infinite matter and its equation of state have important consequences for dense objects like neutron stars or how a supernova evolves in its late stages.

1.0.2 Goals for the Work

I have worked systematically to achieve the goals set up by the introduction to the thesis. The main goals of this thesis can be summarized in a few points:

- A first goal for the thesis has been to present the theory behind four many-body methods. Starting with fundamental many-body quantum mechanics and second quantization before deriving the equations for configuration interaction theory, Hartree-Fock theory, Rayleigh-Schrödinger perturbation theory and coupled-cluster theory.

- The second goal was to implement the Pairing model and the four solvers, coded in c++. The implementations could compute the ground state correlation energy to compare the efficiency of different solvers. The Pairing model could also serve as valuable benchmarking for the solvers.

- Next, I needed to present and implement the homogeneous electron gas system and the infinite nuclear matter system with neutrons. Only the coupled-cluster doubles equations would be used to compute correlation energies for these systems.

- The original, brute force, coupled-cluster solver is too slow to compute correlation energies for large basis sets. I needed to look at how matrix-matrix multiplication and symmetries of the system could be exploited to reduce the computational costs. Presenting and implementing a much more advanced and efficient coupled-cluster doubles code has been the hardest and most time-consuming part of the thesis.

- Finally, the last goal has been to produce results for large basis sets, needing a parallelized code to run more efficiently.

1.0.3 Structure

The first part of the thesis is purely a theoretical part, going through the formalism needed to develop many-body methods. My own contributions are presenented in the chapter on implementation, and in the developed code, open to everyone at gibhub.com [27].

Chapter 2 gives a short introduction to quantum mechanics, with a main focus on presenting the many-body wave function, the many-body Hamiltonian and the calculations of matrix elements.

Chapter 3 presents the formalism of *second quantization*, a powerful formalism that simplifies notation by rewriting states as operators. Wick's theorem gives a powerful tool to perform fast computations of matrix elements. This chapter presents alsothe main goal of post-Hartree Fock methods, the calculation of the *correlation energy*.

Chapter 4 gives a brief introduction to the use of Feynman diagrams to represent states, operators and contractions.

Chapter 5 presents a brief introduction to three many-body methods; full configuration interaction theory, many-body perturbation theory and Hartree-Fock theory.

Chapter 6 gives a deeper introduction to coupled-cluster method and sets up the equations for coupled-cluster theory with double excitations only.

Chapter 7 presents the pairing model, introducing the Hamiltonian and basis states. The chapter focuses on how I implemented Full Configuration Interaction, Hartree-Fock calculations and many-body perturbation theory to calculate the ground state energy.

Chapter 8 presents two different systems; the homogeneous electron gas and infinite nuclear matter with the Minnesota potential.

Chapter 9 gives a thourough explanation of the various computational elements of the coupled-cluster solver. First explaining the general concepts of the direct implementation, before delving into more advanced implementations exploiting symmetries and efficiency of matrix multiplication.

Chapter 10 contains all results produced the pairing model, the homogeneous electron gas and infinite nuclear matter, while chapter 11 contains my summary and perspectives.

Chapter 2

Quantum Mechanics

2.1 Postulates

Quantum mechanics is built upon a few principles [2, 5, 6, 9], often called the postulates of quantum mechanics.

1. **The Wave Function**
   All information on a quantum system is given by the wave function $\Psi(x,t)$. The wave function represents the probability of measuring a particle within a small volume dx and for a given time, t. As the probability cannot exceed 1, the wave function must be normalized, namely

   $$\int_{-\infty}^{\infty} \Psi^*(x,t)\Psi(x,t)\mathrm{dx} = 1. \tag{2.1}$$

   Using Dirac notation, we write the wave function as $|\Psi\rangle$. Physical distinguishable states are orthogonal to each other. Using normalized states, they are orthonormal to each other, meaning that for two unambigously distuingishable states, we have

   $$\langle\lambda|\psi\rangle = \delta_{\lambda\psi}. \tag{2.2}$$

2. **Observables**
   All observables are represented by linear operators, written with a "hat", $\hat{O}$. These linear operators are bound to be hermitian.

3. **Measurements**
   The possible outcomes of an experiment are the eigenvalues of an opera-

tor that represents the observable, given as a number λ. If a state is in the eigenstate $|\lambda\rangle$, the only possible measurement of an experiment is the eigenvalue, λ. We write this as

$$\hat{O}\,|\lambda\rangle = \lambda\,|\lambda\rangle\,. \tag{2.3}$$

4. **Probabilities**
   Given a state $|\alpha\rangle$, the probability of observing λ when measuring the observable $\hat{O}$ is given by

$$P(\lambda) = \langle\alpha|\lambda\rangle\,\langle\lambda|\alpha\rangle = |\,\langle\alpha|\lambda\rangle\,|^2, \tag{2.4}$$

   which measures the overlap of the two states $|\alpha\rangle$ and $|\lambda\rangle$. If they are physically distinguishable, the probability is zero. If the probability is non-zero, we have "mixed states".

5. **Time development and the Schrödinger equation**
   Time developement for states are given by acting on the state with a unitary operator

$$|\Psi(t)\rangle = \hat{U}(t)\,|\Psi(0)\rangle\,. \tag{2.5}$$

   This leads us to the time-independent Schrödinger equation

$$\hat{H}\,|\Psi(x,t)\rangle = i\hbar\frac{\partial}{\partial t}\,|\Psi(x,t)\rangle\,, \tag{2.6}$$

   where we have defined the Hamiltonian operator $\hat{H}$. The Hamiltonian will be used throughout the thesis, as its eigenvalues are the measurable energy. We will primarily focus on solving the *time independent* Schrödinger equation

$$\hat{H}\,|\Psi(x)\rangle = E\,|\Psi(x)\rangle\,. \tag{2.7}$$

2.2 The Many-Body Wave Function

A single particle, in isolation, occupies the single particle wave function [2, 11]

$$\phi_i(\mathbf{x}_1). \tag{2.8}$$

Single particle wave functions are described by the lower case letter ϕ, holding all relevant quantum numbers. The vector $\mathbf{x}_1$ holds information on translational

position as well as spin for particle 1. When aiming to describe a system consisting of many such particles, it is tempting to think of the many-body wave function as a function of each particle's wave function

$$\Phi = \Phi(\phi_1(\mathbf{x}_1), \phi_2(\mathbf{x}_2), ..., \phi_N(\mathbf{x}_N)), \tag{2.9}$$

where we will use the upper case letters Ψ and Φ as the many-body wave functions. This wave function will be sought in the combined Hilbert space of the single particle functions [24]

$$\Phi \in \mathcal{H} = \mathcal{H}_1 \oplus \mathcal{H}_2 \oplus ... \oplus \mathcal{H}_N, \tag{2.10}$$

where $\mathcal{H}_i$ represent the Hilbert space for particle i. This combined space is referred to as the Fock space [24]. A first guess for the wave function can be the *Hartree-product* of single particle functions [2, 3, 4]

$$\Phi_h = \phi_1(\mathbf{x}_1), \phi_2(\mathbf{x}_2), ..., \phi_N(\mathbf{x}_N) = \prod_{i=1}^{N} \phi_i(\mathbf{x}_i). \tag{2.11}$$

2.3 Pauli's Exclusion Principle

Pauli's exclusion principle, also called the antisymmetry principle or the symmetrization requirement [4, 5], is quite often included as one of the underlying postulates of quantum mechanics. Our first guess is to write the two-body wave function on the form of a Hartree-product

$$\Psi(\mathbf{x}_1, \mathbf{x}_2) = \phi_1(\mathbf{x}_1)\phi_b(\mathbf{x}_2). \tag{2.12}$$

All particles, however, are completely identical, with no way of separating them from each other [5]. Therefore, one must require a different form on the wave function, one that does not commit the particles to specific wave functions. Introducing a general wave function

$$\Psi(\mathbf{x}_1, \mathbf{x}_2) = A[\psi_1(\mathbf{x}_1)\psi_2(\mathbf{x}_2) \pm \psi_1(\mathbf{x}_2)\psi_2(\mathbf{x}_1)], \tag{2.13}$$

with A given as a normalization factor. We notice the choice of sign. Particles with spin integers, named bosons, will require the use of the positive sign, and the wave function will therefore remain unchanged through the interchange of particles. Particles with spin half-integers, will require the use of a negative sign. All particles used in calculations in this thesis are fermions, namely electrons, neutrons or protons. We can introduce the specific antisymmetrization requirement

for this thesis as

$$\Psi(\mathbf{x}_1, \mathbf{x}_2) = -\Psi(\mathbf{x}_2, \mathbf{x}_1). \tag{2.14}$$

An exchange of particles can be represented through the use of a permutation operator $\hat{P}$, which gives

$$\hat{P}\Psi(\mathbf{x}_1, \mathbf{x}_2) = \Psi(\mathbf{x}_2, \mathbf{x}_1). \tag{2.15}$$

2.4 Slater Determinant

The antisymmetrized wave function grows rapidly for every added particle, and we need to introduce a more convenient notation, called the Slater Determinant. Written in terms of the permutation operator [2]

$$\Phi_{SD} = \frac{1}{\sqrt{N!}} \sum_{\lambda}^{N!} \hat{P}_\lambda (-1)^{n(\lambda)} \Phi_h, \tag{2.16}$$

where the permutation operator $\hat{P}_\lambda$, performes every permutation possible, and introducing a factor -1 every time a perturbation is performed. Introducing the anti-symmetry operator $\mathcal{A}$, we can write the shorthand equation

$$\Phi_{SD} = \sqrt{N!}\mathcal{A}\Phi_h, \tag{2.17}$$

where we have defined $\mathcal{A}$ as [24]

$$\mathcal{A} = \frac{1}{N!} \sum_{\lambda} (-1)^\lambda \hat{P}. \tag{2.18}$$

This operator holds important properties, like commuting with the Hamiltonian operator

$$\left[\hat{H}, \mathcal{A}\right] = 0, \tag{2.19}$$

and

$$\mathcal{A}^2 = \mathcal{A}, \qquad \mathcal{A} = \mathcal{A}^\dagger. \tag{2.20}$$

A more intuitive representation of the Slater determinant is on a matrix form

$$\Phi_{SD} = \frac{1}{\sqrt{N!}} \begin{vmatrix} \phi_1(\mathbf{x}_1) & \phi_2(\mathbf{x}_1) & \cdots & \phi_N(\mathbf{x}_1) \\ \phi_1(\mathbf{x}_2) & \phi_2(\mathbf{x}_2) & \cdots & \phi_N(\mathbf{x}_2) \\ \vdots & \vdots & \ddots & \vdots \\ \phi_1(\mathbf{x}_N) & \phi_2(\mathbf{x}_N) & \cdots & \phi_N(\mathbf{x}_N) \end{vmatrix}. \tag{2.21}$$

This way of writing the many-body wave function will represent a linear combination of products of the one-body wave functions ϕ_i's and all the electronic coordinates $\mathbf{x}_i$ distributed among them in all possible ways. Exchanging two lines will change the sign such that the Slater determinant will respect the antisymmetric requirement. Introducing a convenient shorthand expression using Dirac-notation, consisting only of the diagonal elements, we can write the Slater determinant as [11]

$$|\Phi\rangle = |\phi_1(\mathbf{x}_1)\phi_2(\mathbf{x}_2)...\phi_N(\mathbf{x}_N)\rangle\,, \tag{2.22}$$

which will be the preferred representation of a Slater determinant until Second quantization is introduced.

2.5 An ansatz for the Wave Function

The true wave function, represented by Ψ is seldomly known. On the contrary, one of the goals of many-body quantum mechanics is to find an expression for Ψ. To find Ψ, one can introduce the Slater determinant as an approximation to the wave function

$$\Psi \approx \Phi_{SD}, \tag{2.23}$$

made up of a set of known single particle wave functions ϕ_i. Choosing a set of single particle functions that lies close to the true state, will provide good results. Calculations will be made easier by using single particle states that are eigenstates of the one-body Hamiltonian operator. One could, for example, choose the hydrogen orbitals as single particle functions when calculating on electrons around an atom. We name Φ_{SD} the ansatz for the true wave function.

2.6 The Hamiltonian

The Hamiltonian operator represents the total energy for the system, namely the kinetic energy and the potential energy

$$\hat{H} = \hat{T} + \hat{V}, \tag{2.24}$$

where we can write the kinetic energy as [24]

$$\hat{T} = \sum_{i=1}^{N} \frac{\mathbf{p}_i^2}{2m_i} \sum_{i=1}^{N} \left(\frac{\hbar^2}{2m_i} \nabla_i^2 \right) = \sum_{i=1} t(x_i). \tag{2.25}$$

A general potential operator can be written as

$$\hat{V} = \sum_{i=1}^{N} \hat{u}_{ext}(x_i) + \sum_{ji=1}^{N} v(x_i, x_j) + \sum_{ijk=1}^{N} v(x_i, x_j, x_k) + \cdots, \tag{2.26}$$

where we have included the possibility of more than two-body interactions. When doing quantum chemistry, it is common to *freeze* the core. This is called the Born-Oppenheimer Approximation, and simplifies the potential a lot. We now need to look at electrons interacting with a positive core through the Coulombic interaction. The Coulombic potential is a two-body potential, and including the interaction between every electron, we can rewrite the Hamiltonian as

$$\hat{H} = \sum_{i=1}^{N_e} t(x_i) - \sum_{i=1}^{N_e} k\frac{Z}{r_i} + \sum_{i<j}^{N_e} \frac{k}{r_{ij}}, \tag{2.27}$$

where N_e is the number of electrons and $k = 1.44\text{eVnm}$. It is useful to group the one- and two-body parts together

$$\hat{H} = \hat{H}_0 + \hat{H}_1, \tag{2.28}$$

where we have the one-electron energy

$$\hat{H}_0 = \sum_{i=1}^{N_e} t(x_i) - \sum_{i=1}^{N_e} k\frac{Z}{r_i}, \tag{2.29}$$

and the interaction term

$$\hat{H}_1 = \sum_{i<j}^{N_e} \frac{k}{r_{ij}}. \tag{2.30}$$

It is very useful to have an ansatz for the wave function that satisfies the relation

$$\hat{H}_0 \left|\phi_\lambda\right\rangle = \epsilon_\lambda \left|\phi_\lambda\right\rangle . \tag{2.31}$$

In this thesis, I have only included a two-body interaction for my potentials, simplifing the calculations on nuclear matter by using easier potentials.

2.7 Matrix Elements

A Slater determinant will have an energy, given by the Hamiltonian operator

$$\hat{H} \left|\Phi_{SD}\right\rangle = \epsilon_{SD} \left|\Phi\right\rangle . \tag{2.32}$$

We want to calculate the energy, and to do that, we need to introduce the concept of expectation values. By taking the Hermitian conjugate of a wave function, one finds the *bra* version of the state

$$(\left|\Phi_{SD}\right\rangle)^\dagger = (\Phi_{SD}^*)^T = \left\langle\Phi_{SD}\right| . \tag{2.33}$$

The original state is known as a *ket* state. The expectation value is defined as taking the inner product of two states, where one is worked on by an operator

$$\int_{-\infty}^{\infty} \Phi_{SD}^\dagger \hat{H} \Phi_{SD} d\tau = \epsilon_{SD}. \tag{2.34}$$

Because of the orthonormality of the states, this calculation will result in the energy. In terms of Dirac notation, this is usually referred to as *multiplying from the left by a bra state*

$$\left\langle\ \Phi_{SD}\right|\hat{H}\left|\Phi_{SD}\ \right\rangle = \epsilon_{SD}. \tag{2.35}$$

By splitting the Hamiltonian into the one-body and two-body part

$$\hat{H} = \hat{H}_0 + \hat{H}_1 = \sum_i \hat{h}_0(x_i) + \sum_{i<j} \hat{v}(i,j), \tag{2.36}$$

we can rephrase the expectation value as a one-body calculation and a two-body calculation

$$\left\langle\Phi_{SD}\right| \hat{H} \left|\Phi_{SD}\right\rangle = \left\langle\Phi_{SD}\right| \hat{H}_0 \left|\Phi_{SD}\right\rangle + \left\langle\Phi_{SD}\right| \hat{H}_1 \left|\Phi_{SD}\right\rangle . \tag{2.37}$$

Written out, this gives

$$\langle \Phi_{SD} | \sum_i \hat{h}_0(x_i) | \Phi_{SD} \rangle + \langle \Phi_{SD} | \sum_{i<j} \hat{v} | \Phi_{SD} \rangle . \tag{2.38}$$

We will commonly refer to these elements as *matrix elements*.

2.7.1 Calculation of matrix elements

Looking at the one-body matrix element, we use equations (**??**,2.20)

$$\langle \Phi_{SD} | \hat{h}_0(x_i) | \Phi_{SD} \rangle = N! \langle \Phi_h | \hat{h}_0(x_i) \mathcal{A} | \Phi_h \rangle , \tag{2.39}$$

which, when written on integral form, gives

$$\sum_i N! \int \Phi_h^* \hat{h}_0(x_i) \mathcal{A} \Phi_h d\tau. \tag{2.40}$$

Substituting out the Hartree-product and $\mathcal{A}$ for the permutation operator, we are left with

$$\sum_i \sum_\lambda (-1)^\lambda \int d\tau \left(\prod_j \phi_j(x_j)^* \right) \hat{h}_0(x_i) \hat{P}_\lambda \left(\prod_k \phi_k(x_k) \right) . \tag{2.41}$$

Because of the orthogonality of the single particle states, we can deduce that any permutation of particles on one Hartree-product, will set up an inner product of different particles and give zero as a result. We can therefore reduce the calculation to a single sum of unpermuted inner products

$$\sum_i \int d\tau \left(\prod_j \phi_j(x_j)^* \right) \hat{h}_0(x_i) \left(\prod_k \phi_k(x_k) \right) . \tag{2.42}$$

Since the operator $\hat{h}_0(x_i)$ only works on $\phi_i(x_i)$, we can split the sum into two parts. Looking at the equation for particle i

$$\langle \phi_i | \hat{h}_0 | \phi_i \rangle \left(\prod_{j \neq i} \int d\tau \, |\phi_j(x_j)|^2 \right) , \tag{2.43}$$

which, using the orthonormality relations, become

$$\langle \phi_i | \hat{h}_0 | \phi_i \rangle . \tag{2.44}$$

We can write the one-body matrix elements as

$$E_0 = \sum_i \langle \phi_i | \, \hat{h}_0 \, | \phi_i \rangle \, . \tag{2.45}$$

If we are using single particle wave functions that are eigenstates for the one-body Hamiltonian operator, we get the simple result

$$\langle \, \hat{H}_0 \, \rangle = E_0 = \sum_i \epsilon_i. \tag{2.46}$$

We can apply the same logic for the two-body part

$$\langle \Phi_{SD} | \, \hat{H}_1 \, | \Phi_{SD} \rangle \, . \tag{2.47}$$

We want to calculate

$$N! \, \langle \Phi_h | \sum_{i<j} \hat{v}_{ij} \mathcal{A} \, | \Phi_h \rangle = N! \sum_{i<j} \int \Phi_h^* \hat{v}(x_i, x_j) \mathcal{A} \Phi_h d\tau. \tag{2.48}$$

Rewritten in terms of the permutation operator

$$\sum_{i<j} \sum_{\sigma} (-1)^{\sigma} \int \Phi_h^* v(x_1, x_2) \hat{P} \Phi_h d\tau, \tag{2.49}$$

the two-body interaction will allow for a single permutation. This is because the interaction is dependent on the distance between the two particles. Every other particle must be unpermuted. We can rewrite the equation by this single permutation as

$$\sum_{i<j} \int \Phi_h^* v(x_i, x_j)(1 - P_{ij}) \Phi_h d\tau, \tag{2.50}$$

where P_{ij} means the interchange of the two particles i and j. By the same argument as for the one-particle operator, most states vanish due to orthonormality, and we are left with the terms that take part in the interaction, giving

$$\frac{1}{2} \sum_{\mu} \sum_{\nu} \left[\int \phi_\mu^*(x_i) \phi_\nu^*(x_j) \hat{v}(x_i, x_j) \phi_\mu(x_i) \phi_\nu(x_j) dx_i dx_j \right. \tag{2.51}$$

$$\left. - \int \phi_\mu^*(x_i) \phi_\nu^*(x_j) \hat{v}(x_i, x_j) \phi_\nu(x_i) \phi_\mu(x_j) dx_i dx_j \right], \tag{2.52}$$

where we have introduced the factor $\frac{1}{2}$ because the sum now counts all states

twice. The first term is known as the direct term, and the second term is known as the *exchange term* or the *Fock* term and it incorporates the Pauli principle. We need to introduce an easier notation to present this matrix element

$$\langle \mu\nu|v|\mu\nu\rangle = \int \phi_\mu^*(x_i)\phi_\nu^*(x_j)\hat{v}(x_i,x_j)\phi_\mu(x_i)\phi_\nu(x_j)dx_i dx_j, \tag{2.53}$$

and

$$\langle \mu\nu|v|\nu\mu\rangle = \int \phi_\mu^*(x_i)\phi_\nu^*(x_j)\hat{v}(x_i,x_j)\phi_\nu(x_i)\phi_\mu(x_j)dx_i dx_j. \tag{2.54}$$

Finally, we can write it on an anti-symmetric form

$$\langle \mu\nu|v|\mu\nu\rangle_{AS} = \langle \mu\nu|v|\mu\nu\rangle - \langle \mu\nu|v|\nu\mu\rangle\,, \tag{2.55}$$

meaning that we can write the expectation value of the interaction as a sum of alle the anti-symmetric matrix elements

$$\langle \Phi_{SD}|\,\hat{H}_1\,|\Phi_{SD}\rangle = E_{\text{interaction}} = \frac{1}{2}\sum_{\mu\nu}\langle \mu\nu|v|\mu\nu\rangle_{AS}\,. \tag{2.56}$$

2.8 The Variational Principle

The variational principle is a very powerful principle, useful when doing many-body quantum theory. It states that, if you have a system with the true many-body wave function $|\Psi\rangle$ and the exact energy

$$\langle \Psi|\,\hat{H}\,|\Psi\rangle = \epsilon_0, \tag{2.57}$$

then, any approximate wave function will produce a larger energy [4]

$$\langle \Phi|\,\hat{H}\,|\Phi\rangle \leq \epsilon_0. \tag{2.58}$$

Meaning that we can search for the wave function providing the lowest possible energy. This is the basis for many many-body methods, including Hartree-Fock theory or for example various Monte Carlo approaches.

Chapter 3

Second Quantization

This chapter is meant to introduce second quantization as an efficient formalism to handle complicated many-body states and their possible expectation values and transition probabilities. This formalism allows us represent states and operators in a much more complex and intuitive way, without integrals. This formalism is used in the remainder part of the thesis. The chapter also introduces a powerful toolbox for large calculations, the time-independent Wick's theorem. The last section, sets the groundwork for many-body methods introduced in chapters 5 and 6, by introducing quantities like the reference energy and the correlation energy, E_{ref} and ΔE. This chapter is based upon, and follows the material in *Many-Body Methods in Chemistry and Physics* by *Shavitt* and *Bartlett* [3].

3.1 Annihilation and Creation operators

We introduce a new way of writing states using the mathematical technique known as second quantization. The main goal is to treat states without paying attention to individual particle coordinates. We represent the empty space with the symbol for vacuum

$$|0\rangle \,. \tag{3.1}$$

To represent a state, we use a creation operator that will add the state to the vacuum

$$\hat{a}_i^\dagger \, |0\rangle = |\phi_i\rangle \,, \tag{3.2}$$

And the annihilation operator will remove the particle again

$$\hat{a}_i \left|\phi_i\right\rangle = \left|0\right\rangle . \tag{3.3}$$

Trying to add a new particle to an already filled state and removing an unoccupied state results in zero

$$\hat{a}_i^\dagger \left|\phi_i\right\rangle = 0, \qquad \hat{a}_i \left|0\right\rangle = 0. \tag{3.4}$$

Bra states are needed, and by looking at the adjoint of a ket state, we get

$$\left(\left|\phi_i\right\rangle\right)^\dagger = \left\langle\phi_i\right| , \tag{3.5}$$

which results in

$$\left(\hat{a}_i^\dagger \left|0\right\rangle\right)^\dagger = \left\langle 0\right| \hat{a}_i = \left\langle\phi_i\right| . \tag{3.6}$$

We see that the creation and annihilator operator are each other's adjoint operator. We can define the counting operator, $\hat{N}$, which will count how many states are occupied in a Slater determinant

$$\hat{N} = \sum_p \hat{a}_p^\dagger \hat{a}_p = \sum_p \hat{n}_p. \tag{3.7}$$

3.2 Strings of Operators

We can now construct the Slater determinant by working on vacuum with a string of creation operators

$$\hat{a}_1^\dagger \hat{a}_2^\dagger ... \hat{a}_N^\dagger \left|0\right\rangle = \left|\phi_1 \phi_2 ... \phi_N\right\rangle . \tag{3.8}$$

Permutations of the operators introduce a sign-change, which is equivalent to interchanging rows in the determinant. We need second quantization to respect the antisymmetrization condition, so a permutation of two states should introduce a sign change

$$\hat{a}_1^\dagger \hat{a}_2^\dagger \left|0\right\rangle = \left|\phi_1 \phi_2\right\rangle = - \left|\phi_2 \phi_1\right\rangle = -\hat{a}_2^\dagger \hat{a}_1^\dagger \left|0\right\rangle . \tag{3.9}$$

We introduce the permutation operator, $\hat{P}$, which permutes two states in the Slater determinant

$$\hat{P}\left|\Phi\right\rangle = (-1)^{\sigma(P)}\left|\Phi\right\rangle, \tag{3.10}$$

where $\sigma(P)$ counts how many times the states are interchanged. Demonstrated with creation operators

$$\hat{a}_1^\dagger\hat{a}_2^\dagger...\hat{a}_i^\dagger\hat{a}_j^\dagger...\hat{a}_n^\dagger = -\hat{a}_1^\dagger\hat{a}_2^\dagger...\hat{a}_j^\dagger\hat{a}_i^\dagger...\hat{a}_n^\dagger. \tag{3.11}$$

3.3 Anticommutator Relations

When working on strings of operators, it is very convenient to introduce anti-commutator relations. We define the relation as

$$\{\hat{A},\hat{B}\} = \hat{A}\hat{B} + \hat{B}\hat{A}. \tag{3.12}$$

By inserting the annihilation and creation operator, we can compute the relations and look at how they work on the vacuum state

$$\{\hat{a}_i^\dagger\hat{a}_j\}\left|0\right\rangle = \hat{a}_i^\dagger\hat{a}_j\left|0\right\rangle + \hat{a}_j\hat{a}_i^\dagger\left|0\right\rangle = 0 + \delta_{ij}\left|0\right\rangle, \tag{3.13}$$

where we have introduced the kroenecker-delta function

$$\delta_{ij} = \begin{cases} 1, & \text{if } i = j \\ 0, & \text{ij } i \neq j \end{cases}. \tag{3.14}$$

The second case gives

$$\{\hat{a}_i\hat{a}_j^\dagger\}\left|0\right\rangle = \hat{a}_i\hat{a}_j^\dagger + \hat{a}_j^\dagger\hat{a}_i\left|0\right\rangle = \delta_{ij}\left|0\right\rangle + 0. \tag{3.15}$$

And the two last cases will be zero

$$\{\hat{a}_i\hat{a}_j\}\left|0\right\rangle = \hat{a}_i\hat{a}_j\left|0\right\rangle + \hat{a}_j\hat{a}_i\left|0\right\rangle = \hat{a}_i\hat{a}_j\left|0\right\rangle - \hat{a}_i\hat{a}_j\left|0\right\rangle = 0, \tag{3.16}$$

$$\{\hat{a}_i^\dagger\hat{a}_j^\dagger\}\left|0\right\rangle = \hat{a}_i^\dagger\hat{a}_j^\dagger\left|0\right\rangle + \hat{a}_j^\dagger\hat{a}_i^\dagger\left|0\right\rangle = \hat{a}_i^\dagger\hat{a}_j^\dagger\left|0\right\rangle - \hat{a}_i^\dagger\hat{a}_j^\dagger\left|0\right\rangle = 0. \tag{3.17}$$

Ending up with the final relations

$$\{\hat{a}_i \hat{a}_j\} = 0, \tag{3.18}$$
$$\{\hat{a}_i^\dagger \hat{a}_j^\dagger\} = 0, \tag{3.19}$$
$$\{\hat{a}_i^\dagger \hat{a}_j\} = \{\hat{a}_i \hat{a}_j^\dagger\} = \delta_{ij}. \tag{3.20}$$

The last result is very useful for rewriting strings of operators, since it allows us to rewrite a set of two operators as

$$\hat{a}_i^\dagger \hat{a}_j = \{\hat{a}_i^\dagger \hat{a}_j\} - \hat{a}_j \hat{a}_i^\dagger = \delta_{ij} - \hat{a}_j \hat{a}_i^\dagger, \tag{3.21}$$

which will be at the center of Wick's theorem.

3.4 Inner products

We assume all states are orthonormal, taking the inner product of two states should give

$$\langle i|j\rangle = \delta_{ij}, \tag{3.22}$$

and for consistency, the vacuum state must also be normalized

$$\langle 0|0\rangle = 1. \tag{3.23}$$

This can be demonstrated by looking at the definition of the inner product for two equal states and using the anticommutator relations

$$1 = \langle i|i\rangle = \langle 0|\, \hat{a}_i \hat{a}_i^\dagger \,|0\rangle\,, \tag{3.24}$$
$$= \langle 0|\, (\delta_{ij} - \hat{a}_i^\dagger \hat{a}_i) \,|0\rangle\,, \tag{3.25}$$
$$= \langle 0|0\rangle - 0 = \langle 0|0\rangle\,. \tag{3.26}$$

It turns out we can use this exact scheme for longer chains of operators as well. Looking at the inner product of two general Slater determinants

$$|A\rangle = |a_1 a_2 ... a_N\rangle = \hat{a}_1^\dagger \hat{a}_2^\dagger ... \hat{a}_N^\dagger \,|0\rangle\,, \tag{3.27}$$
$$|B\rangle = |b_1 b_2 ... b_N\rangle = \hat{b}_1^\dagger \hat{b}_2^\dagger ... \hat{b}_N^\dagger \,|0\rangle\,. \tag{3.28}$$

Writing the inner product of $|A\rangle$ and $|B\rangle$

$$\langle A|B\rangle = \langle 0|\, \hat{a}_N ... \hat{a}_2 \hat{a}_1 \hat{b}_1^\dagger \hat{b}_2^\dagger ... \hat{b}_N^\dagger \,|0\rangle\,. \tag{3.29}$$

By moving the annihilation operators all the way to the right, we know that the inner product becomes zero because $\hat{a}_p |0\rangle = 0$. We utilize the anticommutator relations for interchanging creation and annihilation operators shown in (3.21). By first moving a_1 to the right, we get two possible outcomes:

1. One b_p is equal to a_1 and we get

$$\hat{a}_1 \hat{b}_p^\dagger = \delta_{a_1,b_p} - \hat{b}_p^\dagger \hat{a}_1 = 1 - \hat{b}_p^\dagger \hat{a}_1. \tag{3.30}$$

   This will now give us a new and shorter inner product

$$\langle A|B\rangle = \langle 0| \hat{a}_N ... \hat{a}_2 \hat{b}_1^\dagger ... \hat{b}_{p-1}^\dagger \hat{b}_{p+1}^\dagger ... \hat{b}_N^\dagger |0\rangle (-1)^{p-1} - \langle 0| \hat{a}_N ... \hat{a}_2 \hat{b}_1^\dagger \hat{b}_2^\dagger ... \hat{b}_N^\dagger \hat{a}_1 |0\rangle , \tag{3.31}$$

   where the last term will vanish because of $\hat{a}_1 |0\rangle = 0$. Notice the sign factor coming from $(-1)^{p-1}$. This is due to interchanging creation operators when moving $\hat{b}_p^\dagger$ from position p and $(p-1)$ steps to the left before using (3.30).

2. No b_p is equal to a_1 and all $\delta_{a_1,b_p} = 0$. Applying the same logic as for outcome 1, we get

$$\langle A|B\rangle = 0. \tag{3.32}$$

We do the same for all states and see that this inner product can only be non-zero if all states $a_1..a_N$ have matching states in $b_1..b_N$ and vice versa. If the ordering of states is different, a permutation factor $-1^{\sigma(P)}$ is included.

3.5 Representation of Operators

Consider a symmetric one-body operator represented by a sum of single-particle operators

$$\hat{F} = \sum_{\mu=1}^{N} \hat{f}_\mu \tag{3.33}$$

The number μ tells us on which particle $\hat{F}$ works on. In this case, we are looking at a symmetric operator because it works identically on all particles. Looking at a matrix element of $\hat{F}$ put between two Slater determinants, we get the expectation value

$$\langle a_1 a_2 ... a_N| \hat{F} |b_1 b_2 ... b_N\rangle . \tag{3.34}$$

Written out as a sum over all single-particle operators, this expectation value becomes

$$\sum_{\mu} \langle a_1 a_2 ... a_N | \, \hat{f}_\mu \, | b_1 b_2 ... b_N \rangle \, . \tag{3.35}$$

3.5.1 One-Body Operator

In second quantization, a one-body operator is given as

$$\hat{F} = \sum_{pq} \langle p | \, \hat{f} \, | q \rangle \, \hat{a}_p^\dagger \hat{a}_q, \tag{3.36}$$

where the matrix element $\langle p | \, \hat{f} \, | q \rangle$ is determined on the nature of the operator $\hat{F}$. It is common to denote this matrix element as

$$\hat{F} = \sum_{pq} \langle p | \, \hat{f} \, | q \rangle \, \hat{a}_p^\dagger \hat{a}_q = \sum_{pq} f_{pq} \hat{a}_p^\dagger \hat{a}_q. \tag{3.37}$$

Doing calculations in many-body quantum mechanics, we are primarily interested in expectation values. It is therefore crucial that we develop a solid scheme for calculating these values. This can be done by for example looking at the following inner product between two Slater determinants R and P

$$\langle P | \, \hat{F} \, | R \rangle \, . \tag{3.38}$$

Inserting the definition of $\hat{F}$, we get the expectation value

$$\langle 0 | \, \hat{a}_M ... \hat{a}_s \hat{a}_r \left(\sum_{kl} f_{kl} \hat{a}_k^\dagger \hat{a}_l \right) \hat{a}_p^\dagger \hat{a}_q^\dagger ... \hat{a}_N^\dagger \, | 0 \rangle \, , \tag{3.39}$$

which can be rewritten as

$$\sum_{pq} f_{pq} \, \langle 0 | \, \hat{a}_M ... \hat{a}_s \hat{a}_r (\hat{a}_k^\dagger \hat{a}_l) \hat{a}_p^\dagger \hat{a}_q^\dagger ... \hat{a}_N^\dagger \, | 0 \rangle \, . \tag{3.40}$$

We apply the same logic we used in the section *3.4*, which provides us with three different outcomes for this expectation value

1. The states $p, q, ..., N$ are all identical to the states $r, s, ..., M$. This results

in

$$\langle P|\,\hat{F}\,|R\rangle = \sum_{k}^{N} f_{kk}(-1)^{\sigma(P)}, \tag{3.41}$$

where we have included a permutation factor in case the ordering of states is different in the two states.

2. If all states except one from each Slater determinant are equal, we get a *noncoincidence* [3]

$$(p = r),\ (s = q),\ ...,\ (n \neq m),\ ...,\ (N = N), \tag{3.42}$$

meaning that we can rewrite the expectation value as

$$\sum_{pq} f_{pq}\,\langle 0|\,\hat{a}_M ... \hat{a}_s \hat{a}_r (\hat{a}_k^\dagger \hat{a}_l) \hat{a}_p^\dagger \hat{a}_q^\dagger ... \hat{a}_N^\dagger\,|0\rangle = (-1)^{\sigma(P)} f_{mn}, \tag{3.43}$$

because the operators $\hat{a}_k^\dagger$ and $\hat{a}_l$ must be paired with the non-identical states m and n for us to be left with a orthogonal inner product.

3. If there is more than one noncoincidence, no contributions can survive, and the expectation value is

$$\langle P|\,\hat{F}\,|R\rangle = 0. \tag{3.44}$$

3.5.2 Two-body Operator

I have in this thesis only looked at Hamiltonians consisting of a maximum of two-body interactions. Because of this, I will need a formalism for a two-body operator as well. It is defined almost identically as the one-body operator. We write the general two-body operator as

$$\hat{G} = \frac{1}{2}\sum_{ijkl} \langle i(1)j(2)|\,g_{12}\,|k(1)l(2)\rangle\,\hat{a}_i^\dagger \hat{a}_j^\dagger \hat{a}_l \hat{a}_k, \tag{3.45}$$

where the numbers (1) and (2) show which particle occupies a give single-particle state. We are, as for the one-body operator, interested in how we can calculate expectation values for this operator. We take the inner product with the two

Slater determinants $|P\rangle$ and $|R\rangle$

$$\frac{1}{2}\sum_{ijkl}\langle i(1)j(2)|\, g_{12}\,|k(1)l(2)\rangle\,\langle 0|\,\hat{a}_M...\hat{a}_s\hat{a}_r(\hat{a}_i^\dagger\hat{a}_j^\dagger\hat{a}_l\hat{a}_k)\hat{a}_p^\dagger\hat{a}_q^\dagger...\hat{a}_N^\dagger\,|0\rangle\,. \tag{3.46}$$

There are three possible outcomes here as well

1. If there are none noncoincidences, and all states in SD $|P\rangle$ are equal to all states in SD $|R\rangle$, we get

$$\langle P|\,\hat{G}\,|R\rangle = \frac{1}{2}\sum_{p\in P}\sum_{q\in P}(\langle pq|\,\hat{g}\,|pq\rangle - \langle pq|\,\hat{g}\,|qp\rangle) = \frac{1}{2}\sum_{p\in P}\sum_{q\in P}\langle pq||pq\rangle\,, \tag{3.47}$$

   where it is useful to use the antisymmetric matrix element

$$\langle pq||pq\rangle = \langle pq|\,\hat{g}\,|pq\rangle - \langle pq|\,\hat{g}\,|qp\rangle\,. \tag{3.48}$$

2. If we have a single noncoincidence, where all states except one from each SD are perfectly identical, we get [3]

$$\langle P|\,\hat{G}\,|R\rangle = \sum_{q\in P}\langle p'q||pq\rangle\,, \tag{3.49}$$

   where the states p' and p are the unequal states.

3. If we have two noncoincidences, we get

$$\langle P|\,\hat{G}\,|R\rangle = \langle p'q'||pq\rangle\,. \tag{3.50}$$

4. If more than two states from each SD are unequal, the expectation value will be 0.

3.5.3 The Hamiltonian

We can now write our Hamiltonian using second quantization. The Hamiltonian consists of a one-body and a two-body term

$$\hat{H} = \hat{H}_1 + \hat{H}_2, \tag{3.51}$$

which can be written out as

$$\hat{H}_1 = \sum_{\mu} \hat{h}_\mu, \qquad \hat{H}_2 = \sum_{\mu<\nu} \hat{v}_{\mu\nu}. \tag{3.52}$$

Using atomic units, we can write this as

$$\hat{h}_\mu = -\frac{1}{2}\nabla_\mu^2 - \sum_A \frac{Z_A}{r_{\mu A}}, \qquad \hat{v}_{\mu\nu} = \frac{1}{r_{\mu\nu}}. \tag{3.53}$$

Using the formalism of second quantization, we can write the Hamiltonian as

$$\hat{H} = \hat{H}_1 + \hat{H}_2 = \sum_{ij} \langle i|\, \hat{h}\, |j\rangle\, \hat{a}_i^\dagger \hat{a}_j + \frac{1}{4}\sum_{ijkl} \langle ij||kl\rangle\, \hat{a}_i^\dagger \hat{a}_j^\dagger \hat{a}_l \hat{a}_k, \tag{3.54}$$

where we have used the anti-symmetric form of the two-body operator

$$\langle ij||kl\rangle = \langle i(1)j(2)|\, \hat{v}_{12}\, |k(1)l(2)\rangle - \langle i(1)j(2)|\, \hat{v}_{12}\, |l(1)k(2)\rangle\,. \tag{3.55}$$

3.6 Normal Ordering and Wick's Theorem

As one can see, calculations of inner products can be a tedious affair when utilizing the anticommutator rules. Luckily, one can develop more powerful tools, namely Wick's theorem. Before introducing Wick's theorem, a definition of normal ordering and contractions are needed.

3.6.1 Normal Ordering

As previously shown, when evaluating a string of operators, the general scheme is to place all annihilation operators to the right of creation operators. This is because, when working on the true vacuum state, annihilation operators give zero. The only non-zero results will then arize from kroenecker delta's when permutating creation-annihilation operators according to equation (3.21).

A string of operators with all annihilation operators to the right will be referred to as a *normal ordered* string of operators. Normal ordering of operators

is commonly denoted by a curvy bracket or square bracket

$$n[\hat{A}\hat{B}...\hat{N}] = \{\hat{A}\hat{B}...\hat{N}\}. \tag{3.56}$$

Any expectation value, with respect to the true vacuum, of a set of normal ordered operators will always be zero:

$$\langle 0| \{\hat{A}\hat{B}...\hat{N}\} |0\rangle = 0. \tag{3.57}$$

One can note that the Hamiltonian operator is already written in a *normal ordered* form.

3.6.2 Contractions

The second tool needed for Wick's theorem is the definition of so-called *contractions* of operators. We define the contraction of general creation and annihilation operators as

$$\hat{A}\hat{B} \equiv \hat{A}\hat{B} - \{\hat{A}\hat{B}\}. \tag{3.58}$$

Taking the expectation value of the two operators with respect to the true vacuum, provides the contractions

$$\hat{a}_a^\dagger \hat{a}_b^\dagger = \hat{a}_a \hat{a}_b = \hat{a}_a^\dagger \hat{a}_b = 0. \tag{3.59}$$

The only non-zero results will be for

$$\hat{a}_a \hat{a}_b^\dagger = \delta_{ab}. \tag{3.60}$$

3.6.3 Time-independent Wick's theorem

Wick's theorem states: *A product of a string of creation and annihilation operators is equal to their normal product plus the sum of all possible normal ordered contractions* [3]. Symbolically, this is shown by

$$\hat{A}\hat{B}\hat{C}\hat{D}... = \{\hat{A}\hat{B}\hat{C}\hat{D}...\} + \sum \{\hat{A}\hat{B}\hat{C}\hat{D}....\}. \tag{3.61}$$

The usefulness of this relation is when calculating expectation values. Because of (3.57), the only result that will give a non-zero result, is when all operators are fully contracted. As an example to display the usefulness of Wick's theorem

$$\langle 0|\, \hat{a}_a\hat{a}_b^\dagger\hat{a}_c\hat{a}_d^\dagger\hat{a}_e\hat{a}_f^\dagger\, |0\rangle = \langle 0|\, \{\hat{a}_{\underbrace{a}}\hat{a}_{\underbrace{b}}^\dagger\hat{a}_{\underbrace{c}}\hat{a}_{\underbrace{d}}^\dagger\hat{a}_{\underbrace{e}}\hat{a}_{\underbrace{f}}^\dagger\}\, |0\rangle = \delta_{ab}\delta_{cd}\delta_{ef}, \tag{3.62}$$

where the contractions displayed are the only possible non-zero contractions.

3.7 Particle-Hole Formulation

For larger Slater determinants, it is tedious to write all states in terms of the vacuum state $|0\rangle$. We define a reference state that will be used instead of the pure vacuum. Looking at a general Slater determinant

$$|\Phi_0\rangle = \hat{a}_i^\dagger\hat{a}_j^\dagger ... \hat{a}_n^\dagger\, |0\rangle\,. \tag{3.63}$$

If this Slater determinant is the ground state of our system, we can use it as a reference state. We define the highest lying occupied state as the Fermi level, and name all states above the Fermi level *particle states* or *virtual states*. If a state below the Fermi level is vacant, we name it a *hole state*. Hereafter in this thesis, we will use a distinct naming pattern for indices. Indices using the latin alphabet using letters $i, j, k, l, ...$ are reserved for *hole states*. Latin letters $a, b, c, d, ...$ are reserved for *particle states*. Sometimes, we want to name more general states that can take the form of either a *hole state* or a *particle state*. We use the latin letters $p, q, r, s, ...$ For a more convenient way of writing, operators will be written on a shorter and more convenient form

$$\hat{a}_a = \hat{a} \quad \hat{a}_b^\dagger = \hat{b}^\dagger \quad \hat{a}_i^\dagger = \hat{i}^\dagger \quad ..., \tag{3.64}$$

and so forth. The reference state will be written as

$$|\Phi_0\rangle = \hat{i}^\dagger\hat{j}^\dagger\hat{k}^\dagger ... \hat{n}^\dagger\, |\rangle = |ijk...n\rangle = |\rangle\,, \tag{3.65}$$

and excitations will be written as

$$\text{Single Excitation:} \quad |\Phi_i^a\rangle = |ajk...n\rangle = \hat{i}\hat{a}^\dagger\, |\rangle\,, \tag{3.66}$$

$$\text{Double Excitation:} \quad \left|\Phi_{ij}^{ab}\right\rangle = |abk...n\rangle = \hat{i}\hat{j}\hat{a}^\dagger\hat{b}^\dagger\, |\rangle\,, \tag{3.67}$$

where the use of annihilation operators for *hole states* no longer produce zero when used on the reference state, but simply remove one particle from the refer-

ence state and create a *hole state*:

$$\hat{a}_i \left|\right\rangle = \left|\Phi_i\right\rangle = \left|jk...n\right\rangle . \tag{3.68}$$

This will introduce a small change in Wick's theorem, as the only non-zero contractions are now

$$\hat{i}^\dagger \hat{j} = \delta_{ij}, \tag{3.69}$$

and

$$\hat{a}\hat{b}^\dagger = \delta_{ab}. \tag{3.70}$$

Contractions relative to the Fermi vacuum will now be denoted by brackets *above* the operators instead of below. Apart from this, Wick's theorem is unchanged relative to the Fermi vacuum.

A very important property of the reference state, is the expectation value for the Hamiltonian:

$$\left\langle\right| \hat{H} \left|\right\rangle = \left\langle\Phi_0\right| \hat{H} \left|\Phi_0\right\rangle = \left\langle ijk...n\right| \hat{H} \left|ijk...n\right\rangle . \tag{3.71}$$

We name this the reference Energy. The result is given by [3]

$$E_{\text{ref}} = \left\langle\Phi_0\right| \hat{H} \left|\Phi_0\right\rangle = \sum_i h_{ii} + \frac{1}{2} \sum_{ij} \left\langle ij||ij\right\rangle . \tag{3.72}$$

3.8 Normal ordering of Operators

After defining the new vacuum, we will now write the operators on a normal-ordered form, which will now work with respect to the reference state.

3.8.1 One-Body Operator

Consider a general one-body operator

$$\hat{F} = \sum_{pq} \left\langle p\right| \hat{f} \left|q\right\rangle \hat{p}^\dagger \hat{q}. \tag{3.73}$$

Using Wick's theorem to rewrite the string of operators

$$\hat{p}^\dagger \hat{q} = \{\hat{p}^\dagger \hat{q}\} + \hat{p}^\dagger \hat{q}, \tag{3.74}$$

we get

$$\hat{F} = \sum_{pq} \langle p| \hat{f} |q\rangle \{\hat{p}^\dagger \hat{q}\} + \sum_i \langle i| \hat{f} |i\rangle , \tag{3.75}$$

$$= \hat{F}_N + \sum_i \langle i| \hat{f} |j\rangle . \tag{3.76}$$

We notice that since

$$\langle\, |\hat{F}_N|\, \rangle = 0 \quad \rightarrow \quad \sum_i \langle i| \hat{f} |i\rangle = \langle\, |\hat{F}|\, \rangle , \tag{3.77}$$

we can rewrite the equation as

$$\hat{F} = F_N + \langle\, |\hat{F}|\, \rangle . \tag{3.78}$$

Meaning that F_N represent the difference between $\hat{F}$ and the Fermi expectation value.

3.8.2 Two-Body operators

Consider a general two-body operator, given by

$$\hat{G} = \frac{1}{4} \sum_{pqrs} \langle pq|\hat{g}|rs\rangle_A \, \hat{p}^\dagger \hat{q}^\dagger \hat{s} \hat{r} \tag{3.79}$$

As we did for the one-body operator, we want to use Wick's theorem to find an expression for the normal-ordered two-body operator. Although the method will be identical for the two-body operator as for the one-body operator, we will require a much larger sum over all possible contractions when using Wick's theorem. The calculations, using Wick's theorem can be viewed in [3]. The results are presented as

$$\hat{G} = \frac{1}{4} \sum_{pqrs} \langle pq|\hat{g}|rs\rangle_A \{\hat{p}^\dagger \hat{q}^\dagger \hat{s} \hat{r}\} + \sum_{ipq} \langle pi|\hat{g}|qi\rangle_A \{\hat{p}^\dagger \hat{q}\} + \frac{1}{2} \sum_{ij} \langle ij|\hat{g}|ij\rangle_A . \tag{3.80}$$

As we did for the one-body operator, we will rename the terms for the two-body operator. Starting with the reference part, we get

$$\langle\ |\hat{G}|\ \rangle = \frac{1}{2}\sum_{ij}\langle ij|\hat{g}|ij\rangle_A\,. \tag{3.81}$$

The normal ordered one-body term is labelled

$$\hat{G}'_N = \sum_{ipq}\langle pi|\hat{g}|qi\rangle_A\,\{\hat{p}^\dagger\hat{q}\}, \tag{3.82}$$

and the normal ordered two-body term is labelled

$$\hat{G}_N = \frac{1}{4}\sum_{pqrs}\langle pq|\hat{g}|rs\rangle_A\,\{\hat{p}^\dagger\hat{q}^\dagger\hat{s}\hat{r}\}. \tag{3.83}$$

We can now rewrite the two-body operator, $\hat{G}$ in terms of the respective normal ordered terms

$$\hat{G} = \hat{G}_N + \hat{G}'_N + \langle\ |\hat{G}|\ \rangle\,. \tag{3.84}$$

3.9 Partitioning the Hamiltonian Operator

The Hamiltonian has been shown to consist of a one-body and a two-body term

$$\hat{H} = \hat{H}_1 + \hat{H}_2. \tag{3.85}$$

One can, however, write it in terms of a zero-order term and a perturbation

$$\hat{H} = \hat{H}_0 + \hat{V}. \tag{3.86}$$

It is convenient to choose a zero-order Hamiltonian that is diagonal

$$\hat{H}_0 = \sum_p \epsilon_p \hat{p}^\dagger\hat{p}. \tag{3.87}$$

This means we can write the perturbation as

$$\hat{V} = (\hat{H}_1 - \hat{H}_0) + \hat{H}_2 \tag{3.88}$$

$$= \sum_{pq} (h_{pq} - \epsilon_p \delta_{pq}) \hat{p}^\dagger \hat{q} + \frac{1}{4} \langle pq||rs\rangle \, \hat{p}^\dagger \hat{q}^\dagger \hat{s} \hat{r}. \tag{3.89}$$

First, we define a Fock operator, $\hat{F}$, and a common practice is to choose the orbital energies as the diagonal elements of this Fock operator.

$$\hat{F} = \sum_{pq} f_{pq} \hat{p}^\dagger \hat{q}, \tag{3.90}$$

with the matrix element defined as

$$f_{pq} = h_{pq} + u_{pq}. \tag{3.91}$$

Here u_{pq} is the matrix element of a one-body operator $\hat{U}$. It is commonly implemented to simplify the zeroth-order term $\hat{H}_0$ and the normal ordering of the Hamiltonian. See (3.112). We define the operator $\hat{U}$ as

$$\hat{U} = \sum_{pq} u_{pq} \hat{p}^\dagger \hat{q}, \tag{3.92}$$

$$u_{pq} = \sum_{i} \langle pi||qi\rangle \, . \tag{3.93}$$

This means we can write $\hat{F} = \hat{H}_1 + \hat{U}$. Inserting the Fock operator into the perturbation

$$\hat{V} = \hat{F} - \hat{H}_0 - \hat{U} + \hat{H}_2 \tag{3.94}$$

$$= \sum_{pq} (f_{pq} - \epsilon_p \delta_{pq} - u_{pq}) \hat{p}^\dagger \hat{q} + \frac{1}{4} \sum_{pqrs} \langle pq||rs\rangle \, \hat{p}^\dagger \hat{q}^\dagger \hat{s} \hat{r}. \tag{3.95}$$

For a non-canonical Hartree-Fock case, the Fock matrix is diagonal, namely

$$f_{pq} = \epsilon_p \delta_{pq}. \tag{3.96}$$

This means the perturbation can be rewritten as

$$\hat{V} = -\sum_{pq} u_{pq} \hat{p}^\dagger \hat{q} + \frac{1}{4} \sum_{pqrs} \langle pq||rs\rangle \, \hat{p}^\dagger \hat{q}^\dagger \hat{s} \hat{r}, \tag{3.97}$$

with the zeroth-order energies given by

$$\hat{H}_0 = \sum_p \epsilon_p \hat{p}^\dagger \hat{p} \qquad \epsilon_p = h_{pp} + \sum_i \langle pi||pi\rangle \,. \tag{3.98}$$

The noncanonical case, the Fock operator, $\hat{F}$, is block diagonal, with $f_{ia} = 0$. To cancel out the single orbital energies from the perturbation, we split the Fock operator into a diagonal and an off-diagonal term

$$\hat{F} = \hat{F}^d + \hat{F}^o. \tag{3.99}$$

The diagonal term will now be canceled out, and we are left with the perturbation

$$\hat{V} = -\sum_{pq}(f^o_{pq} - u_{pq})\hat{p}^\dagger \hat{q} + \frac{1}{4}\sum_{pqrs}\langle pq||rs\rangle\, \hat{p}^\dagger \hat{q}^\dagger \hat{s}\hat{r}. \tag{3.100}$$

For convience, we can organize the perturbation into a one-body part and a two-body part, $\hat{V}_1$ and $\hat{V}_2$

$$\hat{V}_1 = \hat{F}^o - \hat{U} = \sum_{pq}(f^o_{pq} - u_{pq})\hat{p}^\dagger \hat{q}, \tag{3.101}$$

$$\hat{V}_2 = \hat{H}_2 = \frac{1}{4}\sum_{pqrs}\langle pq||rs\rangle\, \hat{p}^\dagger \hat{q}^\dagger \hat{s}\hat{r}. \tag{3.102}$$

Resulting in the Hamiltonian

$$\hat{H} = \hat{H}_0 + \hat{V}_1 + \hat{V}_2. \tag{3.103}$$

3.10 Normal Ordering of Hamiltonian

To sum it all up, I will now present a normal ordering of the partitioned Hamiltonian operator. Starting by applying Wick's theorem to the zeroth order term

$$(\hat{H}_0)_N = \hat{H}_0 - E^{(0)} = \sum_p \epsilon_p \hat{p}^\dagger \hat{p} - \sum_i e_i = \sum_p \epsilon_p \{\hat{p}^\dagger \hat{p}\}. \tag{3.104}$$

Then applying Wick's theorem to the one- and two-body perturbations given in equation 3.102, we get

$$\hat{V}_1 = (\hat{V}_1)_N + \langle\, |\hat{V}_1| \,\rangle\,, \tag{3.105}$$

where we have

$$(\hat{V}_1)_N = \hat{F}_N^o - \hat{U}_N = \sum_{pq} (f_{pq}^o - u_{pq})\{\hat{p}^\dagger \hat{q}\}, \tag{3.106}$$

and

$$\langle\, |\hat{V}_1|\, \rangle = -\sum_{ij} \langle ij||ij\rangle = -\langle\, |\hat{U}|\, \rangle\,. \tag{3.107}$$

Turning to the two-body perturbation and using the equation 3.80, we can write the two-body part as

$$\hat{V}_2 = (\hat{V}_2)_N + \hat{V}_N' + \langle\, |\hat{V}_2|\, \rangle\,, \tag{3.108}$$

where we have the following

$$(\hat{V}_2)_N = \frac{1}{4}\sum_{pqrs} \langle pq||rs\rangle\, \{\hat{p}^\dagger \hat{q}^\dagger \hat{s}\hat{r}\}, \tag{3.109}$$

$$V_N' = \sum_{pq} \langle pi||pi\rangle\, \{\hat{p}^\dagger \hat{q}\}, \tag{3.110}$$

$$\langle\, |\hat{V}_2|\, \rangle = \frac{1}{2}\sum_{ij} \langle ij||ij\rangle\,. \tag{3.111}$$

We notice now, that after normal ordering the operators, we are left with many terms that can be reorganized into zero-, one- and two-body parts. We can rewrite the total perturbation as

$$\hat{V} = \hat{F}_N^o - \hat{U}_N + \langle\, |\hat{V}_1|\, \rangle + (\hat{V}_2)_N + \hat{V}_N' + \langle\, |\hat{V}_2|\, \rangle\,. \tag{3.112}$$

Now, by construction of $\hat{U}$, we see that $\hat{U}$ and $\hat{V}_N'$ cancel each other out. Renaming $(\hat{V}_2)_N = \hat{W}_N$, we see that the terms left can be written as

$$\hat{V} = \hat{F}_N^o + \hat{W}_N + \langle\, |\hat{V}|\, \rangle\,. \tag{3.113}$$

By applying the same logic as earlier, we write

$$\hat{V}_N = \hat{V} - \langle\, |\hat{V}|\, \rangle\,, \tag{3.114}$$

so that we finally can write the normal ordered perturbation as

$$\hat{V}_N = \hat{F}_N^o + \hat{W}_N. \tag{3.115}$$

We notice here the use of the diagonal Fock matrix. This matrix is just zero in the canonical Hartree Fock case.

3.11 Correlation Energy

All the many-body quantum mechanics methods described in this thesis will aim to compute the correlation energy. We derive it by substracting

$$\langle\, |\hat{H}|\, \rangle = \langle\, |\hat{H}_0|\, \rangle + \langle\, |\hat{V}|\, \rangle\,, \tag{3.116}$$

from the partitioned hamiltonian $\hat{H} = \hat{H}_0 + \hat{V}$. Resulting in

$$\hat{H} - \langle\, |\hat{H}|\, \rangle = \hat{H}_0 - \langle\, |\hat{H}_0|\, \rangle + \hat{V} - \langle\, |\hat{V}|\, \rangle\,. \tag{3.117}$$

This can be rewritten in terms of normal ordered operators as

$$\hat{H}_N = (\hat{H}_0)_N + \hat{V}_N. \tag{3.118}$$

The Schrödinger equation for this operator is given as

$$\hat{H}_N \Psi = \Delta E \Psi, \tag{3.119}$$

where we have defined the computed energy as

$$\Delta E = E - E_{\text{ref}}, \tag{3.120}$$

or

$$E = E_{\text{ref}} + \Delta E. \tag{3.121}$$

This energy is named the correlation energy, and the goal of my thesis is to implement and compare different methods to compute this energy for different systems. The reference energy, given as

$$E_{\text{ref}} = \langle\, |\hat{H}_0|\, \rangle + \langle\, |\hat{V}|\, \rangle\,, \tag{3.122}$$

is easily computed when the basis is set up. Finally, we can set up the fully partitioned normal ordered Hamiltonian as

$$\hat{H}_N = \hat{F}_N^d + \hat{F}_N^o + \hat{W}_N. \tag{3.123}$$

Chapter 4

Diagramatic Representation

It can be quite cumbersome and error-prone to treat the manipulation of states and operators with second quantization [3]. The soon to be introduced many-body methods will include various sums over states. One can introduce a new formalism originated in quantum field theory in the form of Feynman diagrams to depict and list these sums. It is quite common to refer to these sums simply as *diagrams*.

4.1 The Slater determinant

We begin, as in second quantization, by setting up the Slater determinant. There is a time dependent direction on the diagrams going up. The actual times are irrelevant, but the sequence is important. The reference state, $|\,\rangle = |\Phi\rangle$, is depicted simply as a horizontal line

Figure 4.1: Diagram for the reference state $|\,\rangle$

While the hole states are represented by vertical lines either going up or down, particle and hole states are depicted by a vertical line. An arrow pointing up relates a particle state, while an arrow pointing down means a hole state. Depicting the two states $|\Phi^a\rangle$ and $|\Phi_i\rangle$

Figure 4.2: Diagrams for the addition of a particle and a hole state, $|\Phi^a\rangle$ and $|\Phi_i\rangle$ respectively

The ket-variant of the singly excited Slater determinant $\langle\Phi_i^a|$ can be drawn as

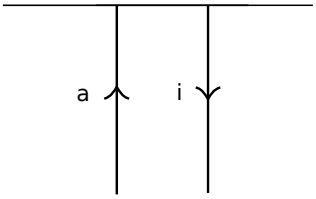

Figure 4.3: Diagram for the singly excited ket state $\langle\Phi_i^a|$

And the doubly excited states $\left|\Phi_{ij}^{ab}\right\rangle$ can be drawn as

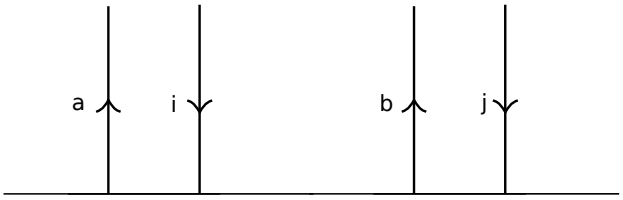

Figure 4.4: Diagram for the doubly excited bra state $\left|\Phi_{ij}^{ab}\right\rangle$

4.2 Operators

We need a convention for one-body operators as well. A general one-body operator is given by

$$\hat{F}_N = \sum_{pq} \langle p| \hat{f} |q\rangle \left\{\hat{p}^\dagger \hat{q}\right\}. \tag{4.1}$$

We will represent the matrix element $\langle p| \hat{f} |q\rangle$ by a dashed line, while there will be one line entering and one line leaving the operator due to the annihilation and creation operator. Because the operator behaves differently depending on whether the general operators p and q are virtual or occupied states, it can be written out as four different diagrams as shown in the figure below (adapted from [3])

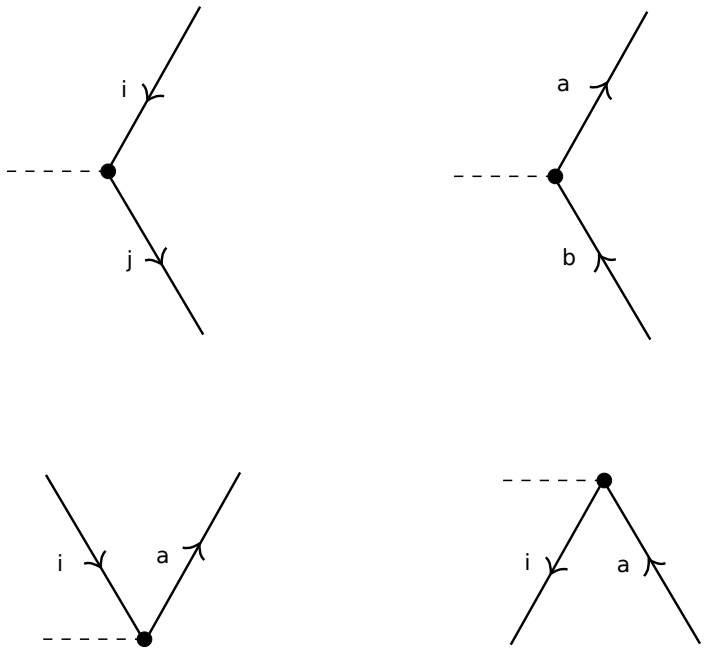

Figure 4.5: Diagrams for four different variants of the one-body operator. From left to right, the operators shown are $\sum_{ij} h_{ij} i^\dagger j$, $\sum_{ab} h_{ab} a^\dagger b$, $\sum_{ai} h_{ai} a^\dagger i$ and $\sum_{ai} h_{ia} i^\dagger a$

The same logic can be applied to the general two-body operator, given by

$$\hat{V}_N = \frac{1}{4}\sum_{pqrs} \langle pq||rs\rangle \left\{\hat{p}^\dagger\hat{q}^\dagger\hat{s}\hat{r}\right\}. \tag{4.2}$$

When we draw this diagram, one will need two outgoing lines representing the creation operators and two incoming lines, representing the annihilation operators. The matrix element will, as for the one-body operator, be drawn as a horizontal *interaction line*

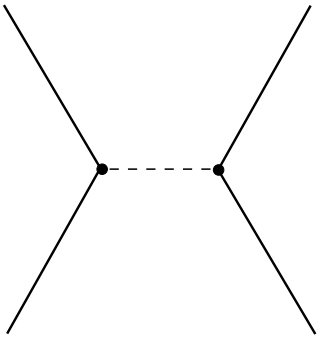

Figure 4.6: two-body operator, showing the horizontal line and four creation or annihilation operators

The left half side of the interaction will represent particle 1, while the right half will represent particle two. We can therefore set up the general relations for the term $\left\{\hat{p}^\dagger\hat{q}^\dagger\hat{s}\hat{r}\right\}$

$$\begin{aligned} \hat{p}^\dagger &\rightarrow \text{left outgoing line}, \quad \hat{q}^\dagger \rightarrow \text{right outgoing line}, \\ \hat{r} &\rightarrow \text{left incoming line}, \quad \hat{s} \rightarrow \text{right incoming line}. \end{aligned}$$

For the matrix element, we use the rules

$$\langle \text{left-out} \;\; \text{right-out} \;||\; \text{left-in} \;\; \text{right-in} \rangle. \tag{4.3}$$

There should be 16 combinations of particle- and hole-states distributed out between the operators $\hat{p}^\dagger$, $\hat{q}^\dagger$, $\hat{s}$ and $\hat{r}$, but since some diagrams will be equivalent, we are left with 9 distuingishable diagrams. The equivalent diagrams will be included by a weight factor 2.

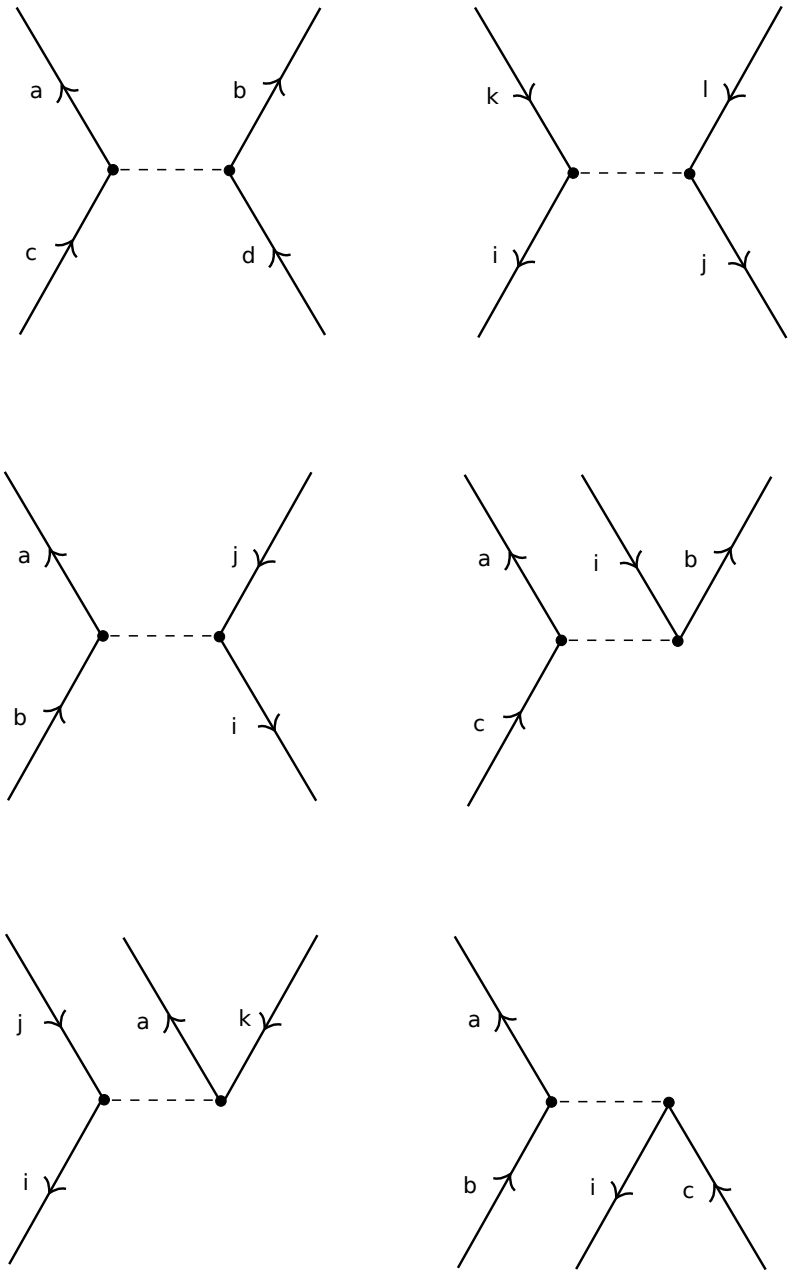

Figure 4.7: A figure showing 6 different Goldstone diagrams for the two-body operator. The matrix elements shown, from left to right, are: $\langle ab||cd\rangle$, $\langle ij||kl\rangle$, $\langle ai||bj\rangle$, $\langle ab||ci\rangle$, $\langle ia||jk\rangle$, $\langle ai||bc\rangle$.

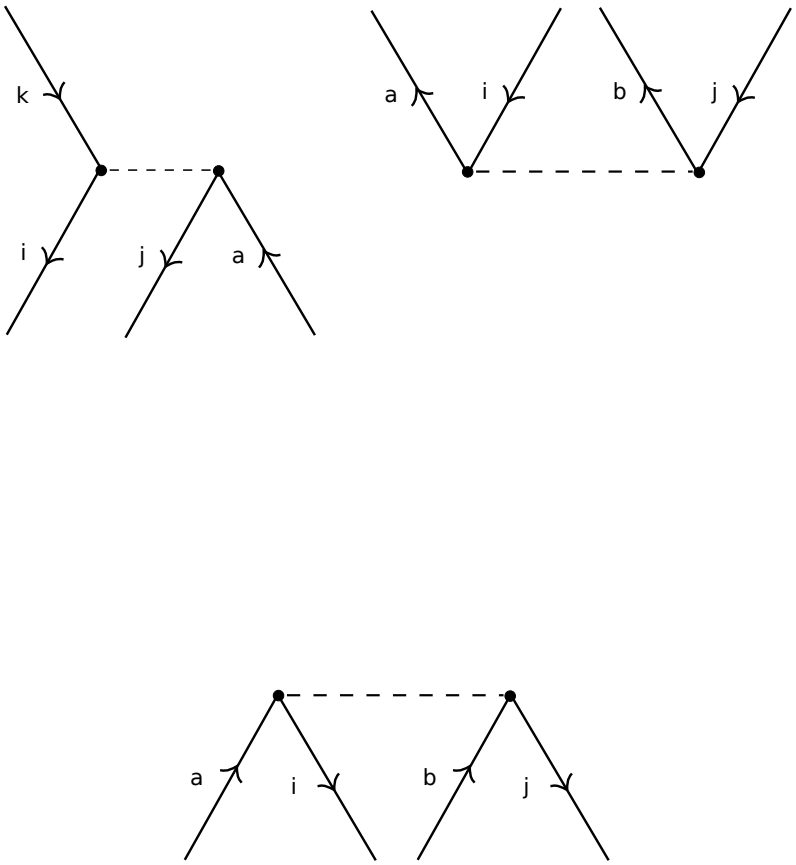

Figure 4.8: A figure showing 3 different Goldstone diagrams for the two-body operator. The matrix elements shown, from left to right, are: $\langle ij||ka\rangle$, $\langle ab||ij\rangle$, $\langle ij||ab\rangle$.

4.3 Contractions and Inner products

As seen, contractions are an important part of many-body methods. Representing contractions is easy when using a diagrammatic approach. It is done by connecting the lines between operators and Slater determinants. Let us for example consider the Slater determinant [2, 3]

$$|\Phi_i^a\rangle = \hat{a}^\dagger\hat{i}|\,\rangle\,, \tag{4.4}$$

and the general one-body operator

$$\hat{U} = \sum_{bc} \langle b|\hat{u}|c\rangle\,\{\hat{b}^\dagger\hat{c}\}. \tag{4.5}$$

When the operator $\hat{U}$ acts on the Slater determinant, the resulting Slater determinant will change

$$\hat{U}\,|\Phi_i^a\rangle = \sum_{bc} \langle b|\hat{u}|c\rangle\,\{\hat{b}^\dagger\hat{c}\}\{\hat{a}^\dagger\hat{i}\}|\,\rangle\,. \tag{4.6}$$

We can write this out using the generalized Wick's theorem, noticing that there is only one possible contraction that is non-zero.

$$= \langle b|\hat{u}|c\rangle\,\{\hat{b}^\dagger\hat{c}\hat{a}^\dagger\hat{i}\} + \langle b|\hat{u}|c\rangle\,\{\hat{b}^\dagger\overbrace{\hat{c}\hat{a}^\dagger}\hat{i}\} = 0 + \langle b|\hat{u}|c\rangle\,\delta_{ac}\left|\Phi_i^b\right\rangle, \tag{4.7}$$

which gives

$$\langle b|\hat{u}|a\rangle\,\{\hat{b}^\dagger\hat{i}\}|\,\rangle = \langle b|\hat{u}|a\rangle\left|\Phi_i^b\right\rangle \tag{4.8}$$

The diagrammatic representation of contractions are given in the following figure.

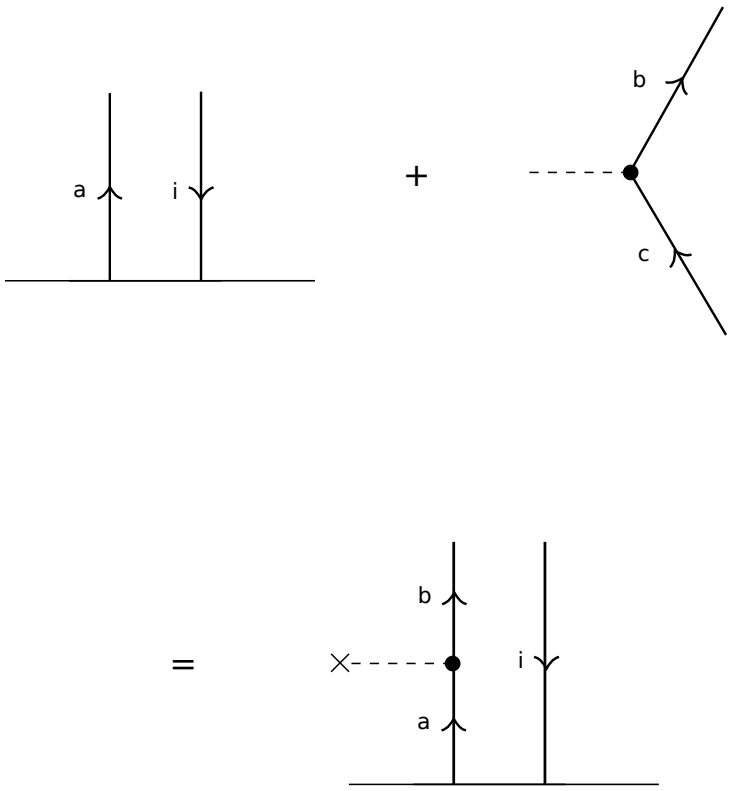

Figure 4.9: The diagrammatic representation of a contraction between the one-body operator and a singly excited Slater determinant.

Representing an inner product of two Slater determinants is done by putting together the diagram for a ket state and the diagram for a bra state. Looking at the previous example, taking the expectation value of the general operator $\hat{U}$, we get

$$\left\langle \Phi_k^d \right| \hat{U} \left| \Phi_i^a \right\rangle , \tag{4.9}$$

which can be written out as

$$\sum_{bj} \langle b|\hat{u}|c\rangle \left\langle \, |\{\hat{k}^\dagger \hat{d}\}\{\hat{b}^\dagger \hat{c}\}\{\hat{a}^\dagger \hat{i}\}| \, \right\rangle . \tag{4.10}$$

A calculating with the generalized Wick's theorem gives us the result

$$= \langle d|\hat{u}|a\rangle \, \delta_{db}\delta_{ac}\delta_{ki}. \tag{4.11}$$

The expectation are represented in the following figure.

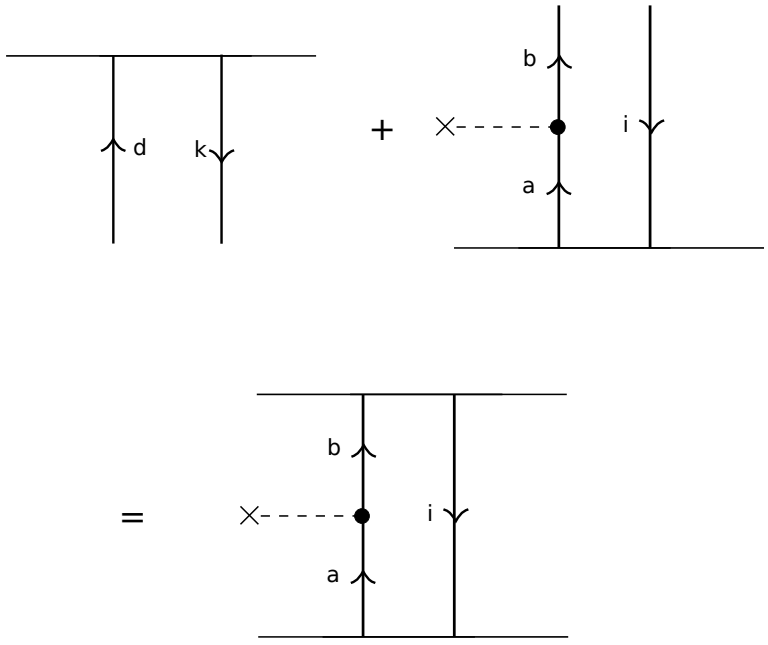

Figure 4.10: Diagrammatic representation of the inner product for a one-body operator between two singly excited Slater determinants.

4.4 Interpreting Diagrams

The many-body methods presented in this thesis rely heavily upon operator expressions and contractions. A common way to utilize the toolset presented in this chapter, is to give a visual representation of equations that are less prone to human errors. Using diagrams to perform contractions is by many considered to be more efficient than to perform calculations using Wick's theorem by hand.

An important part of using diagrams, is to have a consistent toolset to translate diagrams into mathematical expressions. These tools exist, see for example [3], and the implementation of perturbation theory for the pairing model pre-

sented in this thesis.

Chapter 5

Many-Body Methods

We define an ansatz for the ground state, $|\Phi_0\rangle$ as a Slater determinant consisting of the single-particle states, $|\phi_i\rangle$

$$|\Psi\rangle \approx |\Phi_0\rangle = \frac{1}{\sqrt{N!}} \begin{vmatrix} \phi_1(\mathbf{x}_1) & \phi_2(\mathbf{x}_1) & ... & \phi_N(\mathbf{x}_1) \\ \phi_1(\mathbf{x}_2) & \phi_2(\mathbf{x}_2) & ... & \phi_N(\mathbf{x}_2) \\ ... & & & \\ \phi_1(\mathbf{x}_N) & \phi_2(\mathbf{x}_N) & ... & \phi_N(\mathbf{x}_N), \end{vmatrix} \tag{5.1}$$

which can be rewritten using second quantization

$$|\Phi_0\rangle = \left(\prod_{i \leq F} \hat{i}^\dagger \right) |0\rangle = |\,\rangle\,. \tag{5.2}$$

Typically one chooses well-known and mathematically simple single-particle states that are easy to implement. In this thesis, I have used a free particle wave function as single-particle states for infinite matter. Using this basis, I obviously fail to incorporate the interaction between electrons since ϕ_1 remains unchanged if I also add ϕ_2. This can be solved by using a smarter basis, which is the goal of Hartree-Fock. Through an iterative method, the single-particle basis is modified so as to to get an improved representation of the ground state. This can be viewed as incorporating the interaction as a *mean field* approximation.

I will in this thesis present, and use, three *post Hartree-Fock* methods. These are *Full Configuration Interaction Theory*, *Many-Body Perturbation Theory* and *Coupled Cluster Theory*, where the latter is the main focus of my thesis. These methods aim to compute the *Correlation Energy* as presented in the chapter on Second Quantization. It is common to first implement the Hartree-Fock method, providing the most precise reference energy.

5.1 Full Configuration Interaction Theory

The first *Post Hartree-Fock* method to be presented is *Full Configuration Interaction theory*. We expand the true wave function as a linear combination of the ground state ansatz and all possible excitations

$$|\Psi\rangle = C_0 |\Phi_0\rangle + \sum_{ai} C_i^a |\Phi_i^a\rangle + \sum_{abij} C_{ij}^{ab} \left|\Phi_{ij}^{ab}\right\rangle + ..., \tag{5.3}$$

which can be rewritten in terms of a *correlation operator*

$$|\Psi\rangle = (C_0 + \hat{C}) |\Phi_0\rangle , \tag{5.4}$$

with

$$\hat{C} = \sum_{ai} C_i^a \hat{a}^\dagger \hat{i} + \sum_{abij} C_{ij}^{ab} \hat{a}^\dagger \hat{b}^\dagger \hat{j} \hat{i} + ... \tag{5.5}$$

We can name the terms such that

$$\hat{C} = \hat{C}_1 + \hat{C}_2 + ... \tag{5.6}$$

We use intermediate normalization, which gives us $C_0 = 1$, such that we get the relation

$$\langle \Psi | \Phi_0 \rangle = C_0 \langle \Phi_0 | \Phi_0 \rangle = 1. \tag{5.7}$$

We can now rewrite $|\Psi\rangle$

$$|\Psi\rangle = (1 + \hat{C}) |\Phi_0\rangle . \tag{5.8}$$

To simplify the notation, we can write the equation in terms of P and H, which symbolizes all possible chains of creation and annihilation operators

$$|\Psi\rangle = \sum_{PH} C_H^P \left|\Phi_H^P\right\rangle = \left(\sum_{PH} C_H^P \hat{A}_H^P \right) |\Phi_0\rangle . \tag{5.9}$$

We are working with orthonormal states, meaning that

$$\langle \Psi | \Psi \rangle = \sum_{PH} \left| C_H^P \right|^2 = 1. \tag{5.10}$$

The only thing left now, is defining how to compute the correlation energy. We write the expression for the energy as

$$E = \langle \Psi|\hat{H}|\Psi \rangle = \sum_{PHP'H'} (C_H^P)^* \langle \Phi_H^P|\hat{H}|\Phi_{H'}^{P'} \rangle C_{H'}^{P'}. \tag{5.11}$$

5.1.1 The Hamiltonian Matrix

We can build a Hamiltonian matrix consisting of all possible combinations of Slater determinants, i.e. all possible combinations of P, H and P', H'. The matrix elements will be the expectation value for the Hamiltonian, $\hat{\mathcal{H}}$, with respect to the given Slater determinants. The matrix is set up with the inner products of the following excited states

$$\begin{pmatrix} & 0p-0h & 1p-1h & 2p-2h & 3p-3h & 4p-4h & ... & Np-Nh \\ 0p-0h & x & x & x & 0 & 0 & 0 & 0 \\ 1p-1h & x & x & x & x & 0 & 0 & 0 \\ 2p-2h & x & x & x & x & x & \cdots & 0 \\ 3p-3h & 0 & x & x & x & x & \cdots & 0 \\ 4p-4h & 0 & 0 & x & x & x & \cdots & 0 \\ \vdots & 0 & 0 & \vdots & \vdots & \vdots & \ddots & \vdots \\ Np-Nh & 0 & 0 & 0 & 0 & 0 & \ldots & x \end{pmatrix}. \tag{5.12}$$

Above is an example of a general Hamiltonian matrix, $\mathcal{H}$, set up for an N-particles, N-holes, basis. One can notice that many matrix elements are zero. This is because the Hamiltonian only have a two-particle interaction term. If we have performed Hartree-Fock calculations, or start out with a Hartree-Fock basis, we have shifted the basis so that all matrix elements of the type

$$\langle 0p-0h|\,\hat{H}\,|1p-1h\rangle = \langle 1p-1h|\,\hat{H}\,|0p-0h\rangle = 0, \tag{5.13}$$

will be equal to zero. This gives a shifted Hamiltonian matrix, $\hat{\mathcal{H}}$, where the inner products are changed. The shifted matrix is given as

$$\begin{pmatrix} & 0p-0h & 1p-1h & 2p-2h & 3p-3h & 4p-4h & ... & Np-Nh \\ 0p-0h & \tilde{x} & 0 & \tilde{x} & 0 & 0 & 0 & 0 \\ 1p-1h & 0 & \tilde{x} & \tilde{x} & \tilde{x} & 0 & 0 & 0 \\ 2p-2h & \tilde{x} & \tilde{x} & \tilde{x} & \tilde{x} & \tilde{x} & \cdots & 0 \\ 3p-3h & 0 & \tilde{x} & \tilde{x} & \tilde{x} & \tilde{x} & \cdots & 0 \\ 4p-4h & 0 & 0 & \tilde{x} & \tilde{x} & \tilde{x} & \cdots & 0 \\ ... & 0 & 0 & \vdots & \vdots & \vdots & \ddots & \vdots \\ Np-Nh & 0 & 0 & 0 & 0 & 0 & \cdots & \tilde{x} \end{pmatrix} \tag{5.14}$$

To find the ground state correlation energy, the normal procedure is to diagonalize the Hamiltonian matrix through diagonalization algorithms. If we have a finite size Hilbert space, we can set up a finite Hamiltonian matrix which, when diagonalized, will provide us with the exact ground state correlation energy.

Unfortunatly, Full Configuration Interaction Theory is computationally costly. The Hamiltonian matrix will grow exponentially fast for large Hilbert spaces, which both increases the memory usage dramatically and increases the prosessing power associated with diagonalizing the matrix. For infinite and very large Hilbert spaces, one can truncate the number of excitations at some level to reduce the size of Hamiltonian matrix. I will later refer to this as just *Configuration Interaction theory*.

5.1.2 Computational cost

As an example on how costly full configuration interaction theory can be [22], we look at the oxygen nucleus. For a system consisting of N states and n particles, the total number of unique Slater determinants is given by

$$\binom{N}{n} = \frac{n!}{(n-N)!N!}. \tag{5.15}$$

Looking at the oxygen-16, we have 8 protons and 8 neutrons. If we only include the first major shells, we have a total of 40 states that the neutrons and protons can occupy [22]. Using equation (5.15)

$$\binom{40}{8} = \frac{40!}{32!8!} \approx 10^9, \tag{5.16}$$

for both the protons and the neutrons. Multiplying them together, we get

$$10^9 10^9 = 10^{18}, \tag{5.17}$$

Slater determinants for the whole system. This shows how fast the dimensionality explodes!

5.2 Many-body Perturbation Theory

Many-body perturbation theory presents a non-iterative approach to approximating the ground state energy. The approach is similar to previous methods. We start by splitting the Hamiltonian into a solvable part and a perturbation

$$\hat{H} = \hat{H}_0 + \hat{V}, \tag{5.18}$$

where we have chosen our basis such that

$$\hat{H}_0 |\Psi_0\rangle = W_0 |\Psi_0\rangle . \tag{5.19}$$

We also split the basis

$$|\Psi_0\rangle = |\Phi_0\rangle + \sum_i^\infty c_i |\phi_i\rangle . \tag{5.20}$$

Assuming intermediate normalization

$$\langle \Phi_0 | \Psi_0 \rangle = 1, \tag{5.21}$$

we can calculate the total exact energy

$$E = \langle \Phi_0 | \hat{H}_0 |\Psi_0\rangle + \langle \Phi_0 | \hat{V} |\Psi_0\rangle , \tag{5.22}$$

where we know that

$$\langle \Phi_0 | \hat{H}_0 |\Psi_0\rangle = W_0. \tag{5.23}$$

We get the correlation energy

$$E - W_0 = \Delta E = \langle \Phi_0 | \hat{V} |\Psi_0\rangle . \tag{5.24}$$

We will usually aim to compute the correlation energy, ΔE, when doing MBPT.

5.2.1 General derivation of Many-Body Particle Theory equations

Looking at the equation

$$\hat{V}\left|\Psi_0\right\rangle = \hat{H}\left|\Psi_0\right\rangle - \hat{H}_0\left|\Psi_0\right\rangle, \tag{5.25}$$

we reorganize and add the term $\omega\left|\Psi_0\right\rangle$ on both sides

$$\hat{V}\left|\Psi_0\right\rangle + \omega\left|\Psi_0\right\rangle - \hat{H}\left|\Psi_0\right\rangle = \omega\left|\Psi_0\right\rangle - \hat{H}_0\left|\Psi_0\right\rangle. \tag{5.26}$$

Remembering that $\hat{H}\left|\Psi_0\right\rangle = E\left|\Psi_0\right\rangle$, we get

$$\left|\Psi_0\right\rangle = \frac{\hat{V}+\omega-E}{\omega-\hat{H}_0}\left|\Psi_0\right\rangle. \tag{5.27}$$

Before continuing, we introduce the operators $\hat{P}$ and $\hat{Q}$, such that

$$\left|\Psi_0\right\rangle = \hat{P}\left|\Psi_0\right\rangle + \hat{Q}\left|\Psi_0\right\rangle = \left|\Phi_0\right\rangle\left\langle\Phi_0|\Psi_0\right\rangle + \sum_i \left|\Phi_i\right\rangle\left\langle\Phi_i|\Psi_0\right\rangle, \tag{5.28}$$

$$= \left|\Phi_0\right\rangle + \chi, \tag{5.29}$$

which gives

$$\left|\Phi_0\right\rangle = \hat{P}\left|\Psi_0\right\rangle \quad \chi = \hat{Q}\left|\Psi_0\right\rangle. \tag{5.30}$$

Using $\hat{R}(\omega) = \frac{\hat{Q}}{\left(\omega-\hat{H}_0\right)}$ and multiplying both sides with $\hat{Q}$ from the left in equation (5.27) we attain

$$\hat{Q}\left|\Psi_0\right\rangle = \hat{R}(\omega)\left(\hat{V}+\omega-E\right)\left|\Psi_0\right\rangle. \tag{5.31}$$

Using equations (5.28) and (5.30), we get

$$\left|\Psi_0\right\rangle = \left|\Phi_0\right\rangle + \hat{R}(\omega)\left(\hat{V}+\omega-E\right)\left|\Psi_0\right\rangle. \tag{5.32}$$

This sets up an iterative scheme, where we need to know $\left|\Psi_0\right\rangle$ before we can calculate $\left|\Psi_0\right\rangle$. We can substitute the state $\left|\Psi_0\right\rangle$ on the right hand side with the entire right hand side. This results in an infinite sum provided the series converges

$$\left|\Psi_0\right\rangle = \sum_0^\infty \left\{\hat{R}(\omega)(\hat{V}+\omega-E)\right\}^m \left|\Phi_0\right\rangle. \tag{5.33}$$

The right hand side does include the energy, E, which must be computed using $E = W_0 + \Delta E$, and

$$\Delta E = \langle \Phi_0 | \hat{V} | \Psi_0 \rangle = \sum_0^\infty \langle \Phi_0 | \hat{V} \left[\hat{R}(\omega)(\hat{V} - E + \omega) \right]^m | \Phi_0 \rangle . \tag{5.34}$$

5.2.2 Equations for Rayleigh-Schrödinger Perturbation Theory

We can interpret ω in different ways. I here present the Rayleigh-Schrödinger Perturbation Theory which postulates that

$$\omega = E_0^{(0)}, \tag{5.35}$$

such that we get the expression for the resolvent

$$\hat{R}_0 = \frac{\hat{Q}}{E_0^0 - \hat{H}_0}. \tag{5.36}$$

This gives the expression for $|\Psi_0\rangle$

$$|\Psi_0\rangle = \frac{\hat{V} - \Delta E}{\omega - \hat{H}_0} |\Psi_0\rangle , \tag{5.37}$$

and we get the final equation for the wave function

$$|\Psi_0\rangle = \sum_0^\infty \left\{ \hat{R}(\omega)(\hat{V} + -\Delta E) \right\}^m | \Phi_0 \rangle . \tag{5.38}$$

The correlation energy can be calculated by

$$\Delta E = \sum_0^\infty \langle \Phi_0 | \hat{V} \left[\hat{R}(\omega)(\hat{V} - \Delta E) \right]^m | \Phi_0 \rangle . \tag{5.39}$$

Taking a closer look at the energy-equations, we find that we can write the first orders as

$$
\begin{aligned}
E^{(1)} &= \langle\Phi_0|\,\hat{V}\,|\Phi_0\rangle = V_{00},\\
E^{(2)} &= \langle\Phi_0|\,\hat{V}\hat{R}_0\hat{V}\,|\Phi_0\rangle\,,\\
E^{(3)} &= \langle\Phi_0|\,\hat{V}\hat{R}_0(\hat{V}-E^{(1)})\hat{R}_0\hat{V}\,|\Phi_0\rangle\,,\\
E^{(4)} &= \langle\Phi_0|\,\hat{V}\hat{R}_0(\hat{V}-E^{(1)})\hat{R}_0(\hat{V}-E^{(1)})\hat{R}_0\hat{V}\,|\Phi_0\rangle - E^{(2)}\,\langle\Phi_0|\,\hat{V}\hat{R}_0^2\hat{V}\,|\Phi_0\rangle\,.
\end{aligned}
$$

Because of the frequent appearance, we can rewrite $\hat{V}-E^{(1)}$ as

$$
\hat{\Omega} = \hat{V} - E^{(1)} = \hat{V} - \langle\Phi_0|\,\hat{V}\,|\Phi_0\rangle\,. \tag{5.40}
$$

We name this new variable the wave operator, and rewrite the equations in a simpler form

$$
\begin{aligned}
E^{(1)} &= \langle\Phi_0|\,\hat{V}\,|\Phi_0\rangle = V_{00},\\
E^{(2)} &= \langle\Phi_0|\,\hat{V}\hat{R}_0\hat{V}\,|\Phi_0\rangle\,,\\
E^{(3)} &= \langle\Phi_0|\,\hat{V}\hat{R}_0\hat{\Omega}\hat{R}_0\hat{V}\,|\Phi_0\rangle\,,\\
E^{(4)} &= \langle\Phi_0|\,\hat{V}\hat{R}_0\hat{\Omega}\hat{R}_0\hat{\Omega}\hat{R}_0\hat{V}\,|\Phi_0\rangle - E^{(2)}\,\langle\Phi_0|\,\hat{V}\hat{R}_0^2\hat{V}\,|\Phi_0\rangle\,.
\end{aligned}
$$

I am, in this thesis, concerned with calculating the correlation energy, and these four equations will be implemented for the Pairing model.

5.3 Linked Diagram theorem

The linked diagram theorem is an important theorem, presented by Goldstone in 1957 [3, 10] which leads to the cancellation of all unlinked diagrams in Rayleigh-Schrödinger perturbation theory.

The theorem states that the wave function and the energy can be expressed as a sum of linked diagrams *only*, reducing the equations to

$$
E^{(n)} = \langle\ |\hat{W}(\hat{R}_0\hat{W})^{n-1}\ |\rangle_L\,, \tag{5.41}
$$

$$
\left|\Psi^{(n)}\right\rangle = \Big[(\hat{R}_0\hat{W})^n|\ \rangle\Big]_L\,. \tag{5.42}
$$

5.4 Hartree-Fock calculations

When doing Hartree-Fock calculation, we conduct a change of the basis, and instead of expanding our Hamiltonian, we vary the wave function to minimize the energy. We name the original basis by greek letters and the new basis by latin letters. The original basis should be chosen such that we can calculate its expectation value.

$$\langle \Phi_0 | \hat{H} | \Phi_0 \rangle = E^{\mathrm{HF}}. \tag{5.43}$$

The variational principle ensures that

$$E^{\mathrm{HF}} > 0. \tag{5.44}$$

We introduce a change of basis

$$|\psi_a\rangle = \sum_{\lambda} C_{a\lambda} |\psi_\lambda\rangle . \tag{5.45}$$

Varying $C_{p\lambda}$, we can search for the basis which yields the lowest energy. We start by rewriting E^{HF} as a functional

$$E[\psi] = \sum_{a=1}^{N} \langle a| h |a\rangle + \frac{1}{2} \sum_{ab}^{N} \langle ab| v |ab\rangle . \tag{5.46}$$

Rewriting it in terms of the original basis (greek letters), we get the energy functional given as

$$E[\psi] = \sum_{a=1}^{N} \sum_{\alpha\beta} C^*_{a\alpha} C_{a\beta} \langle \alpha| h |\beta\rangle + \frac{1}{2} \sum_{ab}^{N} \sum_{\alpha\beta\gamma\delta} C^*_{a\alpha} C^*_{b\beta} C_{a\gamma} C_{b\delta} \langle \alpha\beta| v |\gamma\delta\rangle . \tag{5.47}$$

To find the minima, we introduce a Lagrange multiplier before differentiating with respect to $C^*_{a\alpha}$. This will give N equations, one for each state a. The equations are given by

$$\sum_{\beta} C_{a\beta} \langle \alpha| h |\beta\rangle + \sum_{b}^{N} \sum_{\beta\gamma\delta} C^*_{b\beta} C_{b\delta} C_{a\gamma} \langle \alpha\beta| v |\gamma\delta\rangle = \epsilon_a C_{a\alpha}. \tag{5.48}$$

Defining

$$h^{\mathrm{HF}}_{\alpha\gamma} = \langle \alpha| h |\gamma\rangle + \sum_{b=1}^{N} \sum_{\beta\delta} C^*_{b\beta} C_{b\delta} \langle \alpha\beta| v |\gamma\delta\rangle , \tag{5.49}$$

we get the short hand iterative equations to be solved

$$\sum_{\gamma} h^{\mathrm{HF}}_{\alpha\gamma} C_{a\gamma} = \epsilon_a C_{a\alpha}. \tag{5.50}$$

A natural starting point for the constants, C, is to set

$$C_{a\lambda} = \delta_{a\lambda}, \tag{5.51}$$

which means that the first guess is to use the original greek basis.

Chapter 6

Coupled-Cluster Theory

Coupled-cluster theory is similar to full configuration interaction theory. Coupled-cluster theory is a post-Hartree-Fock method. The goal of Coupled-cluster theory is to improve the ansatz by including a set of excitations that can be summed to infinite order. Coester and Kümmel initially developed the ideas that led to the coupled-cluster theory in the late 1950's [23].

6.1 The Exponential Ansatz

The basic idea of Coupled-cluster theory is to express the true wave function as an exponential operator working on the Slater determinant [3, 23, 11]

$$|\Psi\rangle \approx e^{\hat{T}} |\Phi_0\rangle . \tag{6.1}$$

The operator $\hat{T}$, is a sum of the excitation operators, also known as cluster operators

$$\hat{T} = \hat{T}_1 + \hat{T}_2 + \hat{T}_3 + ... + \hat{T}_N, \tag{6.2}$$

where the operators are defined as

$$T_1 = \sum_{ia} t_i^a \hat{a}_a^\dagger \hat{a}_i, \tag{6.3}$$

$$T_2 = \frac{1}{2} \sum_{ijab} t_{ij}^{ab} \hat{a}_a^\dagger \hat{a}_b^\dagger \hat{a}_j \hat{a}_i, \tag{6.4}$$

$$T_N = \left(\frac{1}{n!}\right)^2 \sum_{ij..ab..}^{n} t_{ij..n}^{ab..n} \hat{a}_a^\dagger \hat{a}_b^\dagger ... \hat{a}_n^\dagger \hat{a}_n ... \hat{a}_j \hat{a}_i, \tag{6.5}$$

$$\tag{6.6}$$

which we will see is similar to configuration interaction theory.

6.2 Comparison with Configuration Interaction

By doing an expansion of the exponential operator, we can rewrite it as

$$e^{\hat{T}} = 1 + \hat{T} + \frac{\hat{T}^2}{2!} + \frac{\hat{T}^3}{3!} + \cdots . \tag{6.7}$$

Calculating the terms and organizing them in terms of total excitations, we can write the exponential operator as

$$e^{\hat{T}} = (1) + \left(\hat{T}_1\right) + \left(\hat{T}_2 + \frac{\hat{T}_1^2}{2}\right) + \left(\hat{T}_3 + \hat{T}_1\hat{T}_2 + \frac{\hat{T}_1^3}{6}\right) + \cdots . \tag{6.8}$$

Remembering the equation for configuration interaction, given by equation (5.8)

$$|\Psi_{CI}\rangle = (1 + \hat{C}) |\Phi_0\rangle ,$$

where

$$\hat{C} = \hat{C}_1 + \hat{C}_2 + ... = \sum_{ia} c_i^a a_a^\dagger a_i + \frac{1}{4} \sum_{ijab} c_{ij}^{ab} a_a^\dagger a_b^\dagger a_j a_i + ...$$

By comparing configuration interaction with coupled-cluster theory, we see that we can write

$$\hat{C}_0 = 1 \quad , \hat{C}_1 = \hat{T}_1, \tag{6.9}$$

$$\hat{C}_2 = \hat{T}_2 + \frac{1}{2}T_1^2, \tag{6.10}$$

and

$$\hat{C}_3 = \hat{T}_3 + \hat{T}_1\hat{T}_2 + \frac{\hat{T}_1^3}{6}. \tag{6.11}$$

The difference we notice, is that coupled-cluster introduces a mixing of excitation operators for every level of total excitations.

6.3 Truncating the Exponential Ansatz

By including infinite terms, this expansion will represent the true wave function, but the equations cannot be computed unless they are truncated at some point.

1. By including only $\hat{T} = \hat{T}_1$, we are doing coupled-cluster singles, short-handed by *CCS*

2. By truncating the equations at double excitations, $\hat{T} = \hat{T}_1 + \hat{T}_2$, we are doing coupled-cluster singles and doubles, with the short-hand given by *CCSD*

3. By truncating the equations at triple excitations, $\hat{T} = \hat{T}_1 + \hat{T}_2 + \hat{T}_3$, we are doing coupled-cluster singles, doubles and triples, *CCSDT*

4. four excitations are called quadruples, and so on

We introduce a new operator, $\overline{H}$, given by

$$\overline{H} = e^{-\hat{T}}\hat{H}e^{\hat{T}}. \tag{6.12}$$

When calculating the energy, we look at the expectation value for the Hamiltonian

$$\langle\Phi_0|\, e^{-\hat{T}}\hat{H}e^{\hat{T}}\,|\Phi_0\rangle = \langle\Phi_0|\,\overline{H}\,|\Phi_0\rangle = E. \tag{6.13}$$

By subsequent left-projection of various excited states, we get amplitude equations

$$\left\langle\Phi_{ij\cdots}^{ab\cdots}\right|\overline{H}\,|\Phi_0\rangle = 0. \tag{6.14}$$

We have now decoupled the amplitude equations from the energy equations, reducing the complexity of a coupled-cluster solver. The energy-equation is a function of the amplitudes $t_i, t_j, \cdots$ and $t_a, t_b, \cdots$, which can now be found through a different set of iterative equations. We have introduced the similarity transformed Hamiltonian, which can be significantly simplified using the Baker-Campbell-Hausdorff formula [11]

$$\begin{aligned}\overline{H} = e^{-\hat{T}}\hat{H}e^{\hat{T}} =& \hat{H} + [\hat{H},\hat{T}] + \frac{1}{2!}[[\hat{H},\hat{T}],\hat{T}] \\ &+\frac{1}{3!}[[[\hat{H},\hat{T}],\hat{T}],\hat{T}] + \frac{1}{4!}[[[[\hat{H},\hat{T}],\hat{T}],\hat{T}],\hat{T}] + \cdots.\end{aligned} \tag{6.15}$$

At first glance, this equation does not look like a simplification, but based on properties on the system, we can truncate this expansion. The cluster operators, $\hat{T}_1, \hat{T}_2, \hat{T}_3, \cdots$ commute with each other, but they do not generally commute with the Hamiltonian operator. Consider the general commutation of the one-body Hamiltonian and the T_1 cluster operator

$$[\hat{H}_0, \hat{T}_1] = [\hat{p}^\dagger\hat{q}, \hat{a}^\dagger\hat{i}] = \hat{p}^\dagger\hat{q}\hat{a}^\dagger\hat{i} - \hat{a}^\dagger\hat{i}\hat{p}^\dagger\hat{q}. \tag{6.16}$$

We can use the anti-commutator relations to rewrite two terms on the right-hand side

$$\hat{p}^\dagger\delta_{qa}\hat{i} - \hat{a}^\dagger\delta_{ip}\hat{q}. \tag{6.17}$$

Because p and q are summed over of all possible states, and are not limited to virtual or occupied states, we cannot explicitly state that the Kronecker delta functions δ_{qa} or δ_{ip} are either 0 or 1.

Because the cluster operators commute, to get a non-zero result, the Hamiltonian must create one Kronecker-delta function for each of the participating cluster operators. For every system in this thesis, we are only working with a two-body Hamiltonian, so a commutation with more than four cluster operators must provide zero. We will get a natural truncation, that holds for both the energy and amplitude equations. This is true for all systems that have a two-body Hamiltonian. We now write the similarity transformed Hamiltonian as

$$\begin{aligned}\overline{H} = e^{-\hat{T}}\hat{H}e^{\hat{T}} = \hat{H} + [\hat{H},\hat{T}] + \frac{1}{2!}[[\hat{H},\hat{T}],\hat{T}] + \frac{1}{3!}[[[\hat{H},\hat{T}],\hat{T}],\hat{T}] \\ + \frac{1}{4!}[[[[\hat{H},\hat{T}],\hat{T}],\hat{T}],\hat{T}].\end{aligned} \tag{6.18}$$

6.4 The Variational Principle

Using a variational method comes with great advantages. One can be sure to have calculated an upper boundary to the energy, but the coupled-cluster energy equation do not conform to any variational conditions [11]. However, the exponential ansatz does allow for another way of setting up the energy equation

$$E_{\text{exact}} \leq E = \frac{\langle \Phi_0 | \, (e^{\hat{T}})^\dagger \hat{H} e^{\hat{T}} \, | \Phi_0 \rangle}{\langle \Phi_0 | \, (e^{\hat{T}})^\dagger \hat{H} e^{\hat{T}} \, | \Phi_0 \rangle} = \frac{\langle \Psi | \, \hat{H} \, | \Psi \rangle}{\langle \Psi | \, \hat{H} \, | \Psi \rangle}, \tag{6.19}$$

which is variational. Unfortunately, one can not apply the same logic of natural truncation to the variational coupled-cluster energy.

6.5 Size-Extensivity

It can be important to have a wave function that scales with size. Imagine two particles, X and Y, with infinite separation, meaning that they do not interact. This means we should be able to write the total energy as

$$E = E_X + E_Y. \tag{6.20}$$

Rewriting the cluster operators in terms of the two particles

$$\hat{T} = \hat{T}_X + \hat{T}_Y, \tag{6.21}$$

the wave function can be rewritten as

$$|\Psi\rangle_{CC} = e^{\hat{T}_X + \hat{T}_Y} \, |\Phi_0\rangle = e^{\hat{T}_X} e^{\hat{T}_Y} \, |\Psi_0\rangle \, . \tag{6.22}$$

Since we can write the reference state as a product of the two separated parts, we are able to write

$$E_{CC} = E_{CC}^X + E_{CC}^Y. \tag{6.23}$$

For Configuration Interaction, multiplicative separability is not possible

$$\Psi_{CI} = \left(1 + \hat{C}\right) \Phi_0 = \left(1 + \hat{C}_x + \hat{C}_y\right) \Phi_0, \tag{6.24}$$

which cannot be rewritten as two separable parts. This means the coupled-cluster theory produces a *size-extensive* energy, contrary to full configuration interaction. A size-extensive system will scale perfectly with the size of the system, regardless

of the interaction between the particles.

6.6 The Coupled-Cluster Doubles Equations

We need to truncate the cluster operator, $\hat{T}$, and the approximation used in this thesis, is to only allow 2p-2h excitations. This is normally referred to as the coupled-cluster doubles equations, or CCD. We can rewrite the operator as [23]

$$\hat{T} \approx \hat{T}_2. \tag{6.25}$$

The wave function will be approximated by

$$|\Psi_0\rangle \approx |\Psi_{\text{CCD}}\rangle = e^{\hat{T}_2} |\Phi_0\rangle . \tag{6.26}$$

Inserting this ansatz into the Hamiltonian expectation value, we get

$$\langle\Phi_0| e^{-\hat{T}_2} \hat{H} e^{\hat{T}_2} |\Phi_0\rangle , \tag{6.27}$$

which will have the natural truncation at

$$\langle\Phi_0| \hat{H}(1 + \hat{T}_2) |\Phi_0\rangle = E_{\text{CCD}}. \tag{6.28}$$

This leads up to the energy equation

$$E_{\text{CCD}} = E_{\text{ref}} + \frac{1}{4} \sum_{abij} \langle ij|\hat{v}|ab\rangle \, t_{ij}^{ab}, \tag{6.29}$$

with the reference energy defined as

$$E_{ref} = \sum_i \langle i| \hat{h}_0 |j\rangle + \sum_{ij} \langle ij|\hat{v}|ij\rangle + \frac{1}{2} A v_0. \tag{6.30}$$

We have used v_0, which is a constant, nonzero for the finite electron gas. The second part of the energy, is known as the correlation energy. It is given by

$$\Delta E_{CCD} = \frac{1}{4} \sum_{ijab} \langle ij|\hat{v}|ab\rangle \, t_{ij}^{ab}. \tag{6.31}$$

The computation of this correlation energy is the goal of the coupled-cluster theory. This depends on the amplitudes t_{ij}^{ab} and we need the corresopnding amplitude

equations, found by

$$\left\langle \Phi_{ij}^{ab} \right| e^{-\hat{T}_2} \hat{H}_N e^{\hat{T}_2} \left| \Phi_0 \right\rangle = 0. \tag{6.32}$$

After several applications of Wick's theorem, the amplitude equations can be reduced to

$$\begin{aligned}(\epsilon_i + \epsilon_j - \epsilon_a - \epsilon_b) t_{ij}^{ab} &= \langle ab|\hat{v}|ij\rangle + \frac{1}{2}\sum_{cd} \langle ab|\hat{v}|cd\rangle \, t_{ij}^{cd} \\ &+ \frac{1}{2}\sum_{kl} \langle kl|\hat{v}|ij\rangle \, t_{kl}^{ab} + \hat{P}\,(ij|ab) \sum_{kc} \langle kb|\hat{v}|cj\rangle \, t_{ik}^{ac} \\ &+ \frac{1}{4}\sum_{klcd} \langle kl|\hat{v}|cd\rangle \, t_{ij}^{cd} t_{kl}^{ab} + \frac{1}{2}\hat{P}\,(ij|ab) \sum_{klcd} \langle kl|\hat{v}|cd\rangle \, t_{ik}^{ac} t_{lj}^{db} \\ &- \frac{1}{2}\hat{P}(ij) \sum_{klcd} \langle kl|\hat{v}|cd\rangle \, t_{ik}^{ab} t_{jl}^{cd} - \frac{1}{2}\hat{P}(ab) \sum_{klcd} \langle kl|\hat{v}|cd\rangle \, t_{kl}^{bd} t_{ij}^{ac},\end{aligned} \tag{6.33}$$

where we have defined

$$\hat{P}(ij) = 1 - \hat{P}_{ij}. \tag{6.34}$$

The permutation operator, $\hat{P}_{ij}$, interchanges the two particles occupying the quantum states i and j. Furthermore, we define the operator

$$\hat{P}\,(ij|ab) = (1 - \hat{P}_{ij})(1 - \hat{P}_{ab}). \tag{6.35}$$

We notice that some parts are linear in the amplitude, while some are quadratic. Sorting them into the linear and quadratic parts, L and Q respectably, I get

$$L(t_{ij}^{ab}) = \frac{1}{2}\sum_{cd} \langle ab|\hat{v}|cd\rangle \, t_{ij}^{cd} + \frac{1}{2}\sum_{kl} \langle kl|\hat{v}|ij\rangle \, t_{kl}^{ab} + \hat{P}\,(ij|ab) \sum_{kc} \langle kb|\hat{v}|cj\rangle \, t_{ik}^{ac}, \tag{6.36}$$

and

$$\begin{aligned}Q(t_{ij}^{ab} t_{ij}^{ab}) &= \frac{1}{4}\sum_{klcd} \langle kl|\hat{v}|cd\rangle \, t_{ij}^{cd} t_{kl}^{ab} + \frac{1}{2}\hat{P}\,(ij|ab) \sum_{klcd} \langle kl|\hat{v}|cd\rangle \, t_{ik}^{ac} t_{lj}^{db} \\ &- \frac{1}{2}\hat{P}(ij) \sum_{klcd} \langle kl|\hat{v}|cd\rangle \, t_{ik}^{ab} t_{jl}^{cd} - \frac{1}{2}\hat{P}(ab) \sum_{klcd} \langle kl|\hat{v}|cd\rangle \, t_{kl}^{bd} t_{ij}^{ac}.\end{aligned} \tag{6.37}$$

For practical reasons, I label each term

$$L_a = \frac{1}{2} \sum_{cd} \langle ab|\hat{v}|cd\rangle \, t_{ij}^{cd}, \tag{6.38}$$

$$L_b = \frac{1}{2} \sum_{kl} \langle kl|\hat{v}|ij\rangle \, t_{kl}^{ab}, \tag{6.39}$$

$$L_c = \hat{P}\,(ij|ab) \sum_{kc} \langle kb|\hat{v}|cj\rangle \, t_{ik}^{ac}, \tag{6.40}$$

$$Q_a = \frac{1}{4} \sum_{klcd} \langle kl|\hat{v}|cd\rangle \, t_{ij}^{cd} t_{kl}^{ab}, \tag{6.41}$$

$$Q_b = \frac{1}{2} \hat{P}\,(ij|ab) \sum_{klcd} \langle kl|\hat{v}|cd\rangle \, t_{ik}^{ac} t_{lj}^{db}, \tag{6.42}$$

$$Q_c = -\frac{1}{2} \hat{P}(ij) \sum_{klcd} \langle kl|\hat{v}|cd\rangle \, t_{ik}^{ab} t_{jl}^{cd}, \tag{6.43}$$

$$Q_d = -\frac{1}{2} \hat{P}(ab) \sum_{klcd} \langle kl|\hat{v}|cd\rangle \, t_{kl}^{bd} t_{ij}^{ac}. \tag{6.44}$$

6.7 Intermediates

As coupled-cluster computations consume large amounts of computational power, researchers are spending much effort trying to reduce computational cost. One way of reducing the cost is by refactoring the amplitude equations such that we can perform an intermediate computation first and use the result to compute various diagrams later.

Rewriting the equation, (6.34) for CCD amplitudes [1, 2]:

$$
\begin{aligned}
(\epsilon_i + \epsilon_j - \epsilon_a - \epsilon_b) t_{ij}^{ab} = \langle ab|\hat{v}|ij\rangle + \frac{1}{2}\sum_{cd} \langle ab|\hat{v}|cd\rangle\, t_{ij}^{cd} \\
+\frac{1}{2}\sum_{kl} t_{kl}^{ab} \left[\langle kl|\hat{v}|ij\rangle + \frac{1}{2}\sum_{cd} \langle kl|\hat{v}|cd\rangle\, t_{ij}^{cd} \right] \\
+\hat{P}\,(ij|ab) \sum_{kc} t_{ik}^{ac} \left[\langle kb|\hat{v}|cj\rangle + \frac{1}{2}\sum_{ld} \langle kl|\hat{v}|cd\rangle\, t_{lj}^{db} \right] \\
-\frac{1}{2}\hat{P}(ij) \sum_{k} t_{ik}^{ab} \left[\sum_{lcd} \langle kl|\hat{v}|cd\rangle\, t_{jl}^{cd} \right] \\
-\frac{1}{2}\hat{P}(ab) \sum_{c} t_{ij}^{ac} \left[\sum_{kld} \langle kl|\hat{v}|cd\rangle\, t_{kl}^{bd} \right].
\end{aligned}
\tag{6.45}
$$

We can now define, and precompute the following values

$$
I_1 = \langle kl|\hat{v}|ij\rangle + \frac{1}{2}\sum_{cd} \langle kl|\hat{v}|cd\rangle\, t_{ij}^{cd}, \tag{6.46}
$$

$$
I_2 = \langle kb|\hat{v}|cj\rangle + \frac{1}{2}\sum_{ld} \langle kl|\hat{v}|cd\rangle\, t_{lj}^{db}, \tag{6.47}
$$

$$
I_3 = \sum_{lcd} \langle kl|\hat{v}|cd\rangle\, t_{jl}^{cd}, \tag{6.48}
$$

$$
I_4 = \sum_{kld} \langle kl|\hat{v}|cd\rangle\, t_{kl}^{bd}. \tag{6.49}
$$

We can now redefine the CCD equation in terms of the intermediate factorizations,

$$
\begin{aligned}
(\epsilon_i + \epsilon_j - \epsilon_a - \epsilon_b) t_{ij}^{ab} = \langle ab|\hat{v}|ij\rangle + \frac{1}{2}\sum_{cd} \langle ab|\hat{v}|cd\rangle\, t_{ij}^{cd} + \frac{1}{2}\sum_{kl} t_{kl}^{ab} I_1 \\
+\hat{P}\,(ij|ab) \sum_{kc} t_{ik}^{ac} I_2 - \frac{1}{2}\hat{P}(ij) \sum_{k} t_{ik}^{ab} I_3 - \frac{1}{2}\hat{P}(ab) \sum_{c} t_{ij}^{ac} I_4
\end{aligned}
\tag{6.50}
$$

By doing the intermediate calculations, we can achieve a reduction of computational cost from $\mathcal{O}(h^4p^4)$ to $\mathcal{O}(h^4p^2)$, which is significant for large systems approaching the thermodynamic limit. However, storing the intermediate values will require a greater use of memory.

Chapter 7

The Pairing Model

The first system I looked at is the pairing model. I have implemented a pairing model consisting of four energy levels with degeneracy two, one for positive and negative spin. The system consists of four electrons where we fill up the four lower-most states below the Fermi level.

7.1 The Hamiltonian

We limit ourselves to a two-body interaction, writing the Hamiltonian as

$$\hat{H} = \sum_{\alpha\beta} \langle\alpha| \hat{h}_0 |\beta\rangle \hat{a}^\dagger_\alpha \hat{a}_\beta + \frac{1}{4} \sum_{\alpha\beta\gamma\delta} \langle\alpha\beta|\hat{v}_0|\gamma\delta\rangle \hat{a}^\dagger_\alpha \hat{a}^\dagger_\beta \hat{a}_\delta \hat{a}_\gamma. \tag{7.1}$$

We use the complete basis $|\alpha\rangle$ and define the set as eigenvalues of the one-body operator, $\hat{h}_0$.

The system does require that the total spin is equal to 0. In addition we will not allow spin pairs to be broken, i.e. singly excited states are not allowed.

$$|\Psi^a_i\rangle = 0. \tag{7.2}$$

We introduce the double creation operator, $\hat{P}^\dagger_{pq}$

$$\hat{P}^\dagger_{pq} = \hat{a}^\dagger_{p\sigma} \hat{a}^\dagger_{p-\sigma}, \tag{7.3}$$

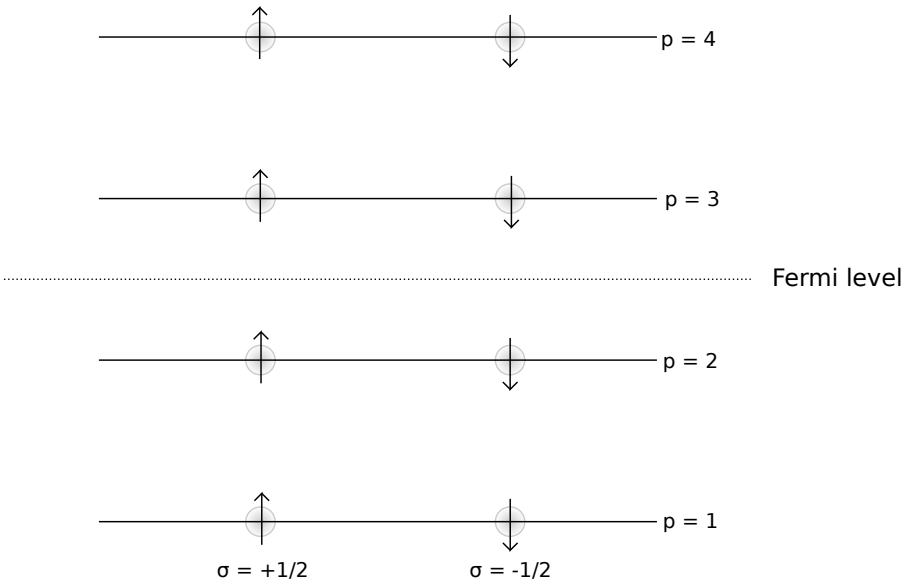

Figure 7.1: A figure depicting a 4 particles-4 holes state. The system consists of occupied particle states below the Fermi level and unoccupied hole states above Fermi level.

and the double annihilation operator, $\hat{P}_{pq}$

$$\hat{P}_{pq} = a_{q\sigma} a_{q-\sigma}. \tag{7.4}$$

We can rewrite the Hamiltonian as an unperturbed part and a perturbation

$$\hat{H} = \hat{H}_0 + \hat{V}, \tag{7.5}$$

Where the unperturbed part is given by

$$\hat{H}_0 = \xi \sum_{p\sigma} (p-1) \hat{a}^\dagger_{p\sigma} \hat{a}_{p\sigma}, \tag{7.6}$$

and the perturbation operator is given by

$$\hat{V} = -\frac{1}{2} g \sum_{pq} \hat{a}^\dagger_{p+} \hat{a}^\dagger_{p-} \hat{a}_{q-} \hat{a}_{q+}. \tag{7.7}$$

The value of ξ determines the spacing between the energy levels, which is set to

1 for the calculations in this thesis. This will not impact the insight attained solving this system. p and q determines the energy level. σ is the spin, with value either $+\frac{1}{2}$ or $-\frac{1}{2}$. Both the unperturbed and perturbed Hamiltonian keeps total spin at 0.

We can normal order the Hamiltonian by Wick's general theorem, which introduces the relations

$$a_p^\dagger a_q = \left\{a_p^\dagger a_q\right\} + \delta_{pq\in i}, \tag{7.8}$$

and

$$\begin{aligned} a_p^\dagger a_q^\dagger a_s a_r = \left\{a_p^\dagger a_q^\dagger a_s a_r\right\} + \left\{a_p^\dagger a_r\right\}\delta_{qs\in i} - \left\{a_p^\dagger a_s\right\}\delta_{qr\in i} \\ + \left\{a_q^\dagger a_s\right\}\delta_{pr\in i} \ - \left\{a_q^\dagger a_r\right\}\delta_{ps\in i} + \delta_{pr\in i}\delta_{qs\in i} - \delta_{ps\in i}\delta_{qr\in i}. \end{aligned} \tag{7.9}$$

The Hamiltonian can be written as a sum of the normal-ordered terms and the reference energy, as shown in equation (3.118). We have

$$\hat{H} = \hat{H}_N + E_{ref},$$

with the reference energy

$$E_{ref} = \sum_i h_{ii} + \frac{1}{2}\sum_{ij}\langle ij||ij\rangle\,. \tag{7.10}$$

We have defined the normal ordered Hamiltonian as

$$\hat{H}_N = \hat{F}_N + \hat{W}. \tag{7.11}$$

The one-body operator can be calculated as

$$\hat{F}_N = \sum_{pq} h_{pq}\left\{\hat{a}_{p\sigma}^\dagger \hat{a}_{p\sigma}\right\} - \sum_{pqi}\langle pi||qi\rangle\left\{\hat{a}_{p+}^\dagger \hat{a}_{q-}\right\}, \tag{7.12}$$

and the two-body operator

$$\hat{W} = -\frac{1}{2}\sum_{pqrs}\langle pq||rs\rangle\left\{\hat{a}_{p+}^\dagger \hat{a}_{p-}^\dagger \hat{a}_{q-}\hat{a}_{q+}\right\}. \tag{7.13}$$

7.2 Configuration Interaction theory

This system is a good way to benchmark various methods as we can compute the exact solution using Full Configuration Interaction.

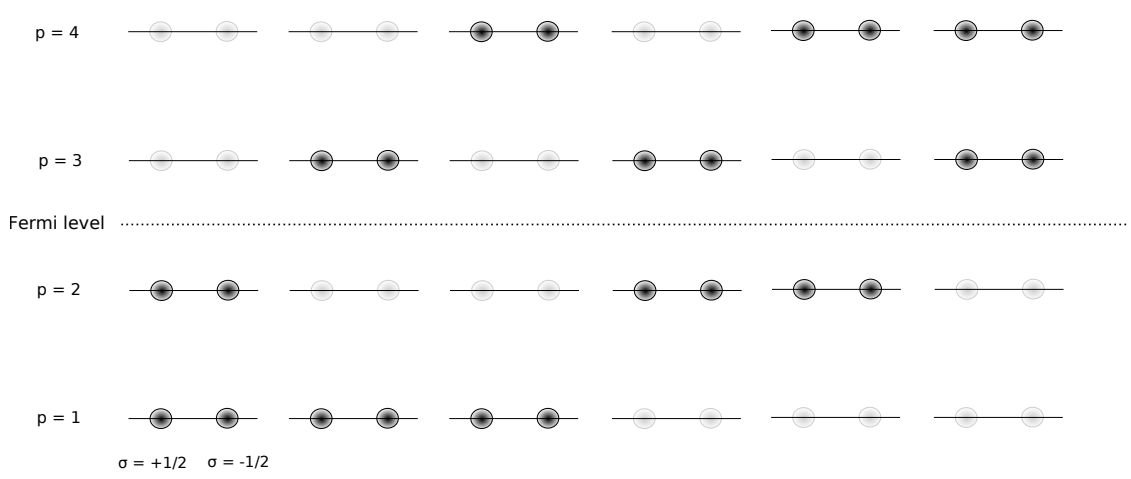

Figure 7.2: Configuration space for given pairing model showing all possible distributions of electrons

We need to diagonalize the Hamiltonian matrix, which is set up by calculating all the expectation values of all combination of states. The matrix elements will be set up as

$$\begin{pmatrix} & |\Phi_0\rangle & |\Phi_{12}^{56}\rangle & |\Phi_{12}^{78}\rangle & |\Phi_{34}^{56}\rangle & |\Phi_{34}^{78}\rangle & |\Phi_{1234}^{5678}\rangle \\ \langle\Phi_0| & & & & & & \\ \langle\Phi_{12}^{56}| & & & & & & \\ \langle\Phi_{12}^{78}| & & & & & & \\ \langle\Phi_{34}^{56}| & & & & & & \\ \langle\Phi_{34}^{78}| & & & & & & \\ \langle\Phi_{1234}^{5678}| & & & & & & \end{pmatrix}. \tag{7.14}$$

Excluding the 4p-4h excitations one does not diagonalize the exact matrix, but rather the approximated matrix known from Configuration Interaction. The diagonal elements are calculated using Wick's theorem. Looking first at the

ground state calculation with the unperturbed Hamiltonian part

$$\langle \Phi_0 | \, \hat{\mathbf{H}}_\mathbf{0} \, | \Phi_0 \rangle \, , \tag{7.15}$$

we rewrite the states with respect to the vacuum state, we get the first equation for $\hat{H}_0$

$$= \langle | \, a_{2\downarrow} a_{2\uparrow} a_{1\downarrow} a_{1\uparrow} \sum_{p\sigma} \delta(p-1) a^\dagger_{p\sigma} a_{p\sigma} a^\dagger_{1\uparrow} a^\dagger_{1\downarrow} a^\dagger_{2\uparrow} a^\dagger_{2\downarrow} \, | \rangle \, . \tag{7.16}$$

This expectation value can be contracted in four different ways, giving the final result

$$= 2\delta(1-1) + 2\delta(2-1) = 2\delta. \tag{7.17}$$

The perturbation part, given by the expectation value

$$\langle \Phi_0 | \, \hat{\mathbf{V}} \, | \Phi_0 \rangle \, , \tag{7.18}$$

written in terms of the vacuum state, this becomes

$$\langle | \, a_{2\downarrow} a_{2\uparrow} a_{1\downarrow} a_{1\uparrow} \left(-g/2 \sum_{pq} a^\dagger_{p\uparrow} a^\dagger_{q\downarrow} a_{q\downarrow} a_{p\uparrow} \right) a^\dagger_{1\uparrow} a^\dagger_{1\downarrow} a^\dagger_{2\uparrow} a^\dagger_{2\downarrow} \, | \rangle \, . \tag{7.19}$$

There are two ways this can contract, each contributing with the constant factor, $-g/2$. Performing similar calculations for all possible expectation values, will result in the final Hamiltonian matrix

$$\hat{\mathcal{H}} = \begin{pmatrix} 2\delta - g & -g/2 & -g/2 & -g/2 & -g/2 & 0 \\ -g/2 & 4\delta - g & -g/2 & -g/2 & 0 & -g/2 \\ -g/2 & -g/2 & 6\delta - g & 0 & -g/2 & -g/2 \\ -g/2 & -g/2 & 0 & 6\delta - g & -g/2 & -g/2 \\ -g/2 & 0 & -g/2 & -g/2 & 8\delta - g & -g/2 \\ 0 & -g/2 & -g/2 & -g/2 & -g/2 & 10\delta - g \end{pmatrix} . \tag{7.20}$$

Diagonalizing this, and finding the smallest eigenvalue, will produce the exact energy for the Pairing model.

7.3 Hartree-Fock calculations

When doing Hartree-Fock calculations on the pairing model, the goal is to minimize the Hamiltonian expectation value through a change in basis. The ground

state energy is given by

$$\langle \Phi_0 | \hat{H} | \Phi_0 \rangle = E^{\mathrm{HF}}. \tag{7.21}$$

This leads to the iterative equation

$$\sum_{\gamma} h^{\mathrm{HF}}_{\alpha\gamma} C_{a\gamma} = \epsilon_a C_{a\alpha}, \tag{7.22}$$

where

$$h^{\mathrm{HF}}_{\alpha\gamma} = \langle \alpha | h | \gamma \rangle + \sum_{b=1}^{N} \sum_{\beta\delta} C^*_{b\beta} C_{b\delta} \langle \alpha\beta | v | \gamma\delta \rangle . \tag{7.23}$$

For the first iteration, we must make a guess on the factors, $C^*_{b\beta}$ and $C_{b\delta}$. A natural starting point is to set

$$C_{b\beta} = \delta_{b\beta} \qquad C_{b\delta} = \delta_{b\delta}. \tag{7.24}$$

This is the same as using the original basis in the first iteration, as there is no overlap between the states

$$|\psi_a\rangle = \sum_{\lambda} \delta_{a\lambda} |\psi_\lambda\rangle . \tag{7.25}$$

To evaluate the Hartree-Fock matrix elements, we look at the states below Fermi level

$$\{p, \sigma\} \in \{1\uparrow, 1\downarrow, 2\uparrow, 2\downarrow\}. \tag{7.26}$$

The greek basis will therefore loop over these four states. The one-electron operator $\hat{H}_0$ is diagonal, so the matrix element

$$\langle \alpha | h | \gamma \rangle , \tag{7.27}$$

will also be diagonal. Because of the starting point for the basis coefficients, we see that the two-electron operator can be written as

$$V = \sum_{b=1}^{4} \langle \alpha b | v | \gamma b \rangle . \tag{7.28}$$

Because the pairing model does not allow broken pairs, this matrix element will only be non-zero when $\alpha = \gamma$ and when $p_\alpha = p_b$, $\sigma_\alpha = \sigma_b$. The Hartree-Fock matrix will therefore be diagonal, meaning the original basis is a canonical Hartree-Fock basis. Hartree-Fock calculations on this basis will not provide any

new results. The Hartree-Fock energy can be calculated

$$E^{\mathrm{HF}} = \langle \Phi_0 | \, \hat{H} \, | \Phi_0 \rangle = \langle \Phi_0 | \, \hat{H}_0 \, | \Phi_0 \rangle + \langle \Phi_0 | \, \hat{V} \, | \Phi_0 \rangle \, , \tag{7.29}$$

which gives the result

$$E^{\mathrm{HF}} = 2 - g \tag{7.30}$$

This energy will be referred to as the reference energy.

7.4 Many-Body Perturbation Theory

When setting up the many-body perturbation theory equations, it is useful to present them as diagrams. All the diagrams from second to fourth order in perturbation theory are presented and translated to equations in this section.

Because of the properties of the pairing model, many of these diagrams can be removed by examination. First, we have no broken pairs, meaning that a general two-body matrix element

$$\langle pq|v|rs\rangle \, , \tag{7.31}$$

is only non-zero if *both* p and q are hole states or *both* are particle states. The same restriction applies to r and s. The second thing to notice, is that we have a canonical Hartree-Fock basis. That means only diagonal one-body matrix elements are non-zero. We will compute the correlation energy ΔE, using the Hamiltonian

$$\hat{H}_N = \hat{F}_N^d + \hat{F}_N^o + \hat{W} = \hat{F}_N^d + \hat{W}, \tag{7.32}$$

where

$$f_{pq} = \epsilon_p \delta_{pq}. \tag{7.33}$$

The diagrams to second and third order, are presented in the following diagram

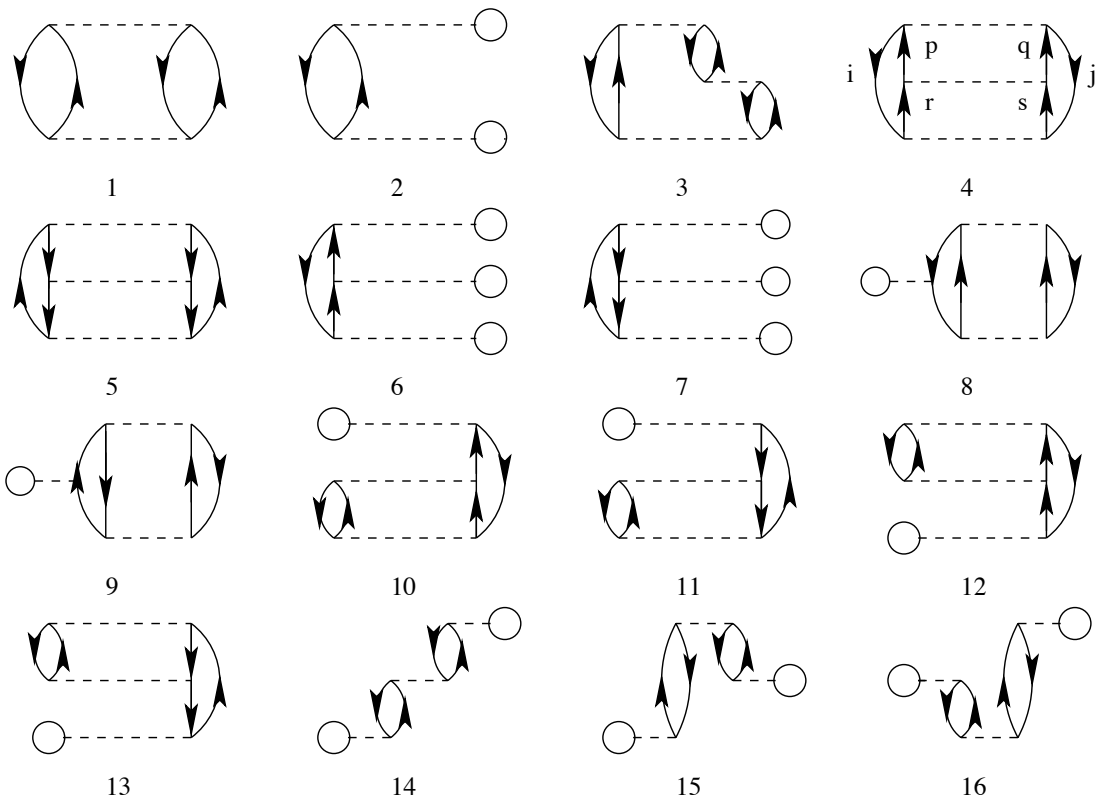

Figure 7.3: Diagrams for Many-Body Perturbation theory to second and third order.

7.4.1 Interpreting diagrams

When reading the diagrams, and connecting them to the equations presented in the equations (5.41), there are a simple set of rules. We have the expression for the resolvent, $\hat{R}_0$ given as

$$\hat{R}_0 = \frac{\hat{Q}}{E_0^{(0)} - \hat{H}_0} = \sum_I \frac{|\Phi_I\rangle \langle \Phi_I|}{E_0^{(0)} - E_I^{(0)}}, \tag{7.34}$$

where we sum over all states apart from $|\Phi_0\rangle$. When this operator operates on any state $|J\rangle$ other than $|\Phi_0\rangle$, it will only produce, as shown in [3],

$$\hat{R}_0 |J\rangle = |J\rangle \frac{1}{E_0^{(0)} - E_J^{(0)}}, \tag{7.35}$$

meaning that the resolvent will only introduce a denominator expressed in terms of zeroth-order energies. We will introduce a more practical notation for this

denominator

$$\epsilon_{ij..}^{ab..} = E_0^{(0)} - E_{\left|\Phi_{ij..}^{ab..}\right\rangle} = \epsilon_i + \epsilon_j + ... - \epsilon_a - \epsilon_b - .... \tag{7.36}$$

The operator $\hat{V}$, as shown in equations (5.41), will give rise to matrix elements. If we have a canonical Hartree-Fock basis, we can rewrite the operator by

$$\hat{V} = \hat{W} + \hat{F}^o = \hat{W}, \tag{7.37}$$

and there will only be two-body matrix elements present. Thich implies that all diagrams with one-body interactions can be removed. In the noncanonical Hartree-Fock case, $\hat{F}^o$ will give non-zero results and must be present. The procedure for interpreting the diagram and write out the corresponding equations can be summed up in the following sequence of operations

7.4.2 Label all lines

First one should identify which lines represent hole states and which represent particle states, and label the lines with the corresponding letter, using $i, j, k, l, ...$ for hole states and $a, b, c, d, ...$ for particle states.

7.4.3 Identify the operators

A one-body vertex should be identified as the one-body operator used for the system, where one sets up the matrix element f_p^q by the labels as

$$f_p^q = \langle \text{line out}| \, \hat{f} \, |\text{line in}\rangle \, . \tag{7.38}$$

The two-body vertices are identified as the two-body operators, and when identified, one should set up the corresponding matrix elements following the interpretation rule

$$\langle pq||rs\rangle = \langle \text{left in, right in}||\text{left out, right out}\rangle \, . \tag{7.39}$$

7.4.4 Identify the denominator

To identify the denominator produced by the resolvent, $\hat{R}_0$, one draws imaginary

lines between the interactions and set up the ϵ for every state-line that was crossed.

7.4.5 Including phase factor

The resulting diagram will get a phase factor depending on how many hole states and how many closed loops there are. The factor is given by

$$(-1)^{\text{Closed loops+Number of holes}}. \tag{7.40}$$

7.4.6 Identify equivalent lines

Equivalent lines are pairs of lines that connect at the same vertices. They must also be of the same kind, either both particle states or both hole states. They will introduce a factor given as

$$\left(\frac{1}{2}\right)^{\text{number of equivalent lines}}. \tag{7.41}$$

7.4.7 Second Order Perturbation Theory

Starting with diagram 1, we see that this diagram is non-zero, because there is no one-body operator and no pairs are broken. We can set up the equation as

$$E_{\text{Diagram 1}} = (-1)^{2+2}\frac{1}{2^2}\sum_{\substack{ab\\ij}}\frac{\langle ij||ab\rangle\langle ab||ij\rangle}{\epsilon_{ij}^{ab}}. \tag{7.42}$$

Diagram 2 can be written out as

$$E_{\text{Diagram 2}} = \sum_{ia}\frac{\langle i|f|a\rangle\langle a|\hat{f}|i\rangle}{\epsilon_i^a} = 0. \tag{7.43}$$

This diagram, however, will be zero. This is because we are operating with a canonical Hartree-Fock basis. By the definition of a non canonical Hartree Fock

basis, $f_i^a = 0$, that basis would provide the same result. That means, only diagram 1 will provide a non-zero result for second order perturbation theory.

7.4.8 Third Order Perturbation Theory

The third order diagrams, shown in figure 7.3, are numbered from 3 to 15. Third order diagrams have three interaction parts: One at the top and one at the bottom of the diagram along with an intermediate interaction part in the middle. Applying the same logic that we applied for diagram 2, we can exclude all diagrams with a one-body interaction term, leaving only diagrams 3, 4 and 5.

$$E_{\text{diagram 3}} = \sum_{\substack{abc \\ ijk}} \frac{\langle ij||ab\rangle \langle bk||jc\rangle \langle ac||ij\rangle}{\epsilon_{ij}^{ac}\epsilon_{ij}^{ab}} = 0. \tag{7.44}$$

However, here we see a problem. We have an interaction term $\langle bk||jc\rangle$, which is a broken pair. The Pairing model does not allow such states, and this must be zero. This is not a problem for the diagrams 4 and 5.

$$E_{\text{diagram 4}} = \frac{1}{2^3} \sum_{\substack{abcd \\ ij}} \frac{\langle cd||ij\rangle \langle ab||cd\rangle \langle ij||ab\rangle}{\epsilon_{ij}^{cd}\epsilon_{ij}^{ab}}, \tag{7.45}$$

$$E_{\text{diagram 4}} = \frac{1}{2^3} \sum_{\substack{ab \\ ijkl}} \frac{\langle ab||kl\rangle \langle kl||ij\rangle \langle ij||ab\rangle}{\epsilon_{kl}^{ab}\epsilon_{ij}^{ab}}. \tag{7.46}$$

When doing many-body perturbation theory to third order with a canonical Hartree-Fock basis for the pairing model, one only needs to calculate diagrams 1, 4 and 5.

7.4.9 Fourth Order Perturbation Theory

When calculating the correlation energy with the fourth order energy, the second and third order are included as well. The amount of diagrams increase dramatically when adding the fourth order, but as we only work with a canonical Hartree-Fock basis, the amount is somewhat limited [3]. We group the diagrams by the excitations they produce, i.e. how many pairs of external lines that are present..

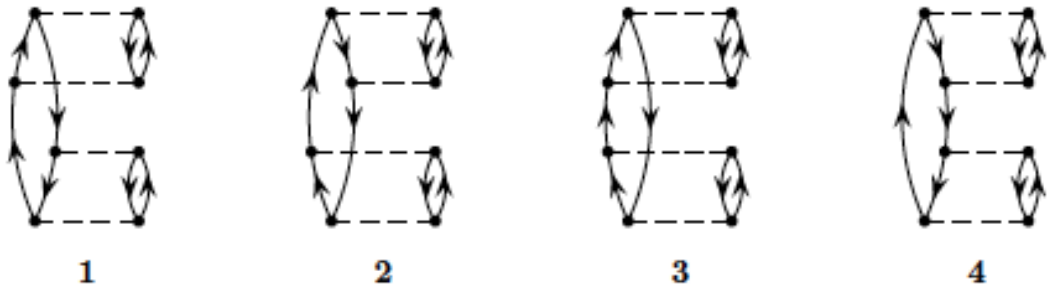

Figure 7.4: Goldstone diagrams for fourth order Rayleigh-Schrödinger perturbation theory with 1p1h excitations

The first set of diagrams in figure (7.4) show diagrams giving rise to a 1particle-1hole excitation. All these diagrams have an intermediate step with a 1p-1h part. The Pairing model does not allow broken pairs, meaning that intermediate steps with 1p-1h or 3p-3h interaction parts must be zero. Therefore none of these diagrams are included in the calculations.

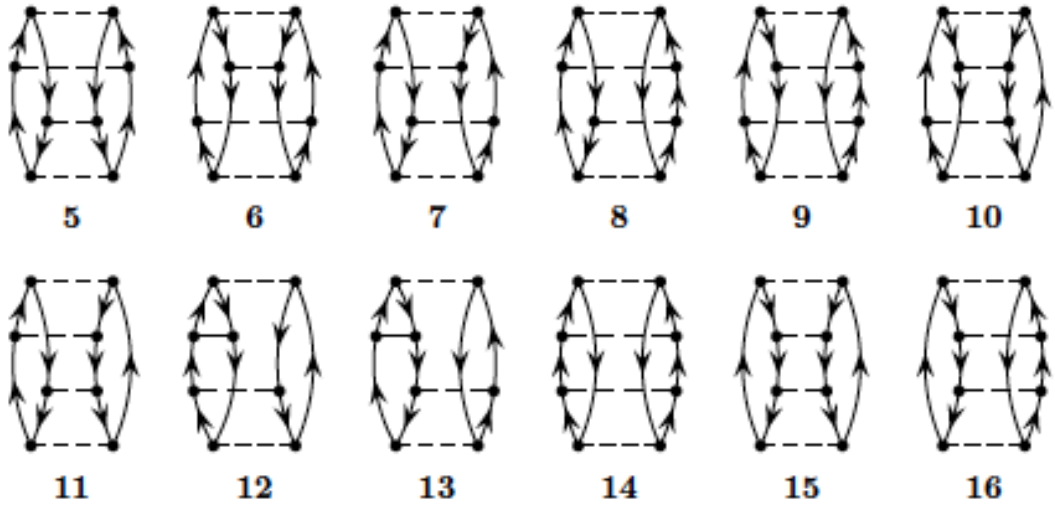

Figure 7.5: Goldstone diagrams for fourth order Rayleigh-Schrödinger perturbation theory with 2p2h excitations

The set of diagrams shown in figure (7.5), give rise to a 2 particle and 2 hole excitation. For all these diagrams, there are only 2p-2h interaction parts for all intermediate steps. However, many of these diagrams give rise to a broken pair interaction of the form

$$\langle ai||pq\rangle \, . \tag{7.47}$$

Only the diagrams 5,6,14 and 15 have no broken pair interactions. They are calculated as

$$E_{\text{diagram 5}} = \frac{1}{2^4} \sum_{\substack{abcd \\ ijkl}} \frac{\langle cd||kl\rangle \langle kl||ij\rangle \langle ab||cd\rangle \langle ij||ab\rangle}{\epsilon_{kl}^{cd} \epsilon_{ij}^{cd} \epsilon_{ij}^{ab}}, \tag{7.48}$$

and diagram 6

$$E_{\text{diagram 6}} = \frac{1}{2^4} \sum_{\substack{abcd \\ ijkl}} \frac{\langle cd||kl\rangle \langle kl||ij\rangle \langle ab||cd\rangle \langle ij||ab\rangle}{\epsilon_{kl}^{ab} \epsilon_{kl}^{cd} \epsilon_{ij}^{ab}}. \tag{7.49}$$

For diagram 14, we get

$$E_{\text{diagram 14}} = \frac{1}{2^4} \sum_{\substack{abcdef \\ ij}} \frac{\langle ij||ab\rangle \langle ab||cd\rangle \langle cd||ef\rangle \langle ef||ij\rangle}{\epsilon_{ij}^{ab} \epsilon_{ij}^{cd} \epsilon_{ij}^{ef}}, \tag{7.50}$$

and for diagram 15

$$E_{\text{diagram 15}} = \frac{1}{2^4} \sum_{\substack{ab \\ ijklmn}} \frac{\langle ij||ab\rangle \langle kl||ij\rangle \langle mn||kl\rangle \langle ab||mn\rangle}{\epsilon_{ij}^{ab} \epsilon_{kl}^{ab} \epsilon_{mn}^{ab}} \tag{7.51}$$

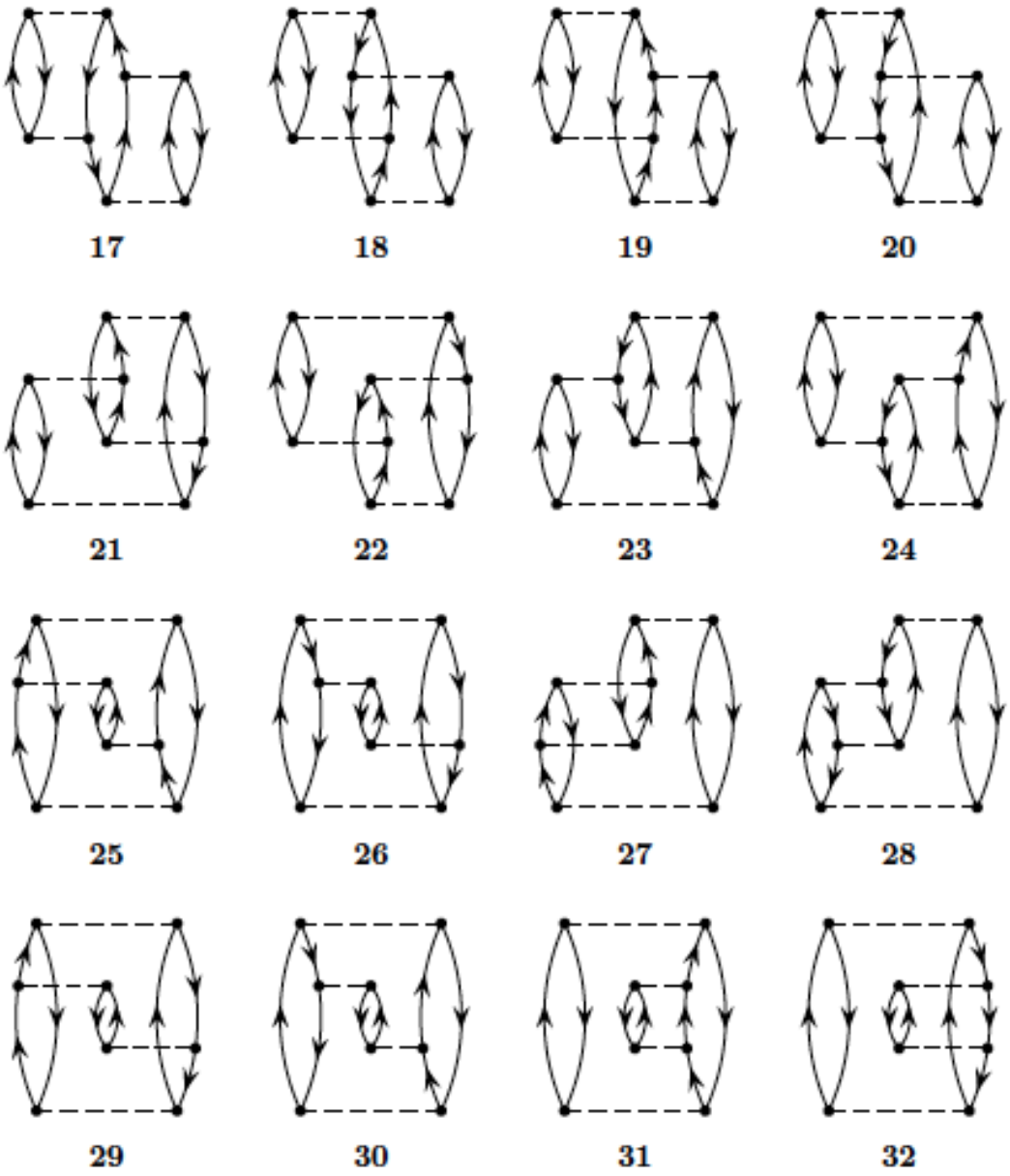

Figure 7.6: Goldstone diagrams for fourth order Rayleigh-Schrödinger perturbation theory with 3p3h excitations

The diagrams depicted in figure (7.6), show the fourth order diagrams giving rise to 3 particles and 3 holes excitations. We notice that all these diagrams include one intermediate step with a 3p-3h excitation. Therefore we can exclude all these diagrams from the calculations.

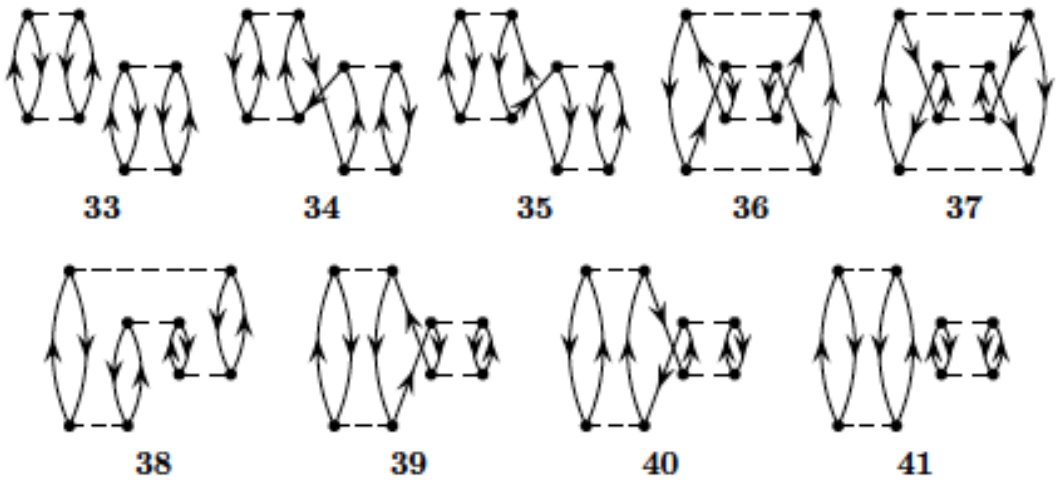

Figure 7.7: Goldstone diagrams for fourth order Rayleigh-Schrödinger perturbation theory with 4p4h excitations

The last set of diagrams, depicted in figure (7.7), show the fourth order diagrams that include a 4 particle and 4 hole part. Invoking the Linked diagram theorem, we can immediatly exclude diagram 33 and diagram 41. Diagram 34 to 40 do will be non-zero, and must be calculated. For diagram 34, we get

$$E_{\text{diagram 34}} = (-1)^{(3+4)} \frac{1}{2^2} \sum_{\substack{abcd \\ ijkl}} \frac{\langle ij||ab\rangle \langle kl||cd\rangle \langle ab||ik\rangle \langle cd||jl\rangle}{\epsilon_{ij}^{ab} \epsilon_{ijkl}^{abcd} \epsilon_{jl}^{cd}}. \tag{7.52}$$

We notice that there are 3 closed loops and 4 hole states, giving rise to the negative phase factor. We also notice that we have two pairs of equivalent lines, arising from the particle states, introducing a factor $\frac{1}{4}$. One can also notice the fourth order denominator term ϵ_{ijkl}^{abcd}, arising from the 4p-4h intermediate excitation part. The last diagrams are calculated following the same principles, giving

$$E_{\text{diagram 35}} = (-1)^{(3+4)} \frac{1}{2^2} \sum_{\substack{abcd \\ ijkl}} \frac{\langle ij||ab\rangle \langle kl||cd\rangle \langle ac||ij\rangle \langle bd||kl\rangle}{\epsilon_{ij}^{ab} \epsilon_{ijkl}^{abcd} \epsilon_{kl}^{bd}}, \tag{7.53}$$

Before calculating diagram 36, please notice that there is a mistake in the drawing of the diagram 36. The right-most particle state is supposed to be a hole state,

giving the correct equation

$$E_{\text{diagram 36}} = \frac{1}{2^4} \sum_{\substack{abcd \\ ijkl}} \frac{\langle ij||ab\rangle \langle kl||cd\rangle \langle ab||kl\rangle \langle cd||ij\rangle}{\epsilon_{ij}^{ab} \epsilon_{ijkl}^{abcd} \epsilon_{ij}^{cd}}. \tag{7.54}$$

Diagram 37 is also depicted with the right-most state wrong. It is supposed to be a particle state, giving

$$E_{\text{diagram 37}} = \frac{1}{2^4} \sum_{\substack{abcd \\ ijkl}} \frac{\langle ij||ab\rangle \langle kl||cd\rangle \langle cd||ij\rangle \langle ab||kl\rangle}{\epsilon_{ij}^{ab} \epsilon_{ijkl}^{abcd} \epsilon_{kl}^{ab}}. \tag{7.55}$$

and for diagram 38, we notice that there are no equal state pairs

$$E_{\text{diagram 38}} = \sum_{\substack{abcd \\ ijkl}} \frac{\langle ij||ab\rangle \langle kl||cd\rangle \langle db||lj\rangle \langle ac||ik\rangle}{\epsilon_{ij}^{ab} \epsilon_{ijkl}^{abcd} \epsilon_{ik}^{ac}}. \tag{7.56}$$

Diagram 39 gives

$$E_{\text{diagram 39}} = (-1)^{(3+4)} \frac{1}{2^2} \sum_{\substack{abcd \\ ijkl}} \frac{\langle ij||ab\rangle \langle kl||cd\rangle \langle bd||kl\rangle \langle ac||ij\rangle}{\epsilon_{ij}^{ab} \epsilon_{ijkl}^{abcd} \epsilon_{ij}^{ac}}. \tag{7.57}$$

And finally, diagram 40 gives the equation

$$E_{\text{diagram 40}} = (-1)^{(3+4)} \frac{1}{2^2} \sum_{\substack{abcd \\ ijkl}} \frac{\langle ij||ab\rangle \langle kl||cd\rangle \langle cd||jl\rangle \langle ab||ik\rangle}{\epsilon_{ij}^{ab} \epsilon_{ijkl}^{abcd} \epsilon_{ik}^{ab}}. \tag{7.58}$$

7.5 Spin Summations

Up to this point, we have not taken into account the effect of spin in the matrix elements. Because of spin orthogonality, terms may vanish from certain two-electron matrix elements. Listed here, are all the different ways spins can be organized, along with the resulting integration. Representing the spin up orbital

with a bar, we get [3]

$$\langle pq||rs\rangle = \langle pq|\hat{v}|rs\rangle - \langle pq|\hat{v}|sr\rangle\,, \tag{7.59}$$
$$\langle p\bar{q}||r\bar{s}\rangle = \langle pq|\hat{v}|rs\rangle\,, \tag{7.60}$$
$$\langle p\bar{q}||\bar{r}s\rangle = -\langle pq|\hat{v}|sr\rangle\,, \tag{7.61}$$
$$\langle \bar{p}q||\bar{r}s\rangle = \langle pq|\hat{v}|rs\rangle\,, \tag{7.62}$$
$$\langle \bar{p}q||r\bar{s}\rangle = -\langle pq|\hat{v}|sr\rangle\,, \tag{7.63}$$
$$\langle \bar{p}\bar{q}||\bar{r}\bar{s}\rangle = \langle pq|\hat{v}|rs\rangle - \langle pq|\hat{v}|sr\rangle\,. \tag{7.64}$$

Because of the restrictions on the pairing model, the first and the last equations will also be zero, because the states are not allowed to exist. Matrix elements, where there are an unequal amount of equal spin orbitals will all give zero as result as well

$$\langle \bar{p}q||rs\rangle = \langle p\bar{q}||rs\rangle = \langle pq||\bar{r}s\rangle = \langle pq||r\bar{s}\rangle = 0, \tag{7.65}$$
$$\langle \bar{p}\bar{q}||rs\rangle = \langle pq||\bar{r}\bar{s}\rangle = 0, \tag{7.66}$$
$$\langle \bar{p}\bar{q}||\bar{r}s\rangle = \langle \bar{p}\bar{q}||r\bar{s}\rangle = \langle \bar{p}q||\bar{r}\bar{s}\rangle = \langle p\bar{q}||\bar{r}\bar{s}\rangle = 0. \tag{7.67}$$

Chapter 8

Infinite Matter

A study of infinite matter can convey important information about the equation of state in dense objects like neutron stars, and hopefully shed light on the strong force acting in a many-body medium. This thesis will study the infinite electron gas before the final study of nuclear matter. This is done for pedagogical reasons and because the electron gas has closed form solutions that provide important benchmarking for the code.

8.1 The Infinite Electron Gas

The infinite electron gas gives a good approximation to valence electrons in metal. The gas consists only of interacting electrons with a uniform background of charged ions. The whole system is charge neutral. We assume a finite cubic box as done in [15] and [16]. The box has a length L and volume $\Omega = L^3$, with N_e as the number of electrons with a charge density $\rho = N_e/\Omega$.

8.1.1 The Hamiltonian

The electrons interact with the central symmetric Colomb potential, $\hat{V}(\mathbf{r}_1, \mathbf{r}_2)$ depending only on the distance $|\mathbf{r}_1 - \mathbf{r}_2|$. The Hamiltonian for infinite electron gas is [1]

$$\hat{H} = \hat{H}_1 + \hat{H}_2 = \hat{H}_{\text{kin}} + \hat{H}_{\text{interaction}}. \tag{8.1}$$

The interaction term will be dependent on both the electron-electron interaction, the electron-background interaction and the background-background interaction

$$\hat{H} = \hat{H}_{\text{kin}} + \hat{H}_{\text{ee}} + \hat{H}_{\text{eb}} + \hat{H}_{\text{bb}}. \tag{8.2}$$

The kinetic energy, $\hat{H}_{\text{kin}}$ is given as

$$\hat{H}_{\text{kin}} = \sum_{p} \frac{\hbar^2 k^2}{2m} a^{\dagger}_{k\sigma} a_{k\sigma}. \tag{8.3}$$

The background-interaction terms will vanish as explained by Fraser et al [18] both for three- and two-dimensional electron gas. When we sum over all particles, we can write the electron-electron interaction term as an Ewald summation term, because it is not possible to use a $1/r$ term for infinite systems [17] [23]. We can write this term as

$$\hat{H}_{ee} = \sum_{i<j}^{N} v_E(\mathbf{r}_i - \mathbf{r}_j) + \frac{1}{2} N e^2 v_0, \tag{8.4}$$

where $v_E(\mathbf{r})$ is an effective two-body interaction. v_0 is the self-interaction term, defined as

$$v_0 = \lim_{\mathbf{r}\to\infty} \left\{ v_E(\mathbf{r}) - \frac{1}{r} \right\}. \tag{8.5}$$

The Ewald summation will account for interactions between all electrons in the finite size system as well as all the image electrons that will arize from self-interaction because of periodic boundaries. We define it as

$$\begin{aligned} v_E(\mathbf{r}) = &\sum_{k\neq 0} \frac{4\pi}{L^3 k^2} e^{i\mathbf{k}\cdot\mathbf{r}} e^{-\eta^2 k^2/4} \\ &+ \sum_{\mathbf{R}} \frac{1}{|\mathbf{r}-\mathbf{R}|} \text{erfc}\left(\frac{|\mathbf{r}-\mathbf{R}|}{\eta} \right) - \frac{\pi\eta^2}{L^3}, \end{aligned} \tag{8.6}$$

where L is the size of the box, $\mathbf{k}$ is the momentum vector, while $\mathbf{r}$ represent the position vectors for all electrons. The translational vector $\mathbf{R}$, is used to obtain all image cells in the entire real space [23]

$$\mathbf{R} = L(n_x \mathbf{u}_x + n_y \mathbf{u}_y + n_z \mathbf{u}_z). \tag{8.7}$$

We have used the error functions

$$\text{erf}(x) = \frac{2}{\sqrt{\pi}} \int_0^x e^{-t^2} \text{dt}, \tag{8.8}$$

and

$$\text{erfc}(x) = 1 - \text{erf}(x) = \frac{2}{\sqrt{\pi}} \int_x^\infty e^{-t^2} \text{dt}. \tag{8.9}$$

We use this relation because an interaction on the form $1/|r|$ is not convergent for an infinite number of particles [2]. Ewald found that one can rewrite the interaction in terms of these error functions [19]

$$\frac{1}{r} = \frac{\text{erf}(\frac{1}{2}\sqrt{\eta}r)}{r} + \frac{\text{erfc}(\frac{1}{2}\sqrt{\eta}r)}{r}. \tag{8.10}$$

One can calculate the two-dimensional Ewald term as well [1], resulting in

$$v_E^{\eta=0,z=0} = \sum_{\mathbf{k}\neq 0} \frac{2\pi}{L^2 k} e^{i\mathbf{k}\cdot\mathbf{r}_{xy}}. \tag{8.11}$$

8.1.2 The Reference Energy

The reference energy for electron gas can be written as [1]

$$E_{\text{ref}} = \sum_i \langle i|h_0|i\rangle + \frac{1}{2}\sum_{ij} \langle ij||ij\rangle + \frac{1}{2}Av_0. \tag{8.12}$$

A is the number of electrons, and the term Av_0 is the so-called Madelung constant. It is how we incorporate the self-interaction term into the system. This factor will be larger for smaller system and vanish as we approach the thermodynamic limit.

8.1.3 The Fock Matrix Elements

The Fock Matrix Elements will be given as

$$\langle p|f|q\rangle = \frac{k_p^2}{2m}\delta_{\mathbf{k}_p\mathbf{k}_q}\delta_{m_{s_p}m_{s_q}} + \sum_i \langle pi||qi\rangle\,. \tag{8.13}$$

We notice that the Fock Matrix elements can be written as a diagonal part plus the $\hat{U}$ operator. As we can see from (3.95) and (3.97), this means the perturbation is given solely by the two-body interaction

$$\hat{V} = \frac{1}{4}\sum_{pqrs} \langle pq||rs\rangle \, \hat{p}^\dagger \hat{q}^\dagger \hat{s}\hat{r}. \tag{8.14}$$

8.1.4 Anti-Symmetric Matrix Elements

We now need to define the matrix elements for the two- and three-dimensional electron gas to calculate the perturbation

$$\begin{aligned} &\left\langle \mathbf{k}_p m_{s_p} \mathbf{k}_q m_{s_q} || \mathbf{k}_r m_{s_r} \mathbf{k}_s m_{s_s} \right\rangle \\ &= \frac{4\pi e^2}{L^3} \delta_{\mathbf{k}_p+\mathbf{k}_q,\mathbf{k}_r+\mathbf{k}_s} \left\{ \delta_{m_{sp},m_{sr}} \delta_{m_{sq},m_{ss}} (1-\delta_{\mathbf{k}_p,\mathbf{k}_r}) \frac{1}{|\mathbf{k}_r-\mathbf{k}_p|^2} \right. \\ &\left. - \delta_{m_{sp},m_{ss}} \delta_{m_{sq},m_{sr}} (1-\delta_{\mathbf{k}_p,\mathbf{k}_s}) \, \frac{1}{|\mathbf{k}_s-\mathbf{k}_p|^2} \right\}. \end{aligned} \tag{8.15}$$

The two-dimensial case is almost identical

$$\begin{aligned} &\left\langle \mathbf{k}_p m_{s_p} \mathbf{k}_q m_{s_q} || \mathbf{k}_r m_{s_r} \mathbf{k}_s m_{s_s} \right\rangle \\ &= \frac{2\pi e^2}{L^2} \delta_{\mathbf{k}_p+\mathbf{k}_q,\mathbf{k}_r+\mathbf{k}_s} \left\{ \delta_{m_{sp},m_{sr}} \delta_{m_{sq},m_{ss}} (1-\delta_{\mathbf{k}_p,\mathbf{k}_r}) \frac{1}{|\mathbf{k}_r-\mathbf{k}_p|} \right. \\ &\left. - \delta_{m_{sp},m_{ss}} \delta_{m_{sq},m_{sr}} (1-\delta_{\mathbf{k}_p,\mathbf{k}_s}) \, \frac{1}{|\mathbf{k}_s-\mathbf{k}_p|} \right\}. \end{aligned} \tag{8.16}$$

8.1.5 The Plane Wave Basis

When set up with periodic boundary conditions, the homogenous electron gas can be set up with free particle normalized wave functions

$$\psi_{\mathbf{k}\sigma}(\mathbf{r}) = \frac{1}{\sqrt{\Omega}} e^{i\mathbf{k}\mathbf{r}} \xi_\sigma, \tag{8.17}$$

where $\mathbf{k}$ is the wave number and ξ_σ is a spin function.

$$\xi_{+\frac{1}{2}} = \begin{pmatrix} 1 \\ 0 \end{pmatrix}, \quad \xi_{-\frac{1}{2}} = \begin{pmatrix} 0 \\ 1 \end{pmatrix}. \tag{8.18}$$

Because of periodic boundary conditions, we acquire the following wave numbers

$$k_i = \frac{2\pi n_i}{L}, \quad i = x, y, z \quad n_i = 0, \pm 1, \pm 2, ... \tag{8.19}$$

and the associated single-particle energies for two dimensions

$$\epsilon_{n_x,n_y} = \frac{\hbar^2}{2m}\left(\frac{2\pi}{L}\right)^2 (n_x^2 + n_y^2). \tag{8.20}$$

For three dimensions, we get the energy

$$\epsilon_{n_x,n_y,n_z} = \frac{\hbar^2}{2m}\left(\frac{2\pi}{L}\right)^2 (n_x^2 + n_y^2 + n_z^2). \tag{8.21}$$

By the nature of the single particle energies, the energy levels will be determined by the value of $n_x^2 + n_y^2 + n_z^2$. There are different combinations of n_x, n_y and n_z that set up each energy level. The cumulative number of particles needed to completely fill these energy states will be named *magic numbers* and are listed in table 8.1.

$n_x^2+n_y^2+n_z^2$	n_x	n_y	n_z	$N_{\uparrow\uparrow}$	$N_{\uparrow\downarrow}$	$N_{\uparrow\downarrow}\hat{\tau}$
0	0	0	0	1	2	4
1	1	0	0			
	-1	0	0			
	0	1	0			
	0	-1	0			
	0	0	1			
	0	0	-1	7	14	28
2	1	1	0			
	1	-1	0			
	1	0	1			
	1	0	-1			
	-1	1	0			
	-1	-1	0			
	-1	0	1			
	-1	0	-1			
	0	1	1			
	0	1	-1			
	0	-1	1			
	0	-1	-1	19	38	76
3	1	1	1			
	1	1	-1			
	1	-1	1			
	1	-1	-1			
	-1	1	1			
	-1	1	-1			
	-1	-1	1			
	-1	-1	-1	27	54	108
4	2	0	0			
	-2	0	0			
	0	2	0			
	0	-2	0			
	0	0	2			
	0	0	-2	33	66	132
5				57	114	228
6				81	162	324
7				81	162	324
8				93	186	372

Table 8.1: All magic numbers for three dimensional infinite matter. The table demonstrates how states will fill up energy levels. n_x, n_y and n_z represent momentum quantum numbers, $n_x^2+n_y^2+n_z^2$ represent energy level. $N_{\uparrow\uparrow}$ shows magic number without spin degeneracy, $N_{\uparrow\downarrow}$ adds two possible spins, and $N_{\uparrow\downarrow}\hat{\tau}$ also adds isospin degeneracy.

8.2 Infinite Nuclear Matter

Central to my thesis, is the study of infinite nuclear matter. I look at baryonic matter similar to the dense baryonic matter found in neutron stars. I limit the study to temperatures far below the Fermi level temperature, assuming thereby that I can treat neutrons and protons as a degenerate Fermi gas. The matter is mostly made up of neutron and protons in β-equilibrium with the relevant leptons. In neutron star matter, we assume the equilibrium consists of protons, neutrons, electrons and muons with densities larger than 0.1fm^{-}3. The equilibrium conditions are specified by

$$b_1 \rightarrow b_2 + l + \bar{\nu}_l \qquad b_2 + l \rightarrow b_1 + \nu_l, \tag{8.22}$$

where b represent either a neutron or a proton and $l$is either an electron or muon. ν_l is the corresponding neutrino.

Nuclear matter is a hypothetical system filling all of space at a uniform density. Symmetric nuclear matter (SNM) consist of equal numbers of protons of neutrons, while pure nuclear matter (PNM) consist only of neutrons. For finite-nucleus systems, the most difficult part is calculating the single particle wave function. For nuclear matter we can use the same plane wave basis that we used for the electron gas. The difficult part is calculating the energy and the effective interaction between particles [13]. In my calculations, I have looked at pure nuclear matter.

8.3 Nuclear Interaction

Nuclear matter is composed of baryons which interacts through the strong force. Here we will employ a simplified model of the nuclear forces, the so-called Minnesota potential. This potential has been widely used and compare different many-body methods.

8.3.1 The Minnesota Potential

The Minnesota Potential is given as

$$v(r) = (v_R + (1 + P_{12}^{\sigma})v_T/2 + (1 - P_{12}^{\sigma})v_S/2) \cdot (\alpha + (2 - \alpha)P_{12}^{r})/2 + (1 + m_{t,1})(1 + m_{t,2})\frac{e^2}{4r}, \tag{8.23}$$

where r is given as $|\mathbf{r_1} - \mathbf{r_2}|$ and m_t is the isospin projection of particle 1 or 2. $m_t = \pm 1$. P_{12}^{σ} and P_{12}^{r} are exchange operators for spin and position, respectively [1]. Furthermore, we have used

$$v_R = v_{0R}e^{-k_R r^2}, \quad v_T = -v_{0T}e^{-k_T r^2}, \quad v_S = -v_{0S}e^{-k_s r^2}, \tag{8.24}$$

where the constants v_{0R}, v_{0T}, v_{0S}, k_R, k_T and k_S are given by [14]

1. $v_{0R} = 200\text{MeV}$, $k_R = 1.487\text{fm}^{-2}$,

2. $v_{0T} = 178\text{MeV}$, $k_T = 0.649\text{fm}^{-2}$,

3. $v_{0S} = 91.85\text{MeV}$, $k_S = 0.465\text{fm}^{-2}$.

In momentum space the interaction reads

$$\langle k_p k_q | v | k_r k_s \rangle = \frac{V_0}{L^3}\left(\frac{\pi}{\alpha}\right)^{3/2} e^{-q^2/4\alpha}\delta_{\mathbf{k}_p+\mathbf{k}_q,\mathbf{k}_r+\mathbf{k}_s}, \tag{8.25}$$

where q is the relative momentum transfer given by

$$\mathbf{q} = \mathbf{p} - \mathbf{p}', \tag{8.26}$$

and the momentum vectors are defined as

$$\mathbf{p} = \frac{1}{2}(\mathbf{k}_p - \mathbf{k}_q), \quad \mathbf{p}' = \frac{1}{2}(\mathbf{k}_r - \mathbf{k}_s). \tag{8.27}$$

We can now set up the two-body Matrix-elements for the Minnesota Potential

$$\begin{aligned}\langle \mathbf{k}_p\mathbf{k}_q|v|\mathbf{k}_r\mathbf{k}_s\rangle &= \langle \mathbf{k}_p\mathbf{k}_q| \frac{1}{2}\left(V_R + \frac{1}{2}V_T + \frac{1}{2}V_S\right)|\mathbf{k}_r\mathbf{k}_s\rangle \\ &+ \langle \mathbf{k}_p\mathbf{k}_q| \frac{1}{4}(V_T - V_S)P_{12}^{\sigma}|\mathbf{k}_r\mathbf{k}_s\rangle \\ &- \langle \mathbf{k}_p\mathbf{k}_q| \frac{1}{2}\left(V_R + \frac{1}{2}V_T + \frac{1}{2}V_S\right)P_{12}^{\sigma}P_{12}^{\tau}|\mathbf{k}_r\mathbf{k}_s\rangle \\ &- \langle \mathbf{k}_p\mathbf{k}_q| \frac{1}{4}(V_T - V_S)P_{12}^{\tau}|\mathbf{k}_r\mathbf{k}_s\rangle \quad .\end{aligned} \tag{8.28}$$

Matrix elements for the spin and isospin exchange operators are

$$\langle \sigma_p\sigma_q| P_{12}^{\sigma}|\sigma_r\sigma_s\rangle = \delta_{\sigma_p,\sigma_s}\delta_{\sigma_q,\sigma_r}. \tag{8.29}$$

One can see that these matrix elements come at a far greater computational cost than the electron-electron interaction in the electron gas. Therefore it is necessary to compute and store all elements instead of computing them "on the fly" [23].

Chapter 9

Implementation of CCD

In this thesis I have created three different solvers for coupled-cluster doubles equations.

1. A naive brute force implementation of the equations summing over all variables.
2. A naive brute force implementation of intermediate equations summing over all variables.
3. Rewriting the summations as matrix-matrix multiplications and exploiting various symmetry arguments that one can set up as a block implementation.

There is a significant performance leap between each method, but I have included the first two solvers for both educational and benchmarking purposes. The pairing model with 4 particles and 4 holes is a small system that one can easily solve using the naive approach. After producing expected results with the naive solver, I have compared the more complicated solvers to the naive solver for all systems.

9.1 Implementing the CCD equations

The basic steps of all implemented CCD algorithms can be explained through the following four steps:

1. Initialize amplitudes $t^{(0)} = 0$and $\Delta E^{(0)}_{CCD} = 0$.

2. Update the amplitudes and calculate $\Delta E^{(1)}_{CCD}$.
3. If $|\Delta E^{(1)}_{CCD} - \Delta E^{(0)}_{CCD}| \geq \epsilon$, update amplitudes and compute ΔE^{2}_{CCD}.
4. Repeat until $|\Delta E^{(n+1)}_{CCD} - \Delta E^{(n)}_{CCD}| \leq \epsilon$.

The difference between the three solvers I have implemented is the way I update amplitudes. The naive brute force solver loops over all indices when computing. An example of diagram L_a is shown below

```
for i in 0, ..., Nholes:
  for j in 0, ..., Nholes:
    for a in Nholes, ..., Nparticles:
      for b in Nholes, ..., Nparticles:
        for c in Nholes, ..., Nparticles:
          for d in Nholes, ..., Nparticles:
            tnew(a,b,i,j) = 0.5 * v(a,b,c,d) *
                told(c,d,i,j) / epsilon(i,j,a,b);
```

A significant cost reduction can be obtained by factorizing the diagrams as shown in equation (7.1). By calculating the four intermediate diagrams, I_1, I_2, I_3 and I_4 beforehand and storing the results reduce the cost of calculation from $\mathcal{O}(h^4p^4)$ to $\mathcal{O}(h^4p^2)$. The second solver applies this method.

9.2 Matrix Representation of Contractions

Diagrams can be viewed as contractions of tensors of varying degree. An example is the matrix-matrix multiplication product

$$(MN)^{\alpha}_{\gamma} = \sum_{\beta} M^{\alpha}_{\beta} N^{\beta}_{\gamma}. \tag{9.1}$$

As our goal is to rewrite the coupled-cluster equations as matrix-matrix products, we will need to map tensors of rank ≥ 2 onto matrices. One mapping that provides systematic and unique matrix elements is

$$\langle pq|\hat{v}|rs\rangle = V_{\alpha(p,q),\beta(r,s)}, \tag{9.2}$$

where

$$\alpha(p,q) = p + qN_p, \quad \beta(r,s) = r + sN_r. \tag{9.3}$$

We need to be careful when mapping tensors this way. Consider first the calculation of the perfectly aligned L_a term

$$L_a = \sum_{cd} \langle ab|\hat{v}|cd\rangle \, t_{ij}^{cd}. \tag{9.4}$$

Mapping this equation using equation (9.3)

$$\langle ab|\hat{v}|cd\rangle = v_{ab}^{cd} \rightarrow V_{\beta(c,d)}^{\alpha(a,b)}, \tag{9.5}$$

and

$$t_{ij}^{cd} \rightarrow T_{\delta(i,j)}^{\beta(c,d)}. \tag{9.6}$$

As we are mapping to unique elements

$$\beta(c,d) = \beta(c,d), \tag{9.7}$$

we can now rewrite the equation

$$(L_a)_{\delta}^{\alpha} = \sum_{\beta} V_{\beta}^{\alpha} T_{\delta}^{\beta}, \tag{9.8}$$

implying by regarding equation (9.1) that we can rewrite the product as a matrix-matrix multiplication

$$L_a = VT. \tag{9.9}$$

9.2.1 Aligning elements

Unfortunately, not all products are perfectly aligned like L_a. Consider, for example, the term L_c

$$L_c = -P\,(ij|ab) \sum_{kc} \langle kb|\hat{v}|cj\rangle \, t_{ik}^{ac}. \tag{9.10}$$

Using the same mapping scheme

$$\langle kb|\hat{v}|cj\rangle = v_{cj}^{kb} \rightarrow V_{\beta(cj)}^{\alpha(kb)}, \tag{9.11}$$

and

$$t_{ik}^{ac} \rightarrow T_{\delta(ik)}^{\gamma(ac)}, \tag{9.12}$$

we notice that this matrix multiplication is misaligned, and if the number of particles is unequal to the number of holes, the size of the matrices will be incompatible

$$(L_c)_\delta^\alpha \neq -P\,(ij|ab)\sum_\beta V_{\beta(cj)}^{\alpha(kb)} T_{\delta(ik)}^{\gamma(ac)}. \tag{9.13}$$

We need to find another mapping, such as

$$v_{cj}^{kb} \rightarrow \tilde{V}_{\beta(ck)}^{\alpha(bj)}, \tag{9.14}$$

and

$$t_{ik}^{ac} \rightarrow \tilde{T}_{\delta(ia)}^{\gamma(ck)}. \tag{9.15}$$

The matrix-matrix multiplication is now properly aligned

$$(\tilde{L}_c)_\delta^\alpha = -P\,(ij|ab)\sum_\beta \tilde{V}_{\beta(ck)}^{\alpha(bj)} \tilde{T}_{\delta(ia)}^{\gamma(ck)}. \tag{9.16}$$

Note, however, that

$$L_c \neq \tilde{L}_c, \tag{9.17}$$

so we need "realign" $\tilde{L}_c$ to match the correct diagram

$$(\tilde{L}_c)_{\delta(i,a)}^{\alpha(b,j)} \rightarrow (L_c)_{\delta(i,k)}^{\alpha(k,b)}. \tag{9.18}$$

Another example is the Qc term

$$Q_c = -\frac{1}{2}\hat{P}(ij)\sum_{klcd} \langle kl|v|cd\rangle\, t_{ik}^{ab} t_{jl}^{cd}. \tag{9.19}$$

We can rewrite this as a matrix-matrix multiplication with the matrix elements given by

$$\langle kl|v|cd\rangle = v_{cd}^{kl} \rightarrow V_{\beta(kl)}^{\alpha(cd)}, \tag{9.20}$$

$$t_{ik}^{ab} \rightarrow (T_1)_{\gamma(ik)}^{\delta(ab)}, \tag{9.21}$$

$$t_{jl}^{cd} \rightarrow (T_2)_{\omega(jl)}^{\eta(cd)}. \tag{9.22}$$

Because we sum over the coefficients $klcd$, we must make sure that they belong to the "inner" indexes. This can only be done by creating a hole, particle-particle-

hole configuration. We must also change the order of multiplication

$$V_{\beta(kl)}^{\alpha(cd)} \rightarrow \tilde{V}_{\gamma(cdl)}^{\delta(k)}, \tag{9.23}$$

$$(T_1)_{\gamma(ik)}^{\delta(ab)} \rightarrow \tilde{(T_1)}_{\delta(k)}^{\alpha(abi)}, \tag{9.24}$$

$$(T_2)_{\omega(jl)}^{\eta(cd)} \rightarrow \tilde{(T_2)}_{\beta(j)}^{\gamma(cdl)}. \tag{9.25}$$

This gives us

$$(\tilde{Q}_c)_{\beta(j)}^{\alpha(abi)} = -\frac{1}{2}\hat{P}(ij)\sum_{klcd}(\tilde{T_1})_{\delta(k)}^{\alpha(abi)}\tilde{V}_{\gamma(cdl)}^{\delta(k)}(\tilde{T_2})_{\beta(j)}^{\gamma(cdl)}. \tag{9.26}$$

Which must be realigned back to the properly aligned Q_c before it can be added to the amplitude equations

$$(\tilde{Q}_c)_{\beta(j)}^{\alpha(abi)} \rightarrow (Q_c)_{\beta(ij)}^{\alpha(ab)}. \tag{9.27}$$

We will need a general mapping function that can be used regardless of the amount of states used. It turns out that we can use the same mapping as before, just generalized to N states.

$$\alpha(p_1, p_2, p_3, ..., p_N) = p_1 + p_2N_1 + p_3N_1N_2 + ... + p_NN_1N_2...N_{N-1}, \tag{9.28}$$

where N_n determines the maximum number of states for p_n. If for example $p_n \in i$, i.e. p_n is a hole-state, $N_n = N_{holes}$.

Writing the diagrams as matrix-matrix multiplications serves as a significant reduction of computational time due to the efficient algortithms in the BLAS-packages for matrix-matrix multiplications. However, since one has to save all the matrices, memory usage will be a problem for large basis sets.

9.3 Block Implementation

One can both greatly reduce memory usage and improve computational speed by exploiting symmetries for infinite matter. Due to the kroenecker delta's in the interaction, one such symmetry is the conservation of momentum

$$\delta_{\mathbf{k}_p+\mathbf{k}_q,\mathbf{k}_r+\mathbf{k}_s} \rightarrow \mathbf{k}_p + \mathbf{k}_q = \mathbf{k}_r + \mathbf{k}_s. \tag{9.29}$$

We also conserve spin

$$m_{s_p} + m_{s_q} = m_{s_r} + m_{s_s}, \tag{9.30}$$

and for nuclear matter, we will conserve isospin as well

$$m_{t_p} + m_{t_q} = m_{t_r} + m_{t_s}. \tag{9.31}$$

The amplitudes will be subject to the same restrictions, vizualised by the first order amplitude generated by perturbation theory

$$(t_{ij}^{ab})^{t=0} = \frac{\langle ab|\hat{v}|ij\rangle}{\epsilon_i + \epsilon_j - \epsilon_a - \epsilon_b}. \tag{9.32}$$

Looking at the L_a term

$$L_a = \sum_{cd} \langle ab|\hat{v}|cd\rangle \, t_{ij}^{ab}, \tag{9.33}$$

we see that we have conservation of momentum

$$\mathbf{k}_a + \mathbf{k}_b = \mathbf{k}_c + \mathbf{k}_d = \mathbf{k}_i + \mathbf{k}_j, \tag{9.34}$$

and conservation of spin

$$m_{s_a} + m_{s_b} = m_{s_c} + m_{s_d} = m_{s_i} + m_{s_j}. \tag{9.35}$$

When summing over all variations of contractions, only the quantum numbers preserving the symmetry requirements are non-zero. When storing the interactions in a matrix, most of it will have zero-elements. The blocking method will store the non-zero parts in blocks inside the matrix. By keeping track of the blocks, we can reduce the full matrix-matrix multiplication to a series of multiplications of the blocks. We will hereby refer to the series of blocks as *channels*.

9.3.1 Two-state configurations

As we can see from the L_a diagram, the conservation laws apply for a combination of two states. The next step is then to set up all two-state configurations that will be needed. We start by setting up the direct two-state channels, T, which consist of all two-hole and two-particle configurations. A unique identifier must be set up for the combination of quantum numbers. The identifier is used to aligning the non-zero combinations of two-body states to the same channel. Without this identifier, we will have to loop over all channels for each two-body state. I have used the following function

$$\begin{aligned} \text{Index}(N_x, N_y, N_z, S_z, T_z) =& 2(N_x + m)M^3 + 2(N_y + m)M^2 \\ &+ 2(N_z + m)M + 2(S_z + 1) + (T_z + 1). \end{aligned} \tag{9.36}$$

We use the same logic as in equation (9.3) to get a unique identifier for every combination of N_x, N_y, N_z, S_z and T_z. This implies that the two-body states have the same momentum, spin and isospin projection, which satisfies our conservation laws. We need m and M to be sufficiently large. I have used

$$m = 2|\sqrt{N_{\max}}|, \qquad M = 2m + 1. \tag{9.37}$$

As a consequence of the Pauli principle, two particles cannot occupy the same state, so we can further reduce the amount of two-body states by excluding equal one-body states from the channels. An algorithm for setting up the direct channels can be portraied as

for one-body state 1 $\in$ STATES :
  for one-body state 2 $\in$ STATES :
    if one-body state 1 $\neq$ one-body state 2 :
    $N_x = n_{x,1} + n_{x,2}$
    $N_y = n_{y,1} + n_{y,2}$
    $N_z = n_{z,1} + n_{z,2}$
    $S_z = m_{s,1} + m_{s,2}$
    $T_z = m_{t,1} + m_{t,2}$
    Id = Index$(N_x, N_y, N_z, S_z, T_z)$
    $T \leftarrow$ (one-body state 1, one-body state 2, Id)

9.3.2 Unaligned channels

Diagram L_a, L_b and Q_a have the same conservation requirements as shown previously for L_a

$$\mathbf{k}_a + \mathbf{k}_b = \mathbf{k}_c + \mathbf{k}_d = \mathbf{k}_i + \mathbf{k}_j, \tag{9.38}$$

The direct channels satisfy this conservation requirement. We will however run into some trouble when computing the unaligned diagrams L_c, Q_b, Q_c and Q_d. Looking first at the diagram L_c, given by

$$L_c = -\hat{P}(ij|ab) \sum_{kc} \langle kb|\hat{v}|cj\rangle \, t_{ik}^{ac}, \tag{9.39}$$

with the corresponding conservation requirement for momentum, given by

$$\mathbf{k}_k + \mathbf{k}_b = \mathbf{k}_c + \mathbf{k}_j = \mathbf{k}_a + \mathbf{k}_c = \mathbf{k}_i + \mathbf{k}_k, \tag{9.40}$$

and for spin and isospin, we have

$$m_{s,k} + m_{s,b} = m_{s,c} + m_{s,j}, \qquad m_{t,k} + m_{t,b} = m_{t,c} + m_{t,j}. \tag{9.41}$$

When realigning the equation, we want it to be on the form

$$\tilde{L}c = -\hat{P}(ij|ab) \sum_{kc} \langle bj|\tilde{v}|ck\rangle \langle ck|\,\tilde{t}\,|ai\rangle\,. \tag{9.42}$$

We reorganize the conservation requirements in terms of the realigned matrix multiplication. This is to make sure we only calculate the non-zero terms. The momentum requirement becomes

$$\mathbf{k}_b - \mathbf{k}_j = \mathbf{k}_c - \mathbf{k}_k = \mathbf{k}_c - \mathbf{k}_k = \mathbf{k}_i - \mathbf{k}_a, \tag{9.43}$$

and spin and isospin will be subject to the same reorganizing. We see that the direct channels do not represent the right conservation requirement, so we must set up the cross channels, X, that consist of particle-hole or hole-particle two-body configurations. An algorithm can be set up as

for one-body state 1 $\in$ STATES :
 for one-body state 2 $\in$ STATES :
  if one-body state 1 $\neq$ one-body state 2 :
  $N_x = n_{x,1} - n_{x,2}$
  $N_y = n_{y,1} - n_{y,2}$
  $N_z = n_{z,1} - n_{z,2}$
  $S_z = m_{s,1} - m_{s,2}$
  $T_z = m_{t,1} - m_{t,2}$
  Id = Index$(N_x, N_y, N_z, S_z, T_z)$
  $X \leftarrow$ (one-body state 1, one-body state 2, Id)
  Id$'$ = Index$(-N_x, -N_y, -N_z, -S_z, -T_z)$
  $X' \leftarrow$ (one-body state 2, one-body state 1, Id')

where X' is the cross channel compliment, $X(pq) = X'(qp)$. The cross-channels are used for calculating the diagrams Q_b and L_c.

Looking at the diagram Q_c

$$Q_c = -\frac{1}{2}\hat{P}(ij) \sum_{klcd} \langle kl|\hat{v}|cd\rangle\, t_{ik}^{ab} t_{jl}^{cd}, \tag{9.44}$$

with the momentum conservation requirement

$$\mathbf{k}_k + \mathbf{k}_l = \mathbf{k}_c\mathbf{k}_d = \mathbf{k}_i + \mathbf{k}_k = \mathbf{k}_a + \mathbf{k}_b = \mathbf{k}_j + \mathbf{k}_l = \mathbf{k}_c + \mathbf{k}_d. \tag{9.45}$$

We see that we must realign the diagram as

$$\tilde{Q}_c = -\frac{1}{2}\hat{P}(ij)\sum_{klcd} \langle abi|\,\tilde{t}\,|k\rangle\,\langle k|\,\tilde{v}\,|cdl\rangle\,\langle cdl|\,\tilde{t}\,|j\rangle\,, \tag{9.46}$$

which sets the conservation requirement as

$$\mathbf{k}_a + \mathbf{k}_b - \mathbf{k}_i = \mathbf{k}_k = \mathbf{k}_k = \mathbf{k}_c + \mathbf{k}_d - \mathbf{k}_l = \mathbf{k}_c + \mathbf{k}_d - \mathbf{k}_l = \mathbf{k}_j. \tag{9.47}$$

We set up three-body and corresponding one-body channels to calculate Q_c and Q_d. An example algorithm for the K_h and $K_{p,p,h}$ channels can be outlined as

for one-body state 1 $\in$ HOLES :
$N_x = n_{x,1}$
$N_y = n_{y,1}$
$N_z = n_{z,1}$
$S_z = m_{s,1}$
$T_z = m_{t,1}$
Id = Index$(N_x, N_y, N_z, S_z, T_z)$
$K_h \leftarrow$ (one-body state 1, Id)

for one-body state 1 $\in$ PARTICLES :
for one-body state 2 $\in$ PARTICLES :
for one-body state 3 $\in$ HOLES :
if one-body state 1 $\neq$ one-body state 2 :
$N_x = n_{x,1} + n_{x,2} - n_{x,3}$
$N_y = n_{y,1} + n_{y,2} - n_{y,3}$
$N_z = n_{z,1} + n_{z,2} - n_{z,3}$
$S_z = m_{s,1} + m_{s,2} - n_{s,3}$
$T_z = m_{t,1} + m_{t,2} - n_{t,3}$
Id = Index$(N_x, N_y, N_z, S_z, T_z)$
$K_{p,p,h} \leftarrow$ (one-body state 1, one-body state 2, one-body state 3, Id)

9.3.3 Permutations

Some diagrams come with permutations. These are easy to handle by simply interchanging indices when adding the diagram to $t^{(n+1)}$.

for i ∈ Holes :
 for j ∈ Holes :
  for a ∈ Particles :
   for b ∈ Particles :
    $t^{(n+1)}(a,b,i,j) = t^{(n+1)} - \frac{1}{2}\left(Q_c(a,b,i,j) - Q_c(a,b,j,i)\right)$

9.4 Setting Up Basis

Before doing coupled-cluster calculations, the basis must be set up. An important property of this basis, is represented by the occupied and the virtual states. For infinite nuclear matter, the following algorithm can be used to set up the states. This algorithm should reproduce the magic numbers presented.

for shell ∈ All Shells :
 for $n_x, n_y, n_z \in [-\text{shell}, \text{shell}]$:
  $n = n_x^2 + n_y^2 + n_z^2$
  if $n =$ shell :
   for $m_s \in \{-1, 1\}$
    for $m_t \in \{-1, 1\}$
     States $\leftarrow (e, n_x, n_y, n_z, m_s, m_t)$
     $N_s = N_s + 1$
     if shell < Fermi level :
      $N_h = N_h + 1$

9.5 Parallelization

To fully utilize the computational power in modern processors, one must use a parallelized code. Modern processors usually come with more than one core to save power output at the same effiency [25]. A standard code written in C++ will be processed using only 1 *thread*, meaning that a single core only will be used. The super computer, *Smaug*, located at the department of Physics at the University of Oslo is built of processors with many but low performing cores given todays standards. If one can split the program into multiple threads, each executed at the same time in different cores, one can hope to reduce computational time substansially.

Measuring time on various parts of the solver, shows that the main bulk of the computational cost is spent when looping over states to fill matrices before multiplications. Particularly, a huge amount of time is spent on the L_a term because of the double sum over particle-states. The other very costly operation is computing the e_{ij}^{ab} values. Because of this, I have focused on parallellizing these loops to reduce cost. The general idea behind this implementation can be described by the following algorithm

```
mat Matrix = zeros<mat>(max_iteration, max_iteration)
#pragma omp parallel
{

  int N = omp_get_num_threads();
  int n = omp_get_thread_num();

  for (int i=n; i<max_iteration; i += N){
    for (int j=0; j<max_iteration; j ++){

      Matrix(i,j) = value(i,j);
    }
  }
}
```

where three new functions has been utilized to parallelize using OpenMP. The first function is

```
#pragma omp parallel
{}
```

which will define an enviroment that will be run in parallel. Each thread will execute the complete code written in this enviroment. By default, the command

will utilize all available threads. The next function used is

```
int N = omp_get_num_threads();
```

This code will find out the total number of threads.

```
int n = omp_get_thread_num();
```

This section checks which particular thread is used. This number will be different for each thread, and numbered from 0 to $N_{\text{maxthread}}$. This is the only part that will be different for each thread, and is the key to utilizing paralelization. The loop for i is set up as to calculate different values for i depending on which thread is executing the code. As an example, looking at thread 2 for an enviroment set up with four threads, the computed values of i will be in the set

$$i \in \{2, 6, 10, 14, \cdots\}. \tag{9.48}$$

In addition, OpenMP has functions for computing the time spent on each calculation, shown by the algorithm

```
double time0 = omp_get_wtime();
[Insert code]
double time1 = omp_get_wtime();
double time_spent = time1 - time0;
```

Which has been used for comparing computational cost of various solvers and loops.

Chapter 10

Results

10.1 The Pairing Model

The pairing Model serves as a valuable benchmark for implemented solvers. As I have looked at a 4p4h configuration, a full configuration interaction solver can be implemented giving the exact solution. One can also calculate the exact solution for second order perturbation theory by hand [7].

$$\Delta E_{MBPT2} = \frac{1}{4}\sum_{abij}\frac{\langle ij||ab\rangle\langle ab||ij\rangle}{\epsilon_{ij}^{ab}} = \sum_{a<b,i<j}\frac{\langle ij||ab\rangle\langle ab||ij\rangle}{\epsilon_{ij}^{ab}}, \tag{10.1}$$

where we have used

$$\epsilon_{ij}^{ab} = \epsilon_i + \epsilon_j - \epsilon_a - \epsilon_b, \tag{10.2}$$

and

$$\epsilon_p = h_{pp} + \sum_i \langle pi||pi\rangle\,. \tag{10.3}$$

This results in

$$\Delta E_{MBPT2} = \frac{\langle 01||45\rangle^2}{\epsilon_{01}^{45}} + \frac{\langle 01||67\rangle^2}{\epsilon_{01}^{67}} + \frac{\langle 23||45\rangle^2}{\epsilon_{23}^{45}}\,\frac{\langle 23||67\rangle^2}{\epsilon_{23}^{67}}, \tag{10.4}$$

which can easily be calculated to give

$$\Delta E_{MBPT2} = -\frac{g^2}{4}\left(\frac{1}{4+g} + \frac{1}{6+g} + \frac{1}{2+g} + \frac{1}{4+g}\right), \tag{10.5}$$

where g represents the interaction strength. The table below shows my results for various g's both using the exact mbpt2 calculations and my numerically computed results. All results can be accessed on github [27]

g	E_0	exact ΔE_{MBPT2}	ΔE_{MBPT2}
-1	3	-0.466667	-0.466667
-0.5	2.5	-0.0887446	-0.0887446
0	2	0	0
0.5	1.5	-0.0623932	-0.0623932
1	1	-0.219048	-0.219048

Table 10.1: A table showing correlation energies for the simple pairing model with 4 particle-states and 4 hole-states. The table presents a comparison of the exact result for second order Rayleigh-Scrödinger perturbation theory, to a numerically implemented solver.

As one can see, the correlation energies computed perfectly matches. This tells us that the basis set is set up correctly and that the MBPT2 solver is set up correctly. The results presented also match the results found in [7]

The second order perturbation theory result is valuable for benchmarking my implementation of the Coupled Cluster doubles equations. By initializing the first set of amplitudes, t, as zero, I get

$$t_{ij}^{ab(0)} = 0, \tag{10.6}$$

and the first iteration becomes

$$t_{ij}^{ab(1)} = \frac{1}{4}\sum_{ijab}\frac{\langle ab||ij\rangle}{\epsilon_{ij}^{ab}}. \tag{10.7}$$

This is equal to second order pertubation theory. The solvers should produce the same results.

g	ΔE_{MBPT2}	$\Delta E^{(1)}_{CCD}$
-1	-0.466667	-0.466667
-0.5	-0.0887446	-0.0887446
0	0	0
0.5	-0.0623932	-0.0623932
1	-0.219048	-0.219048

Table 10.2: A table comparing correlation energies for pairing model with 4 particle-states and 4 hole-states. This table shows that the CCD solver used with only a single iteration produces results exactly equal to mbpt2. This was done with the naive implementation of CCD equations

10.1.1 Comparison of CCD solvers

In this thesis I have created three different solvers for Coupled Cluster Doubles equations.

1. A naive brute force implementation of the equations summing over all variables.

2. A naive brute force implementation of intermediate equations summing over all variables.

3. Rewriting summations as matrix-matrix multiplications and exploiting various symmetry arguments one can set up a block implementation.

As shown in table (10.2), the naive implementation reproduces the mbpt2 energies as expected. I have used both the naive and intermediate CCD solver to compute correlation energies for the Pairing model, and again, [7] provides us with a good benchmark for the CCD equations.

g	ΔE_{CCD} Naive	ΔE_{CCD} Intermediates
0	-0.940891	-0.940891
-0.5	-0.0630564	-0.0630562
0	0	0
0.5	-0.0833621	-0.0833623
1	-0.369557	-0.369557

Table 10.3: A table comparing correlation energies for Pairing model with 4 particle-states and 4 hole-states. This table compare results from Naive and Intermediate implementation of CCD equations. A relaxing factor of $w = 0.3$ has been used because of divergence around $g = -1$

As one can see, my solvers reproduce results presented in [7]. For values of g close to -1, one will see a divergence for CCD equations. By introducing a relaxing factor of $w = 0.3$, this problem was solved.

10.1.2 Comparison of various solvers

The full configuration interaction provides us with the exact solution for the 4p4h Pairing model. It can therefore be useful to compare the performance of Perturbation theory to second, third and fourth order with coupled-cluster doubles and configuration interaction without the four-particle excitation.

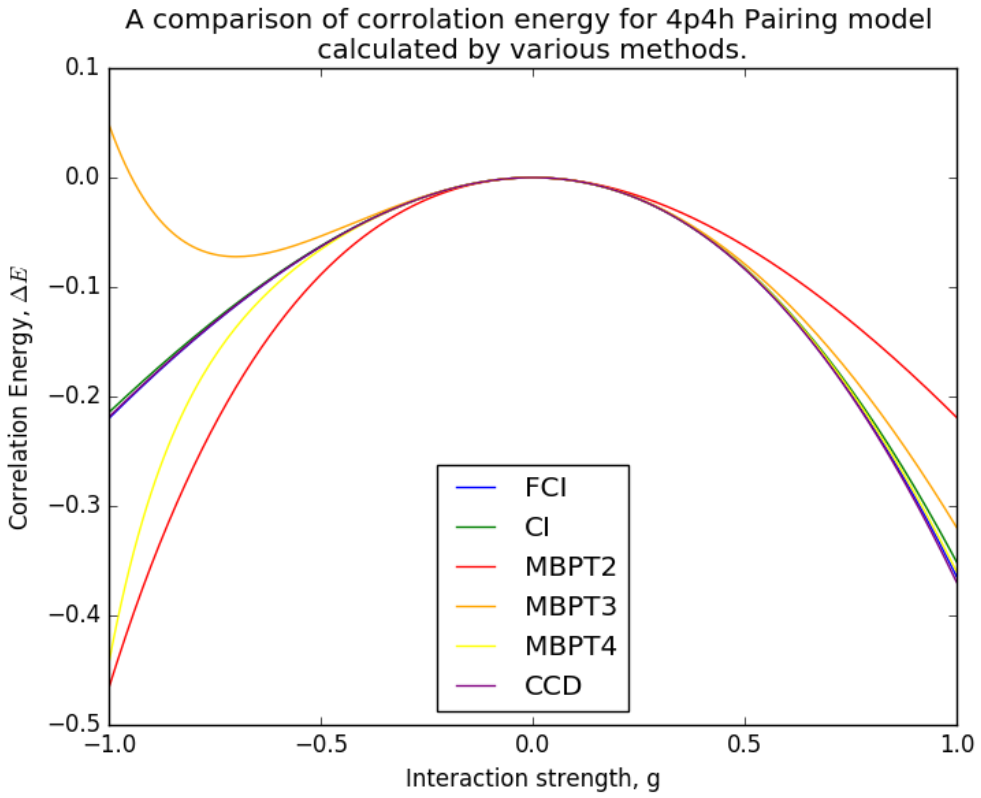

Figure 10.1: Comparing the correlation energy for a 4 particle, 4 hole Pairing model. This has been calculated for various interaction terms, $g \in [-1, 1]$ and for the single particle energy factor $\xi = 1$. The figure show relative performance for various solvers.

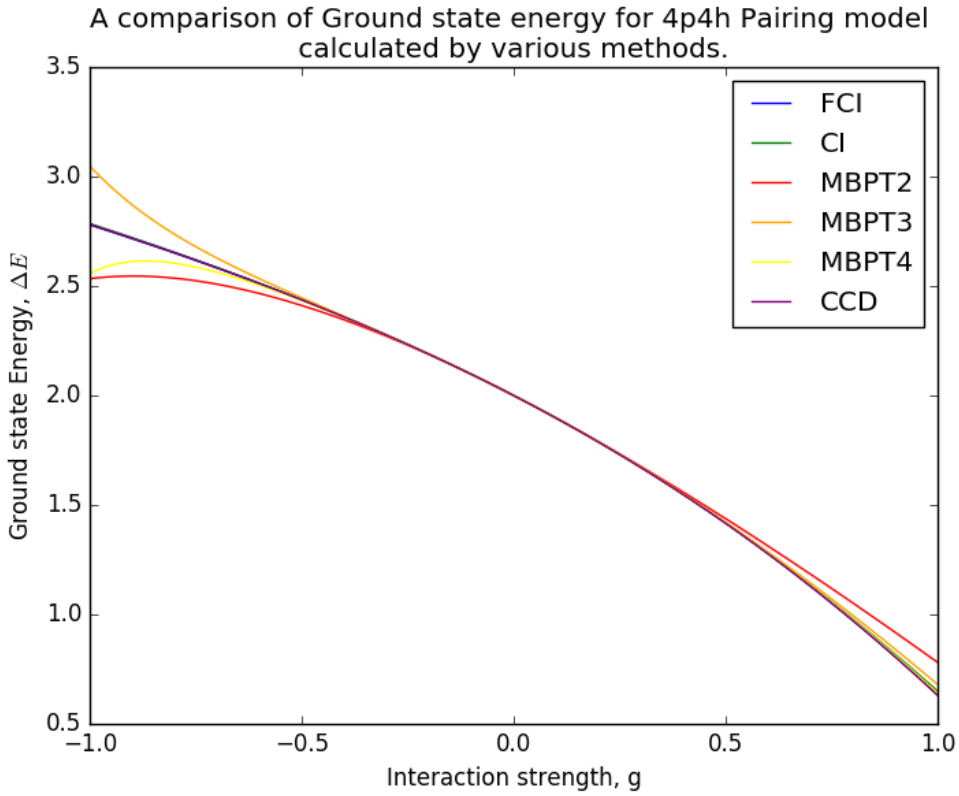

Figure 10.2: Comparing the ground state energy for a 4 particle, 4 hole Pairing model, given by $E_{\text{ref}} + \Delta E$ This has been calculated for various interaction terms, $g \in [-1, 1]$ and for the single particle energy factor $\xi = 1$. The figure show relative performance for various solvers.

One can see from figures (10.1,10.2) that the performance is good across the board close to $g = 0$, where the interaction is weak or non-existent. Once the interaction grows stronger, one notice that perturbation theory starts deviating a lot from the exact solution given by Full Configuration Interaction. That is particularly obvious for a negative interaction term. The cupled-cluster doubles equations perform very well, barely distinguishable from FCI even at very strong interactions. The same can be said for Configuration Interaction without the 4p-4h excitation term.

10.2 The Homogeneous Electron Gas

The homogeneous electron gas is a good system for benchmarking solvers, both in terms of produced results and computational cost. The coupled-cluster solver based on a matrix-matrix multiplications block implementation, has been implemented for this system along with the naive bruto force and intermediate solver.

10.2.1 The Reference Energy

A benchmark on the reference energy is useful to test the implementation of the basis states and the interaction. It does not require any coupled-cluster solver, because it is not dependent on the amplitudes. It serves as a good first hand benchmark for the system, and Audun Skau Hansen and Gustav Baardsen [1, 2] present results that have been reproduced in this thesis

r_s	E_{ref}/N_p	E_{ref}/N_p [1]	E_{ref}/N_p [2]
1.0	0.971682666829	0.971682666826	0.9717
0.5	4.185191069164		
2.0	0.205613116474		

Table 10.4: Reference energy, computed for three different r_s for the homogenous electron gas with 14 particles, compared with results from [1, 2]. The results are given in atomic units. My results are from [27]

10.2.2 Comparison of solvers

As shown, both the naive and intermediate solver reproduces satisfying results for the Pairing model, and can be further used for benchmarking of the implementation of the more advanced solver.

$N_{\text{particles}}$	N_{states}	ΔE_{CCD} naive	ΔE_{CCD} interm.	ΔE_{CCD} block
2	14	-0.0148277	-0.0148277	-0.0148277
14	38	-0.276498	-0.276498	-0.276498
14	52	N/A	-0.317821	-0.317821

Table 10.5: Calculations on the Homogeneous electron gas, using three different implementations of CCD equations. Showing results to benchmark the block solver, which was not benchmarked on the Pairing model. The System has been calculated with 2 or 14 particles and the total states either 14, 38 or 54. The calculations has been made with a relaxing factor of 0.3 and $r_s = 1.0$. The results are given in atomic units. Results can be found [27]

As we can see, the three solvers produce the exact same results, serving as a succesful benchmark for the block solver. These are relatively small calculations, at least compared to the thermodynamic limit. To fully grasp the point of using the block solver for larger computations, I have compared the time spent on performing the calculations for all three solvers

$N_{\text{particles}}$	N_{states}	ΔE_{CCD} naive	ΔE_{CCD} intermediates	ΔE_{CCD} block
2	14	17.54 s	1.28 s	0.01 s
14	38	7.5 days	28.4 mins	0.49 s
14	52	N/A	2.9 hours	0.73 s

Table 10.6: Calculations on the Homogeneous electron gas, using three different implementations of CCD equations. Showing time needed for every solver to calculate results in figure (10.5. The System has been calculated with 2 or 14 particles and the total states either 38 or 54. The calculations has been made with a relaxing factor of 0.3 and $r_s = 1.0$. The results are given in atomic units. Results found in file *CompareTimeNaiveBlock.txt* [27]

One see the enormous leap of computational time, where the intermediate solver needs almost 10 000 times the computational time and the naive solver even more for the small system with 38 states.

For a more thurough benchmark of the block solver, I have compared results for different states, r_s and weights, to compare with results from Audun Skau Hansen's results [2]. I present only the results achieved by the use of a weight factor $\alpha = 0.3$. The results are equal for other weights, and the number of iterations needed are around 1/3 for $\alpha = 1.0$, but for $r_s = 2.0$, the results are unstable without using the relaxing factor. The results are found in various files on github [27].

r_s	N_s	ΔE_{CCD} block	ΔE_{CCD} interm.	ΔE_{CCD} [2]
1.0	54	-0.3178228436888623	-0.3178228436888617	-0.317822843688933
	66	-0.3926965898061108	-0.392696589806104	-0.3926965898061966
	114	-0.4479105961756186		-0.4479105961757175
	162	-0.4805572589305356		-0.4805572589306416
	186	-0.485522931752024		-0.4855229317521318
	246	-0.4929245740022883		-0.4929245740023975
	294	-0.4984909094065708		-0.4984909094066818
	342	-0.5019526761546675		-0.5019526761547779
	358	-0.5025196736075309		-0.502519673607641
0.5	54	-0.3589655739945123	-0.3589655739945096	
	66	-0.4498148680442147	-0.4498148680442103	
	114	-0.5120153541477088		-0.5120153541478306
	162	-0.5476011323717939		
	186	-0.5533296597612266		
	246	-0.5622035867753152		
	294	-0.5687413543469695		
	342	-0.5729645498902303		-0.572964549890367
	358	-0.5736805652891426		
2.0	54	-0.2589156130046963	-0.2589156130046975	
	66	-0.313408288753419	-0.3134082887534144	
	114	-0.3577968843144314		-0.3577968843144996
	162	-0.3855831022718059		
	186	-0.3894387566078363		
	246	-0.3947792888408948		
	294	-0.3989857639655124		
	342	-0.401413618466477		-0.4014136184665555
	358	-0.4017831726474148		

Table 10.7: A comparison of the block solver and the intermediate solver for different systems. The results have been compared to the results found in Audun Skau Hansen's thesis [2]. The results are computed with a weight factor $\alpha = 0.3$. The results are given in atomic units.

10.2.3 The Thermodynamic limit

When setting up the homogeneous electron gas, one is trying to simulate an infinite gas of electrons. One is, however, forced to truncate the number of wave functions. This leads to a system that is not infinite, and we do not get the right results when using many-body methods to compute the ground state energy for

the electrons. As one increases the number of electrons, we will move closer to the real system. As one can see from figure (10.5), by adding more states, the energy converges towards the *thermodynamic limit*, which is the true energy for the system.

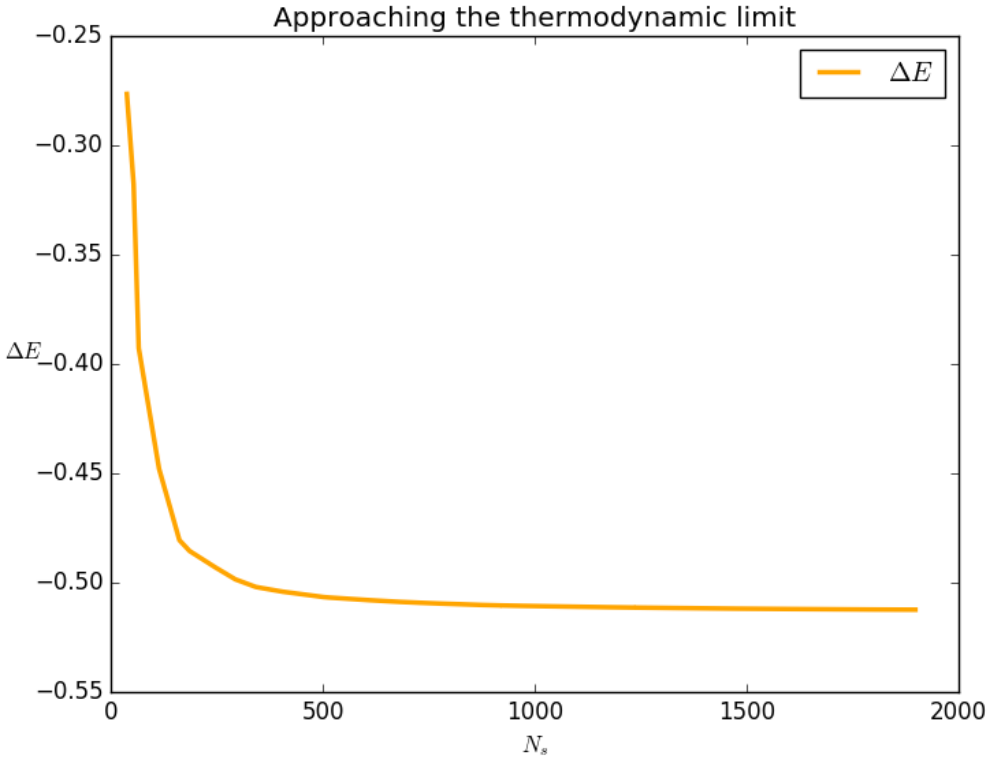

Figure 10.3: Correlation energy for a system consisting of 14 particles, with $r_s = 1.0$. The results are produced with a relaxing factor $\alpha = 0.3$. The results are given in atomic units.

The results for different amount of particles follow in the tables (10.8,10.9,10.10,10.11,10.12). I have computed energies for smaller and smaller system sizes. The memory usage expands rapidly for many particles and states, so these are the largest systems computed.

N_h	N_s	ΔE_{CCD}	$\Delta E_{CCD}/N_\mathrm{h}$
14	38	-0.2764993874198891	-0.01974996
14	54	-0.3178228436888623	-0.02270163
14	66	-0.3926965898061108	-0.02804976
14	114	-0.4479105961756186	-0.03199361
14	162	-0.4805572589305356	-0.03432552
14	186	-0.485522931752024	-0.03468021
14	246	-0.4929245740022883	-0.0352089
14	294	-0.4984909094065708	-0.03560649
14	342	-0.5019526761546675	-0.03585376
14	358	-0.5025196736075309	-0.03589426
14	406	-0.5041428350345967	-0.0360102
14	502	-0.5065799526613661	-0.03618428
14	514	-0.506781381408595	-0.03619867
14	610	-0.5080057508848216	-0.03628613
14	682	-0.508790105475187	-0.03634215
14	730	-0.5091947506339534	-0.03637105
14	778	-0.5095611843519957	-0.03639723
14	874	-0.5101903217890488	-0.03644217
14	922	-0.5104161052302821	-0.03645829
14	970	-0.5106074895685655	-0.03647196
14	1030	-0.5107995654154656	-0.03648568
14	1174	-0.5112320650408912	-0.03651658
14	1238	-0.5113982335227241	-0.03652845
14	1382	-0.5116958244764185	-0.0365497
14	1478	-0.5118827825222959	-0.03656306
14	1502	-0.5119149735422388	-0.03656536
14	1598	-0.5120443934671698	-0.0365746
14	1694	-0.5121557267165306	-0.03658255
14	1790	-0.512269185709	-0.03659066
14	1850	-0.512326660012	-0.03659476
14	1898	-0.512367897375	-0.03659771

Table 10.8: Correlation energies computed with coupled-cluster doubles equations for a system of 14 particles. The value of r_s is set to $r_s = 1$. All results have been computed with a relaxing factor $\alpha = 0.3$. The columns show the number of particles, number of states, correlation energy for all particles and the correlation energy for each particle. The results are given in atomic units.

N_h	N_s	ΔE_{CCD}	$\Delta E_{CCD}/N_\mathrm{h}$
38	38	0	0
38	54	-0.252944115	-0.00665642
38	66	-0.370737565	-0.00975625
38	114	-0.871764141	-0.02294116
38	162	-1.13154477	-0.02977749
38	186	-1.19804172	-0.03152741
38	246	-1.29346208	-0.03403848
38	294	-1.34391772	-0.03536626
38	342	-1.38535934	-0.03645682
38	358	-1.39471117	-0.03670293
38	406	-1.41770717	-0.03730808
38	502	-1.45075296	-0.03817771
38	514	-1.45292878	-0.03823497
38	610	-1.46803297	-0.03863245
38	682	-1.47722483	-0.03887434
38	730	-1.4823711	-0.03900977
38	778	-1.48652184	-0.039119

Table 10.9: Correlation energies computed with coupled-cluster doubles equations for a system of 38 particles. The value of r_s is set to $r_s = 1$. All results have been computed with a relaxing factor $\alpha = 0.3$. The columns show the number of particles, number of states, correlation energy for all particles and the correlation energy for each particle. The results are given in atomic units.

N_h	N_s	ΔE_{CCD}	$\Delta E_{CCD}/N_\mathrm{h}$
54	36	0	0
54	54	0	0
54	66	-0.0421954494	-0.0007813972
54	114	-0.524183851	-0.0097071084
54	162	-1.16644846	-0.0216008974
54	186	-1.29585369	-0.0239972906
54	246	-1.53905245	-0.0285009713
54	294	-1.63508823	-0.0302794117
54	342	-1.71780253	-0.0318111580
54	358	-1.74678467	-0.0323478646
54	406	-1.79566209	-0.0332530017
54	502	-1.87835721	-0.0347843928
54	514	-1.88337624	-0.0348773379
54	610	-1.92179323	-0.0355887635
54	682	-1.9446975	-0.0360129167
54	730	-1.95772367	-0.0362541423

Table 10.10: Correlation energies computed with coupled-cluster doubles equations for a system of 54 particles. The value of r_s is set to $r_s = 1$. All results have been computed with a relaxing factor $\alpha = 0.3$. The columns show the number of particles, number of states, correlation energy for all particles and the correlation energy for each particle. The results are given in atomic units.

N_h	N_s	ΔE_{CCD}	$\Delta E_{CCD}/N_\mathrm{h}$
66	38	0	0
66	54	0	0
66	66	0	0
66	114	-0.69213050	-0.01048683
66	162	-1.51007005	-0.02287985
66	186	-1.65129650	-0.02501964
66	246	-2.01158657	-0.03047858
66	294	-2.23052988	-0.03379591
66	342	-2.37274100	-0.03595062
66	358	-2.40766203	-0.03647973
66	406	-2.48442087	-0.03764274
66	502	-2.61023699	-0.03954905
66	514	-2.62135316	-0.03971747

Table 10.11: Correlation energies computed with coupled-cluster doubles equations for a system of 66 particles. The value of r_s is set to $r_s = 1$. All results have been computed with a relaxing factor $\alpha = 0.3$. The columns show the number of particles, number of states, correlation energy for all particles and the correlation energy for each particle. The results are given in atomic units.

N_h	N_s	ΔE_{CCD}	$\Delta E_{CCD}/N_\mathrm{h}$
114	38	0	0
114	54	0	0
114	66	0	0
114	114	0	0
114	162	-1.21746415	-0.01067951
114	186	-1.76124711	-0.01544954
114	246	-2.47264211	-0.02168984
114	294	-3.24858002	-0.02849632
114	342	-3.70744788	-0.03252147
114	358	-3.79981471	-0.03333171

Table 10.12: Correlation energies computed with coupled-cluster doubles equations for a system of 114 particles. The value of r_s is set to $r_s = 1$. All results have been computed with a relaxing factor $\alpha = 0.3$. The columns show the number of particles, number of states, correlation energy for all particles and the correlation energy for each particle. The results are given in atomic units.

10.3 Neutron Matter

The final set of results are for infinite nuclear matter. I have in this thesis chosen to only look at neutron matter, so there will be no variation of isospin for the particles. Therefore, every shell will contain the same amount of particles as the electron gas. Because of the constants introduced in the Minnesota potential, one will need to use real units, not atomic units. That introduces some changes to the calculation of one-particle energy. The results are calculated as a function of densities, ρ, which sets the volume,

$$V = L^3 = \frac{N_{\text{particles}}}{\rho}. \tag{10.8}$$

The one-particle energies are defined as

$$\frac{\hbar^2 c^2}{2mc^2}\frac{4\pi^2}{L^2}. \tag{10.9}$$

I have used the values

$$\hbar c = 197.3269788 \text{ MeVfm}, \quad mc^2 = 939.565 \text{ MeV} \tag{10.10}$$

I first produced the correlation energies as the correlation energy approached the thermodynamic limit, as I did for the electron gas

These results, do not seem to exactly match the results found in [7]. After extensive searching for the bug without finding a solution, I am presenting the results from my code. The problem most likely lies in the Minnesota potential, because I have used the same coupled-cluster solver for both the electron gas and the neutron matter.

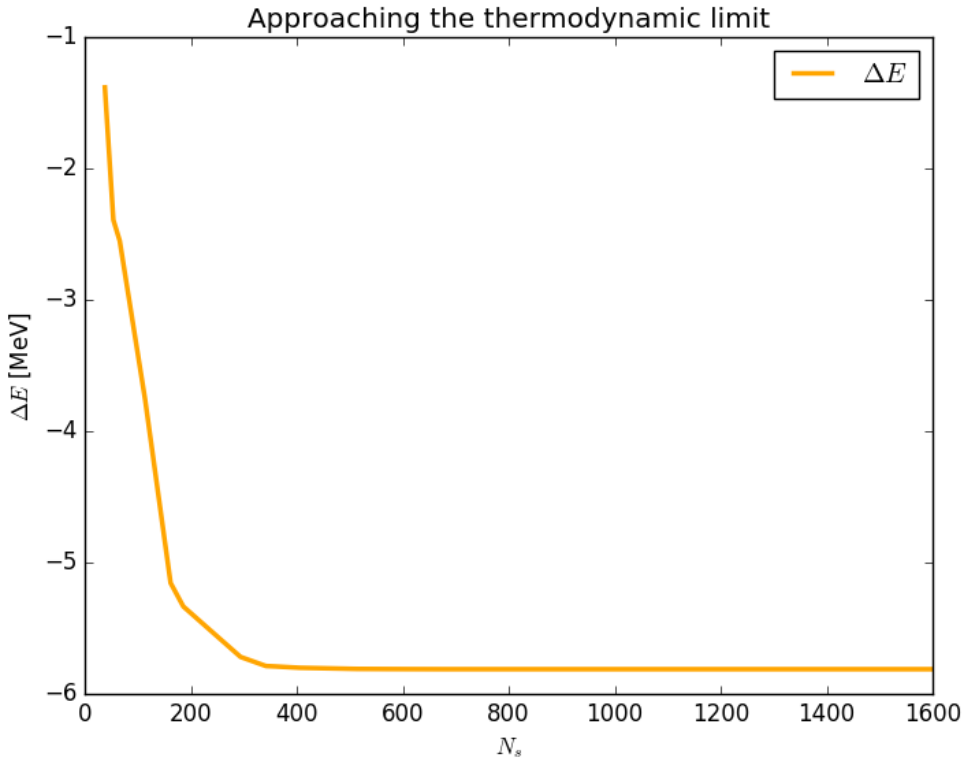

Figure 10.4: Correlation energy for a system consisting of 14 neutrons interacting by the Minnesota potential, with $\rho = 0.2$ fm^{-3}. The results are produced with a relaxing factor $\alpha = 0.3$.

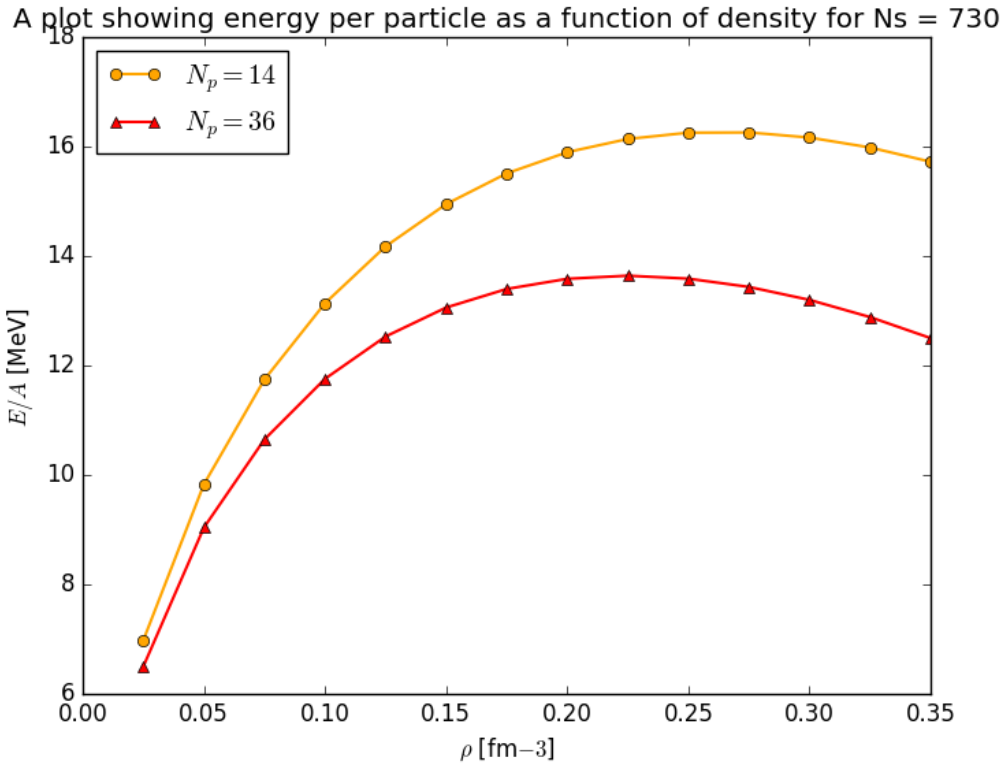

Figure 10.5: Correlation energy for a system consisting of 14 neutrons interacting by the Minnesota potential, with $\rho = 0.2$ fm^{-3}. The results are produced with a relaxing factor $\alpha = 0.3$.

Chapter 11

Conclusion and future prospects

Looking back on the goals defined in the introduction, I have fulfilled all main goals set for this thesis. Laying out the ground work for developing many-body methods, I have presented and explained the implementation of full configuration interaction, Hartree-Fock theory, Rayleigh-Schrödinger perturbation theory and coupled-cluster theory. I have also presented the three quantum mechanical systems that were investigated in the thesis. I have tried to write a complete and well-explained theoretical introduction to many-body quantum mechanics. Hopefully, these sections can be useful for a future generation of students.

I developed a brute force solver for all four methods, and applied them to the small and easy pairing model. The coupled-cluster doubles equations performed very well compared to many-body perturbation theory for the pairing model. This was easily shown, as the full configuration interaction provided a true result for benchmarking all solver. As expected, perturbation theory did not perform well when the interaction became stronger. When developing the equations for perturbation theory, one the ratio $\Delta E/E_{\text{ref}}$ to be small. The code for this system is openly available for further development and testing at github.

I moved on to develop code for the infinite electron gas in three dimensions, which was tested and benchmarked to previous literature. I tried testing the same brute force coupled-cluster doubles implementation to calculate the energy for this system, and found that even for the smallest systems, a brute force implementation is far too costly for systematic use. The first attempt at optimizing the coupled-cluster doubles code, used a factorization of diagrams and intermediate storage of values. This significantly reduced the computational cost from the brute force method. The code was benchmarked against the brute force method, and it also could reproduce som results from literature. This code is also available

for the public on github.

As I wanted to compute results for large systems approaching the thermodynamic limit, the solver based on intermediates proved to be far too costly on both cpu and memory. Most of the developing effort has been spent on implementing a more effiecient solver for the coupled-cluster equations. The first step was to rewrite equations as matrix-matrix multiplications. Because of the packages LAPAK/BLAS, matrix-matrix multiplication offers a significant speed improvement. However, the matrices consume a large amount of memory. To reduce this problem, one can exploit symmetries present in infinite matter to rewrite the full matrix-matrix multiplication as a large set of smaller multiplications. To further reduce cpu time, the code was rewritten to run in parallel. Compared to the brute force implementation, the difference in computational cost was huge, reducing computational time from 7.5 days to 0.49 seconds for a system with 14 particles and 38 states. The code reproduced results from literature exceptionaly well for three-dimensional infinite electron gas. There seems to be some problems for the neutron matter, which I did not manage to correct. The problem is probably connected to the Minnesota potential, because the solver worked without problems for the electron gas.

Further improvements on the coupled-cluster solver can be achieved by adding singles, triples and quadruples excitations to the equations. Further optimizations can be done to memory handeling of amplitues. My work can be used as a foundation for further implementations or it can be used for educational purposes for future students. For this reason, I have tried to write a clean and well documented code that can be understood by an educated reader. It can be interesting to calculate results for infinite nuclear matter with a more complex potential than the Minnesota potential.

Bibliography

[1] Gustav Baardsen *Coupled-cluster theory for infinite matter* 2014

[2] Audun Skau Hansen *Coupled Cluster studies of infinite systems,* Master thesis, University of Oslo, 2015

[3] Isaiah Shavitt and Rodney J. Bartlett *Many-Body Methods in Chemistry and Physics* 2009

[4] Attila Szabo and Neil S. Ostlund *Modern Quantum Chemistry. Introduction to Advanced Electronic Structure Theory* 1982

[5] David J. Griffiths *Introduction to Quantum Mechanics* Second edition 2005.

[6] J.J. Sakurai *Modern Quantum Mechanics* Revised Edition 1993.

[7] Morten Hjorth-Jensen, Maria Paola Lombardo and Ubiraja van Kolck *An Advanced Course in Computational Nuclear Physics* 2016.

[8] Stanley Raimes *Many-Electron Theory* 1972.

[9] Leonard Susskind and Art Friedman *Quantum Mechanics, The Theoretical Minimum* 2014.

[10] J. Goldstone *Derivation of the Brueckner Many-Body Theory, Proc. R. Soc. (London)* 1957.

[11] T. Daniel Crawford and Henry F. Schaefer III *An Introduction to Coupled Cluster Theory for Computational Chemists*

[12] Hermann G. Kummel. A biography of the coupled cluster method. *International Journal of Modern Physics B,* 17(28), 2003.

[13] B. D. Day *Rev. Mod. Phys.,* 39:719, 1967.

[14] D. R. Thompson, M. Lemere and Y.C. Tang. *Nucl. Phys. A,* 286:53 1977.

[15] J. J. Shepherd, A. Grneis, G.H. Booth, G. Kresse and A. Alavi *Phys. Rev. B,* 86:035111, 2012.

[16] J.J. Shepherd and A. Grneis *Phys. Rev. Lett.,* 110:226401, 2013.

[17] N. D. Drummond, R. J. Needs, A. Sorouri and W. M. C. Foulkes *Phys. Rev. B,* 78:125106

[18] L. M. Fraser, W. M. C. Foulkes, G. Rajagopal, R. J. Needs, S.D. Kenny and A. J. Williamson *Phys. Rev. B,* 53:1814, 1996

[19] P.P. Ewald. Die berechnung optischer und elektrostatischer gitterpotentiale. *Annalen der Physik,* 369(3), 1921. ISSN 1521-3889. doi: 10.1002/andp.19213690304

[20] Hans Petter Langtangen *A Primer on Scientific Programming with Python* Scond Edition, Springer 2011

[21] William H. Press, Saul A. Teukolsky, William T. Vetterling, Brian P. Flannery *Numerical Recipes, The Art of Scientific Computing* Third Edition, Cambridge 2007

[22] Morten Hjorth-Jensen *Nuclear Shell Model, Nuclear Talent course 2* URL (14. july, 2016): http://nucleartalent.github.io/Course2ManyBodyMethods/doc/pub/fci/pdf/fci-print.pdf

[23] Carlo Barbieri, Wim Dickhoff, Gaute Hagen, Morten Hjorth-Jensen, Artur Polls *Many-body Methods for Nuclear Physics, Nuclear Talent course 2* URL: *http://nucleartalent.github.io/Course2ManyBodyMethods/doc/web/course.html*

[24] Morten Hjorth-Jensen *Slides from the course FYS-KJM4480 2013/2014* URL: *http://www.uio.no/studier/emner/matnat/fys/FYS-KJM4480/h13/undervisningsmateriale/Slides%20from%20lectures/fys4480.pdf*

[25] Tim Mattson *Intel Youtube Course in OpenMp: Introduction to OpenMP - Tim Mattson (Intel)* URL: *https://www.youtube.com/playlist?list=PLLX-Q6B8xqZ8n8bwjGdzBJ25X2utwnoEG.*

[26] *Computational physics homepage on use of computational cluster, Smaug.* URL: *http://comp-phys.net/cluster-info/using-smaug/*

[27] Fredrik Wilhelm Holmen *https://github.com/wholmen/Master*

[28] Conrad Sanderson. Armadillo: An open source c++ linear algebra library for fast prototyping and computationally intensive experiments, 2010. URL: *http://arma.sourceforge.net/docs.html.*